Characterizations and sources of ambient particles in Augsburg, Germany

Dissertation

zur Erlangung des akademischen Grades eines

Doktors der Naturwissenschaften,

der Mathematisch-Naturwissenschaftlichen Fakultät

der Universität Augsburg vorgelegt

von

Jianwei Gu

Institut für Physik

Universität Augsburg

Augsburg, Oktober 2012

Erster Gutachter:	Prof. Dr. Armin Reller
Zweiter Gutachter:	Prof. Dr. Annette Peters
Tag der mündlichen Prüfung:	18.10.2012

Contents

1 Introduction and aims

Ambient particulate matter (PM) has been found to have adverse health effects by a great many epidemiological studies (Schwartz, 1999; Peters et al., 2000; Dominici et al., 2005; Brook et al., 2010). Particulate matter is a complex mixture of particles, and is emitted by different sources or formed from gas to particle conversion. A detailed identification of the major sources of particulate matter is important in order to investigate the associations between specific particle sources and health, and for policy makers to introduce suitable legislation for air quality control.

Source apportionment based on particulate chemical composition (PCC) has been carried out extensively (Lee et al., 1999; Kim et al., 2003a; Song et al., 2006; Baumann et al., 2008). In the study area of Augsburg, it was found that the regional aerosol accounted for 55% of PM_{10}, whereas the urban background and local traffic contributed to 22% and 24% of PM_{10}, respectively in Augsburg in 2005 (RVS, 2009). Five organic particulate sources have been resolved based on PMF analysis of semi-volatile organic compounds (SVOC) in $PM_{2.5}$ (Schnelle-Kreis et al., 2007). In spite of these studies, more information on the PM sources is needed, especially in winter when higher PM levels occur.

In contrast to PCC data, there are quite limited studies using particle size distribution (PSD) data for source apportionment (Zhou et al., 2004b; Ogulei et al., 2007b; Yue et al., 2008; Costabile et al., 2009). Unlike chemical composition which is relatively stable in the air, particle size distribution changes more rapidly and makes the source apportionment based on PSD data difficult. However, in a proper distance from particle sources the dynamic processes (condensation and coagulation etc) slow down and the particle size distribution becomes relatively stable. A quasi-stationary profile can be assumed (Kim et al., 2004b). As ultrafine particles (UFP) dominate the particle number concentration, this approach provides insight into the sources of UFP which is inadequately addressed by source apportionment based on PCC. Source profiles based on PSD data provide the source information from the physical aspect, which differs from the chemical aspect of PCC method. But the relationship of the source apportionment results from the two kinds of data set is not clear. There is an urgent need to know the consistency or discrepancy of sources obtained from PCC and PSD data, respectively.

The adverse health effects of particulate matter were observed primarily using the mass concentration (MC). Studies also demonstrate that particle number concentration (NC) has systemic inflammatory effects (Ferin, 1994) and is associated with respiratory and cardiovascular diseases (Peters et al., 1997; Pekkanen et al., 2002; Delfino et al., 2005). Studies also revealed that surface area concentration (SC) is associated with excess mortality (Maynard and Maynard, 2002) and lung inflammation (Tran et al., 2000; Brown et al., 2001; Stoeger et al., 2006). Particle length concentration (LC), described as the particle number times the particle diameter, was found to be highly correlated with surface area concentration deposited in the lung (Fissan et al., 2007; Wilson et al., 2007). Therefore, it is necessary to characterize the physical and chemical properties of PM, so as to aid in finding the most health relevant PM characteristics and components.

Long-term continuous measurements of particle-specific parameters like number of ultrafine particles or particle size distribution, particle length, surface and other particulate parameters have been scarcely available. To collect an enhanced PM data set and study the effects of different particulate pollutants on human health, a fixed monitoring station was established in an urban background area of Augsburg, Germany in 2004. The station measured a number of physical and chemical aerosol variables which provide input, on a continuous basis, for epidemiological studies. Measured variables were carefully selected according to the currently available measurement methods and their long-term stability.

As indicated above, NC, LC, SC and MC are variables that potentially impair health. Physical and chemical properties of particles also vary with particle size, thus size-segregated NC, LC, SC and MC were calculated from PSD data. Other variables (such as black carbon and sulfate) were also collected at this monitoring station by independent instruments, resulting in a total of 96 different particle variables. Current epidemiological models typically use a single-pollutant approach to estimate health effects. The analysis of the association between health effects and all 96 variables would not only be very time-consuming but also would not meet the current standards for epidemiological analysis, particularly with regard to the problem of multiple testing. Moreover, different pollutants are often correlated with each other (interdependency) and, therefore, there is a

need to divide the large data set into smaller data sets consisting of relatively independent variables (Dominici et al., 2010).

Environmental epidemiology, which focuses on the environmental exposure and resulted harmful effects as human health, often utilizes the air pollution measured at central sites to approximate the average population exposure with the underlying assumption that air pollution at central monitoring station is representative for exposure in a community (Pekkanen et al., 2002; Stoelzel et al., 2007). In many cases the assumption is valid, especially for PM mass concentration and regional background aerosols (Kim et al., 2005b). However, larger discrepancies among urban area are expected for particulate components with high spatial variability (e.g., traffic emission), which would in turn lead to uncertainties and misclassification of exposure estimate. Meanwhile, individuals who have different daily activity patterns can have different total exposures. Furthermore, it is meaningful to know in what degree the personal exposures agree with stationary measurements, which pollutants can be well approximated by stationary measurement. Such information is important for epidemiology when approximating stationary measured particulate pollutants as average exposure.

The exposure assessment is to provide accurate, precise, and biologically relevant exposure estimates for epidemiological study. Personal measurements provide a direct way to estimate exposure, but it is too costly for large study cohorts. Personal measurements in different microenvironments are less costly, require less effort but also can provide improved exposure estimate.

The aims of the thesis are I) to resolve and characterize particle sources, in terms of both particulate chemical composition and particle size distribution, and to compare both source apportionment methods for agreement, the advantages and disadvantages, and to evaluate the spatial and temporal variation of particulate sources across the urban area; II) to select key particulate variables from a number of measured variables for the use in epidemiological study; and III) to measure the personal exposure to different microenvironments in urban area and public transport, and to study the relationship between personal and stationary measurement.

2 State of the knowledge

2.1 Particulate matter and its physical properties

Airborne particulate matter is defined as particles with diameter ranges from 0.002 μm to 100 μm, the lower edge is not strictly cut as the boundary between gas and particle is not absolute (Finlayson-pitts and Pitts, 2000). Aerosol, defined as solid or liquid particles steadily suspended in the gas, refer to both particles and gas phase. However, in atmospheric science, the term aerosol is often used to represent the particles only. By definition, particulate matter or aerosol is a complex system. There are a lot of important parameters describing particulate matter including the size, number concentration, mass concentration, chemical composition, optical properties, and airborne lifetime etc. In following sections particle size, size distribution, as well as their measurement techniques will be introduced in detail.

2.1.1 Particle size

The size of particle influences its growth rate (Holmes and Morawska, 2006), the airborne residence time (Slinn and Slinn, 1980), and is often related to different sources (Costabile et al., 2009). Ambient particles are distributed not at one size, but spread over a wide range up to several orders of magnitudes (e.g., from a few nanometers to over 10 micrometer). There are several ways to indicate the size of particles, including geometric diameter, aerodynamic diameter and stokes diameter etc. As particles have many irregular shapes, the geometric diameter is thus difficult to characterize the particle size. In fact, the particle size is defined by the method of measurement utilizing inertial, optical, or electrical properties of particles. Among many effective diameters, the aerodynamic diameter is most commonly used. Aerodynamic diameter is defined as the diameter of a sphere with unit density (1.0 g cm^{-3}) has the same terminal velocity in the gas as the particle of interest (Finlayson-pitts and Pitts, 2000). It can be calculated by

$$D_a = D_g k \sqrt{\frac{\rho_P}{\rho_0}}, \qquad 2.1$$

where D_a is the aerodynamic diameter of the particle of interest, D_g is the geometric diameter, ρ_P is particle density, ρ_0 is the unit particle density (1.0 g cm^{-3}), and k is the particle shape factor.

By using aerodynamic diameter, the size of different shaped particles can be expressed in one term, depending on their aerodynamic properties. Aerodynamic size is very useful in sampling specific sized particles (e.g., particle size inlet and cascade impactor), and studying the deposition location of particles in human respiratory system.

Stokes diameter is another diameter defined as the diameter of a sphere with same density has the same terminal velocity in the gas as the particle of interest (Finlayson-pitts and Pitts, 2000). Aerodynamic size can be approximated from stokes diameter as follows:

$$D_a = D_S\sqrt{\rho_P}, \qquad 2.2$$

where D_s is the stokes diameter. Diameter measured by electric mobility method (will be discussed below) is stokes diameter.

2.1.2 Particle size distribution measurement

There are several different methods used to determine particle sizes. These methods are based on particle inertial characteristics, optical and electrical properties etc. Cascade impactors have been widely used to collect particles with different sizes on filters and for gravitational weighting and chemical analysis. Cascade impactor employs a series of impactor stages and each stage is designed to have a respective cutting size point. The cascade impactor normally can separate particles in 6 - 10 size bins (Hering et al., 1978; Hering et al., 1979; Hillamo and Kauppinen, 1991). The MOUDI (Micro-Orifice Uniform-Deposit Impactor), for example, can collect particles in 10 stages between 18 μm and 0.056 μm (Marple et al., 1991).

Aerodynamic particle size (APS) is a technique used to continuously measure particle number size distribution between 0.5 μm to 10 μm. It accelerates the particles through a nozzle and the particle velocity is measured by a Laser-Doppler Velocimetry. The particle velocity is also dependant on their aerodynamic diameter, thus the particle size can be determined by measuring the velocity (Wilson and Liu, 1980).

Another approach determines the particle size distribution by measuring the particle's electric mobility, among which a method called differential mobility analysis (DMA) has been widely used. An electric field is applied to classify charged particles with different electric mobility, which is dependent on particle sizes (Whitby et al., 1972b; Flagan, 2008). Particles are firstly charged (e.g., by ^{85}Kr) and then directed into a cylinder. In the centre of the cylinder there is an electric rod. The wall of cylinder is earthed thus an electric field is created in the cylinder between the rod and the wall. The charged particles are accelerated under the electric force but the acceleration rate becomes slower due to the drag force caused by the viscosity when particles move in the gas. Once electric force and drag force are balanced, the particle reaches its terminal velocity. The electric mobility, defined as the ratio of terminal velocity to the magnitude of electric field (Equation 2.3), is dependent on the particle size under a given electric field strength.

$$\mu = \frac{v_d}{E}, \qquad 2.3$$

where μ is electric mobility, v_d is the terminal drift velocity of a charged particle and E is magnitude of the electric field.

In a DMA, particles with higher mobilities reach the central rod and particles with lower mobilities pass out with exhaust flow. Particles with desired mobility pass through to a detector such as condensation particle counter (CPC), and are measured for numbers. A full particle size distribution can be obtained by changing the applied voltages.

In addition to above mentioned methods, other methods including electrical low pressure impactor (ELPI), fast mobility particle sizer (FMPS) and GRIMM nanoparticle measuring systems are summarized in Kumar et al. (2010).

2.1.3 Typical particle size distribution

Particle number concentration is dominated by particles in the size range < 100 nm. Particle volume or mass concentration mainly locates in the size range > 100 nm. Surface distribution lies in the size range between number and volume distribution. As particles spread over a wide size range, number, surface or volume alone can inadequately address the characteristics of size distribution.

Based on the studies on particle number, surface and volume distribution, Whitby (1972a; 1978) proposed a typical particle size distribution in urban environment which is composed of three modes: Aitken mode, accumulation mode and coarse mode. Coarse mode is composed of particles with diameter larger than 2.5 µm. Particles with diameter smaller than 2.5 µm is considered as fine particles and can be divided into accumulation mode and Aitken mode. Accumulation mode consists of particles with diameter in the range of 0.08-1 µm, and Aitken mode consists of particles in the size range of 0.01- 0.08 µm. Recently with the development of measurement technique of particles with diameter smaller than 10 nm, a fourth mode, nucleation mode was proposed which may be generated from nucleation and condensation. A schematic particulate matter size distribution is shown in Figure 2-1.

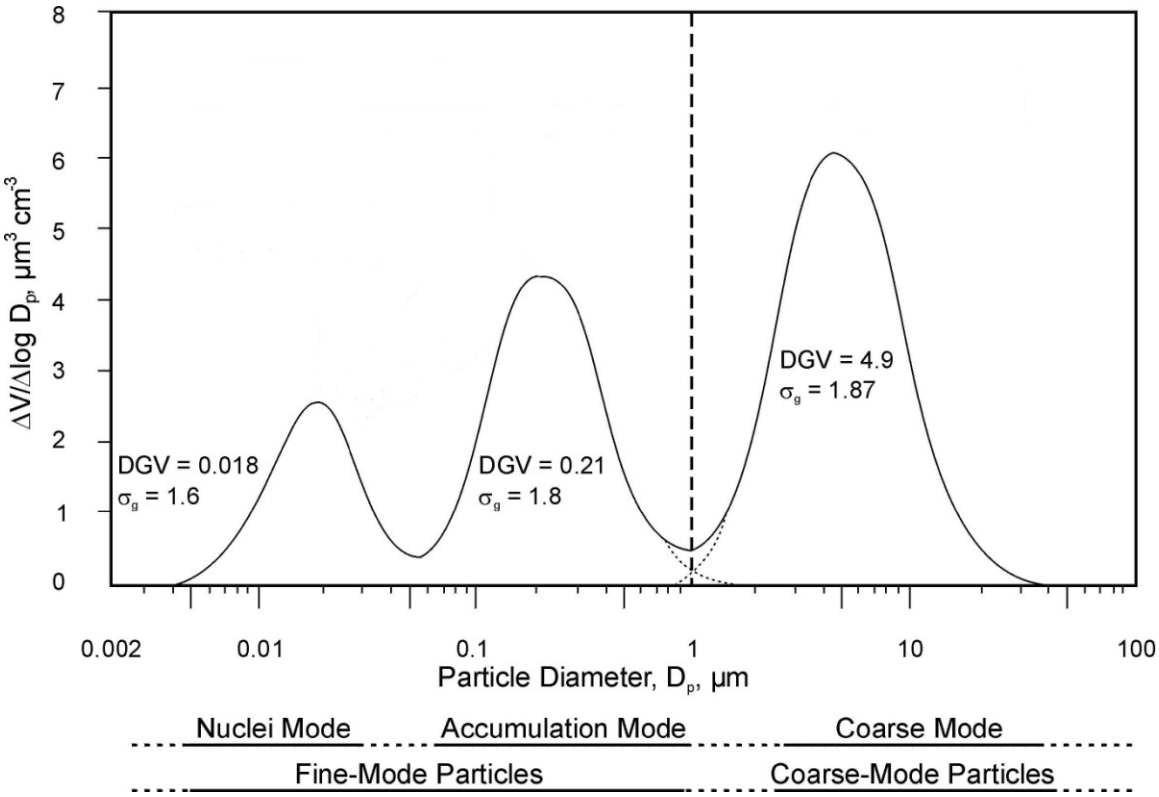

Figure 2-1: Schematic particulate matter size distributions in traffic (adapted from (Wilson and Suh, 1997)).

Coarse particles are considered to be generated from mechanical processes including wind erosion, construction, and sea spray etc. Biogenic emitted particles such as spore and pollen are also in the coarse particle mode. Coarse particles contribute to a fraction of particle mass concentration depending on locations and weather conditions but negligibly to particle number concentration.

Particles in accumulation mode, typically in the size range of 0.1-1 μm, have much lower gravitational deposition rate than coarse particles and smaller coagulation speed compared with ultrafine particles. Thus accumulation particles have longer atmospheric lifetime. Accumulation particles are considered to come from condensation of low-volatile gas and coagulation process. The coagulation can occur either among smaller particles in Aiken nuclei mode, or between nuclei mode and accumulation mode particles. The coagulation rate for the latter is higher than the former (Whitby, 1978). Accumulation particles normally contribute to a majority of particle mass but a small fraction of particle number (Figure 2-1).

Aiken nuclei mode particles arise from gas to particle conversion and combustion. It dominates the particle number concentration. Aiken nuclei mode particles arise from condensation of hot combustion vapor, followed by coagulation (Finlayson-pitts and Pitts, 2000). Aiken mode contributes to the majority of particle number concentrations (Figure 2-2).

Nucleation mode often refers to particles smaller than 10 nm, which arises from nucleation and condensation processes. A few nucleation models have been proposed including binary nucleation of sulfuric acid and water vapor, ternary nucleation with sulfuric acid, water and NH_3, as well as ion-induced nucleation (Holmes, 2007). However, up till now, much remains unknown for the mechanism of nucleation and new particle formation.

Figure 2-2 shows the averaged ambient particle number and mass size distribution in Augsburg. The number concentration locates mainly in Aitken mode, and particle mass distributes in accumulation mode, accompanied with a minor peak in coarse mode.

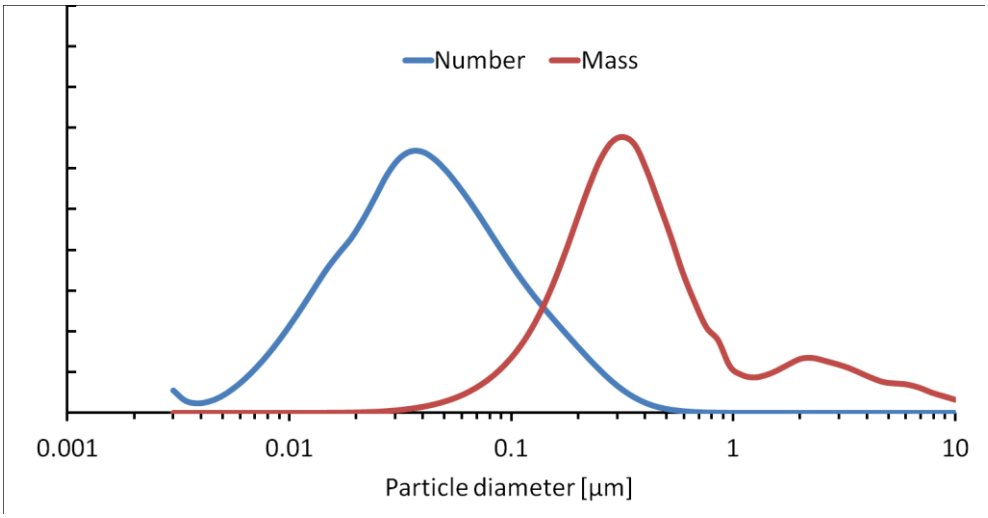

Figure 2-2: Particle number and mass size distribution in Augsburg (hourly average between November 2004 and December 2008).

2.2 Sources of particulate matter

2.2.1 Source types of particulate matter

According to whether physical or chemical transformation occurs from sources to receptor sites, particulate matter can be classified into primary and secondary particles. Primary particles are emitted directly from sources and include windblown dust, sea spray, combustion generated soot and fly ash, and some organic matter from biomass burning etc. Secondary aerosols refer to particles that not emitted directly from sources, but formed in the atmosphere through chemical reactions (mainly gas to particle formation). Typical secondary aerosols include particulate sulfate and nitrate which are mostly formed through the oxidation of SO_2 and nitrogen oxides, respectively. A part of organic matter is formed through the oxidation of volatile organic compounds (VOCs) emitted from vegetation or combustion process (Kroll and Seinfeld, 2008).

Particulate sources can be divided into natural and anthropogenic sources according to whether human activities are the major cause. Particles are emitted from a wide range of natural sources such as volcanic eruption, dust storm and biogenic emissions (spore and

pollen) etc. Anthropogenic sources include industrial emission, transportation (vehicles and ships), residential combustion and power generation etc.

From a management point of view, particulate matter can also be classified as local sources and transported sources. Local sources refer to particles emitted in local area. The transported sources are those not emitted locally but transported from hundreds of kilometers or more to the studied locations with atmospheric movement. This information is important for policy makers to determine how much pollution is within its jurisdiction and how much is from transport.

2.2.2 Chemical composition and related sources

The major components of particulate matter include water soluble inorganic ions (mainly sulfate, nitrate and ammonium), black carbon, organic compounds and trace elements (Putaud et al., 2010).

Sulfate is mainly formed through the atmospheric oxidation of gaseous SO_2 and to a less extent by oxidation of DMS (dimethyl sulfide) emitted by marine phytoplankton. SO_2 is released to the atmosphere with the combustion of fossil fuels containing sulfur or from volcanic eruption. SO_2 is oxidized through gas phase oxidation induced by OH radical or through aqueous phase oxidation by various oxidants including H_2O_2 and O_3 (e.g. in cloud). Nitrate is the oxidation product of photochemical reaction at the presence of NO_x, VOCs and oxidation radicals (e.g. OH). The produced HNO_3 is neutralized by NH_3 to form HN_4NO_3, or reacted with NaCl to form $NaNO_3$ (Hewitt, 2001). Sulfate and nitrate contribute to a big part of $PM_{2.5}$ and PM_{10} mass concentrations.

Apart from sulfate and nitrate, many other inorganic elements have been identified in particulate matter. These include elements that commonly found in earth's crust including Si, Al, Fe, Mg, Ca, Na, and Ti. Many other elements in airborne particles have a high crustal enrichment factors (EF_{crust}) (Duce et al., 1975).

$$EF_{crust} = (X_{air} / Al_{air}) / (X_{crust} / Al_{crust}), \quad 2.4$$

where subscript $_{air}$ indicates the concentration in airborne particles, subscript $_{crust}$ indicates the concentration in crust. In Equation 2.4, aluminum is chosen as the reference element.

High EF_{crust} values indicate the elements have strong sources other than crust, often anthropogenic sources. High EF values have been reported for heavy metals like Sb, Cu, Cd, Se, Hg, Zn, As, Cl, Br and others (Parekh and Husain, 1981; Salam et al., 2003). For example, the brake abrasion dust generated from friction of brake ware and brake pad were considered as the main source of Sb, as well as for Cu but to a less extent (Weckwerth, 2001; Furuta et al., 2005; Iijima et al., 2007). V and Ni were found mainly related to oil combustion (Krudysz et al., 2008). K is considered as an inorganic tracer for biomass burning (Hildemann et al., 1991).

Trace elements, however, can be emitted from multiple sources. For example, Zn is related to tyre ware, fossil fuel combustion, and industrial emissions (Allen et al., 2001). Some sources emitting trace elements are site specific, like metal processing, pigment production and incineration. Moreover, the elements emitted can vary substantially with the change of source contents (e.g. the additives of automobile tyres, the chemical composition of brake linings).

Organic matter accounts for a large part of PM mass concentration, and the composition is complex. There are hundreds of organic compounds that have been identified, which include alkanes, alkenes, aromatic hydrocarbons, alcohols, aldehydes, ketones, organic acids etc (Schauer et al., 1996). Organic compounds are either emitted directly from sources, or formed by secondary atmospheric formation, which refers to primary and secondary organics, respectively. For primary organics, Schauer et al. (1999a; 1999b; 2001; 2002a; 2002b) studied the organic profiles from a variety of emissions ranging from meat charbroiling, cooking and seed oil, diesel trucks, gasoline powered motor vehicles and wood combustion. Moreover, a great many organic compounds are from the secondary formation (Griffin et al., 1999; Hallquist et al., 2009).

Black carbon (BC), also called soot, is a byproduct of combustion (Mansurov, 2005). Bond et al. (2004) estimated the BC emitted from combustion in a global scale, and found fossil fuel, biofuel and open burning contributed to 38%, 20% and 42% of total BC, respectively. In urban environments, traffic is considered one of the major sources of BC (Bhugwant et al., 2000). In term of the mass concentration, BC is normally less abundant than sulfate, nitrate or organic matter.

2.2.3 Size related chemical composition and sources

Particles of different size modes are often related to different emission sources and chemical composition. As discussed above, coarse particles are mainly emitted from mechanical processes. Mineral dusts, which are mainly composed of Si, Al, Ca, Fe and Mg etc, are mainly in the coarse particle mode (Milford and Davidson, 1985; Finlayson-pitts and Pitts, 2000). The mass size distribution of mineral dust particles when blown up has been measured and was in the range of 0.2 μm to over 20 μm with the peak centered at about 10 μm (Sow et al., 2009; Kok, 2011; Shao et al., 2011). Although large particles normally deposit more rapidly than smaller particles, mineral dust arises from deserts can transport over a long distance. Many studies observed Saharan dust be transported to Mediterranean area (Blanco et al., 2003), the Atlantic Ocean (Haywood et al., 2003), and Caribbean Sea (Maring et al., 2003). Asian dust, originated from desert in central Asia, northwest China and Mongolia, had also been found in Japan (Zhang et al., 2006), and North Pacific Ocean (Clarke et al., 2001). Mori et al. (2003) observed a slightly shift in the mineral dust mode from 4.7 μm in Beijing to 3.3 μm in Yamaguchi, Japan. However, the study on the change of particle size distribution during dust transport is still quite limited. As addressed in a recent review paper by Formenti et al. (2011), the particle size distribution of mineral dust, as well as its evolution during transport should be considered with high priority. Nitrate has been found in both coarse mode and accumulation mode (John et al., 1990). The coarse nitrate is often related to marine area, which may be a result of the reaction of HNO_3 on coarse mode sea salt. Sea salt generated NaCl, sulfate are also in the coarse mode.

Accumulation mode contains a large fraction of particle mass. A great many studies showed that sulfate and nitrate were in the accumulation mode between 0.1 and 1 μm. Hering et al. (1997) studied the size distribution of particulate sulfate and discovered two peaks in accumulation mode with one around 0.2 μm and the other around 0.7 μm. The two peaks of PM mass concentration or sulfate and nitrate in accumulation mode have also been found in other studies (Eldering et al., 1994; Liu et al., 2008). The smaller mode in condensation mode, named “condensation mode”, refers to the gas phase oxidation of SO_2 to sulfate, while the larger mode, named “droplet mode”, refers to in droplet oxidation. Plaza et al. (2011) reported the sulfate and ammonium concentrated in

accumulation mode between 0.18 and 0.56 μm indicating the gas phase oxidation process, with the exception in fog event when sulfate and ammonium were in the 0.56 - 1 μm and 1 - 1.8 μm. However, the two-peak style in accumulation mode for sulfate has been only reported in some of the studies. In addition to sulfate and nitrate, accumulation mode contains a large fraction of organic matter. Kleeman et al. (1999; 2008) found the mass distribution of wood combustion, biomass burning and meat cooking were located in the accumulation mode with the peak at 0.1 - 0.2 μm for wood combustion, 0.6-0.9 μm for straw burning, and 0.2 - 0.3 μm for meat cooking. Rauncmaa et al. (1996) found the size range of 0.1 - 0.32 μm was related to black carbon.

Particles in Aitken mode are considered to be composed of soot, or ash core which absorbs volatile material in outer layer (Kumar et al., 2010). The chemical composition of particles in Aitken mode has been reported using cascade impactors, which can collect particles smaller than 100 nm. Generally, carbonaceous materials and sulfate are major components of Aitken mode particles (Puxbaum and Wopenka, 1984; Cass et al., 2000; Cabada et al., 2004).

The nucleation particles, due to their rapid conversion, are more complicated when apportioning their sources. In urban environment, vehicles are the major sources of particle number concentrations. However, particle size, number, as well as their composition go through a rapid and dynamic physical and chemical transformation (Kumar et al., 2011). Within a few seconds after the tail pipe emission, the hot, dense exhaust was quickly diluted with background air and its temperature goes down. New particles are formed through homogenous nucleation and condensation. Condensation process occurred with the condensable vapors condensed on the primary emitted particles. Vaporized lubricant oil and unburned fuel also condensed to form new particles. The measurement of chemical composition of nucleation particles is very difficult due to extremely low amount of mass (Curtius, 2006). A measurement for particles in the range of 6-15 nm in Atlanta showed ammonium sulfate contributed to all of the nucleation particles mass (Smith et al., 2005). In later studies, organics were found to be the main components of nucleation particles, besides sulfate. Smith (2008) found the nanoparticles consisted mainly of organics with a molar ratio of 86%, while sulfur accounted for 10%. Schneider et al., (2005) studied the chemical composition of nucleation particles from

diesel exhaust and found both volatile sulfate and organics. A study in coastal area of Ireland showed nucleation particles included a remarkable fraction of secondary organics besides iodine oxides (Vaattovaara et al., 2006). In spite of this, the study on chemical composition of nucleation particles is quite limited.

2.3 Health effects of particulate matter

2.3.1 Particulate matter and health effects

In 1940s and 1950s several air pollution episodes in Netherland and England which caused great increase in mortality rate triggered the epidemiologic studies on air pollutions ((Anderson, 2009) and references therein). Since then a great number of studies had shown a consistent adverse effect of ambient particles on population mortality and morbidity (Katsouyanni et al., 1997; Schwartz, 1999; Brook et al., 2010). Cardiovascular mortality was estimated to increase for nearly 1% for 10 μg m^{-3} PM_{10} increased by summarizing a number of time-series epidemiologic studies (Anderson, 2009). Based on evidence of the zero-effect threshold for air pollutants from epidemiologic studies, the World Health Organization (WHO) recommended the guideline for air pollution in 1971, 1986 and 2005, respectively. Since then, adverse health effect was found at lower and lower concentrations of particulate matter and then it was accepted that and there is no observable threshold (Pope et al., 2002; Samoli et al., 2005). In 2006, annual means of 10 μg m^{-3} for $PM_{2.5}$ and 20 μg m^{-3} for PM_{10} were recommended by WHO, which is far less than the guideline of 60 - 90 μg m^{-3} PM_{10} in 1971 (WHO, 2006).

In spite of this, the PM mass concentrations far exceeded the WHO recommended values in many countries, as well as in Europe. For many situations with very high particulate concentrations, it is almost impossible to reach the WHO guidelines rapidly. Moreover, the WHO guidelines are neither standards nor legally criteria (Krzyzanowski and Cohen, 2008), rather, they act as a final target value for air quality management. The European Commission launched the Thematic strategy on air pollution and Clean air for Europe

(CAFE) in 2005, with a aim "to achieve levels of air quality that do not result in unacceptable impacts on, and risks to, human health and the environment". The standard for PM_{10} was established in 2005 with the annual average of 40 µg m^{-3}. The limit value for daily mean PM_{10} concentration is 50 µg m^{-3} and should not be exceeded 35 times per year. In order to regulate the smaller particles, the target value for $PM_{2.5}$ standard (annual mean: 25 µg m^{-3}) entered into force in Europe since 2010 (EC 2005; EC 2008).

2.3.2 Particle size and health effect

Epidemiological studies have demonstrated larger health effects for PM_{10} (which can be deposited in the upper (thoracic) regions of the human respiratory tract) and $PM_{2.5}$ (which penetrates more deeply into the lung and may reach the alveolar region (Oberdorster et al., 2005)) than for total suspended particulates (TSP). Several studies have shown that especially the fine fraction ($PM_{2.5}$) of PM_{10} is associated with increased mortality and morbidity. As a direct consequence of this knowledge air quality standards and limit values for PM_{10} and $PM_{2.5}$ (replacing limit values for TSP) were introduced leading to a continuous evolution from TSP (total suspended particulate matter) to PM_{10} and further to $PM_{2.5}$ in government air quality networks (EC 1980; EC 1999; EC 2008).

In addition to particulate mass, evidence from many studies also indicated that particle number concentrations might be another cause for adverse health effects, especially for the cardiovascular diseases (Wichmann et al., 2000). Particle number concentration (NC), which is dominated by UFP, is suggested to have systematic inflammatory effects (Ferin, 1994) and is associated with respiratory and cardiovascular diseases (Peters et al., 1997; Pekkanen et al., 2002; Delfino et al., 2005). Because of the small contribution of ultrafine particles to mass concentration, UFP could not be sufficiently characterized by mass concentration.

2.3.3 Other particle parameters and health effect

In addition to NC, other parameters have been identified as potential health effects indicators. The particulate surface area and percent of surface molecules increased exponentially with decreased sizes. The surface area concentrations became important when considering that the surface molecules play an important role in determining bulk concentration, and exhibit greater biologic activity (Oberdorster et al., 2005). Some

studies revealed that surface area concentration (SC) is associated with excess mortality (Maynard and Maynard, 2002) and lung inflammation (Tran et al., 2000; Brown et al., 2001; Stoeger et al., 2006). Some toxicological studies reported the surface area concentration is a better indicator of dose metric than particle mass or particle number for predicting lung inflammation (Stoeger et al., 2006; Sager and Castranova, 2009).

Particle length concentration (LC), described as the particle number times the particle diameter, was found to be highly correlated with surface area deposited in the lung. Hence, the role of LC in association with health effects should also be considered (Fissan et al., 2007; Wilson et al., 2007).

2.3.4 Particle components and health effect

Although a consensus has been reached upon the adverse effect of particulate matter, there remain some questions and problems to be solved. One of these is which dominant component in particulate matter drives the adverse effect. Grahame et al. (2007) suggested identifying the most health relevant components of ambient particulate, rather than those may have little to no significant health effect. In contrast to the use of total mass concentration of particulate matter, some studies tried to identify the health risk related to a specific type of source. Studies observed higher risks for mortality, morbidity or other indicators for adverse health effect such as heart rate variability for those living nearer to the urban roads or highway (Hoek et al., 2002a; Gehring et al., 2006), and the risk caused by vehicular emissions was stronger than for total $PM_{2.5}$ mass concentration (Schwartz et al., 2005). Industrial sources like steel mills were highly related to mortality (Jerrett et al., 2005). While for particulate sulfate and nitrate, epidemiological studies provided no support for a causal association with adverse health effect (Reiss et al., 2007).

These studies, however, normally focused on only a few species including $PM_{2.5}$, PM_{10}, BC, NO_2 and SO_2, which were chosen mainly due to the limited available species measured at official environmental monitoring networks, rather than being selected for the representatives from a complete chemical speciation. Particles in the ambient air are in general mixtures of materials directly released from different sources or formed as a product from gas to particle conversion. Furthermore, a single chemical species can be emitted from multiple sources. Thus a detailed identification of the most important

sources of atmospheric particles is important in order to investigate the associations between specific particle sources and health, and for policy makers to introduce suitable legislation for air quality control. Studies have also been performed for studying association between source specific particulate matter from source apportionment and adverse health effect (Grahame and Hidy, 2004; Ito et al., 2006; Andersen et al., 2007; Yue et al., 2007).

2.4 Some aspects of exposure assessment to air pollutants

2.4.1 Spatial variability of particulate matter

Air quality monitoring usually measures particulate matter at central monitoring stations to represent the concentrations of a community. The EU directives require the urban background sites shall be located to be representative for several square kilometers. Their pollution level is influenced by the integrated contribution from all sources and should not be dominated by a single source (EC 2008). Epidemiologic studies often rely on single monitoring data to approximate the average exposure for a population (Pekkanen et al., 2002; Stoelzel et al., 2007). There underlies a homogeneous assumption of particulate matter. The assumption is true for $PM_{2.5}$ or PM_{10} mass concentration in many urban areas but is valid mostly only for urban background sites (Figure 2-3).

Figure 2-3 shows a schematic profile of PM mass concentration in and out an urban area (Lenschow et al., 2001). The PM mass concentrations in the great urban background are is higher than at regional background sites due to urban agglomeration. Within the urban area, higher PM mass concentrations near traffic are attributed to the local traffic. It demonstrates how PM mass concentration can vary in intra-urban area, particularly for certain sources (traffic or other single source). These sources maybe more toxic than regional background aerosols like sulfate and nitrate (Schwartz et al., 2005; Reiss et al., 2007). Thus the study on the spatial variability of particulate matter, as well as respective sources is important.

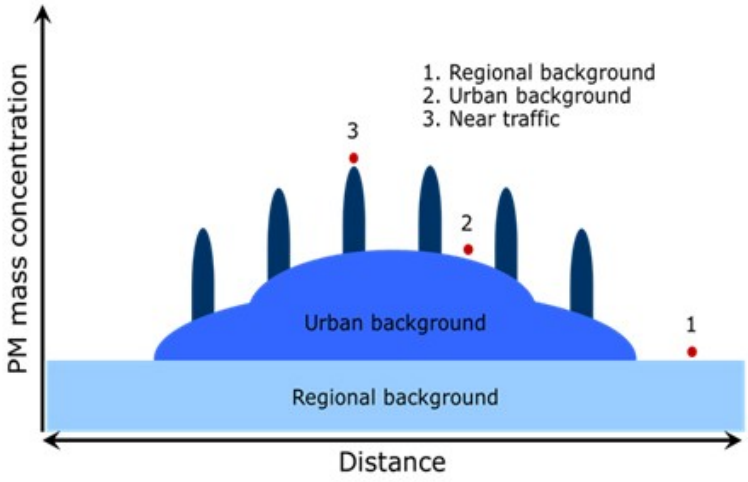

Figure 2-3: Schematic horizontal profile of PM mass concentration in an urban area (adapted from (Lenschow et al., 2001)).

There exist a number of studies dealing with the spatial variability of PM mass concentration in urban areas. The homogeneous assumption of PM was verified by many studies (Burton et al., 1996; Oglesby et al., 2000; DeGaetano and Doherty, 2004; Sajani et al., 2004). Many other studies, however, found PM to be heterogeneous in urban areas (Cyrys et al., 1998; Grivas et al., 2004; Nerriere et al., 2005). In a study of 27 U.S. urban areas, Pinto et al. (2004) found spatial homogeneity or heterogeneity varied between urban areas across the country, and he pointed out that the conclusion of spatial variability of PM mass concentration of an individual urban area cannot be made until the data is investigated.

One thing is certain that particulate source is an important factor controlling the intra-urban spatial variability (Monn, 2001). Even PM mass was found homogeneously distributed in urban area, certain particulate components can be heterogeneous (Krudysz et al., 2008). Fine particles tend to be more homogeneously distributed than coarse particles. Secondary sulfate and nitrate, which mainly originated from long range transport, have less spatial variability on an urban or regional scale. Chemical composition emitted from traffic is highly variable from road side to urban background (Hueglin et al., 2005).

Spatial variation of sources using receptor model also showed different sources of particulate matter had varying spatial variability. Kim et al., (2005b) found high uniformity of secondary sulfate and high heterogeneity for incinerator emission and pigment/metal emission. Kim and Hopke (2008) found $PM_{2.5}$ sources such as wood smoke, diesel and metal were heterogeneous distributed in Seattle urban area.

2.4.2 Personal exposure

In atmospheric environment, the air pollution is depicted by mass concentration (the mass in a unit volume of air). While in environmental epidemiology, the exposure, other than ambient concentration is focused. Personal exposure describes the pollution level that a human being is in contact with. By definition, personal exposure can vary between individuals who have different activities and go through different microenvironments. Personal exposure can be measured directly or indirectly (Monn, 2001). The direct method includes personal measurement with portable monitors, the passive sampler for certain gaseous pollutants like NO_2, and measure of biological marker. The indirect method includes the using of fixed monitoring sites, measurement of the pollutants concentration in different microenvironments and modeling of the exposure by dispersion, receptor model and/or GIS method.

The using of fixed monitoring sites utilizes the widespread air pollution monitoring networks to approximate the exposure for a population. However, there may be potential bias when taking the ambient concentrations as average exposure. This is particularly significant for vehicular emissions, which can be highly variable in different communities in one urban area. Microenvironment measurement measures the concentrations at a set of “microenvironments”, which is defined as a volume of space within which the concentration is homogeneous, or the variance of concentration in a microenvironment is less than the variance between microenvironments (Duan, 1982). Direct personal measurement using portable devices can accurately measure the exposure of individuals. The accuracy of exposure estimate decreases from personal measurement to microenvironment measurement to ambient measurement, but the cost increases greatly from ambient measurement to personal measurement (Mage, 1985). For population based

epidemiology studies, to directly measure the individual exposure for a large population will be very difficult and costly.

Several microenvironment models have been summarized by Duan (1982). The basic formula for calculating personal exposure can be expressed as

$$E = \sum_j \gamma_j \tau_j, \quad 2.5$$

where E is the personal exposure, γ_j is the concentration in microenvironment j, τ_j is the time spent in microenvironment j.

The microenvironment model has been used to calculate the personal exposure to particulate matter; however, the measurement on microenvironment is quite limited. Hänninen et al., (2009) simulated the microenvironment concentrations in Turin and Bologna in Italy from other European cities. Kaur and Nieuwenhuijsen (2009) measured the personal exposure to $PM_{2.5}$, UFP and CO in transport microenvironment. The pedestrian exposure along major road in central London was reported by Kaur et al., (2005). Other studies classified the direct personal measurement into several microenvironments according to the volunteers' activity diary (Vallejo et al., 2004; Dons et al., 2011).

$PM_{2.5}$ and PM_{10} mass concentrations are regulated species and have been extensively studied in epidemiologic studies. However, air pollutants are a mixture of a great many species, the source specific exposure measurement has to rely on the markers, or indicators of the mixtures. Often BC and NO_2 were used to represent air pollutants emitted from vehicles, while ozone represents the photochemical pollutants. And BC, measured by the attenuation of particles to light, is a good surrogate for soot, or elemental carbon, which is emitted from incomplete combustion of fossil fuels and biogenic fuels. Recent studies indicated BC is a appropriate indicator for vehicular emission in urban area (Reche et al., 2011). Particle number concentration may be more toxic to human health but the exposure to NC in different microenvironment is scarce.

3 Sampling sites and measurement program

For the analyses described in the thesis I used data collected at different monitoring sites located across the city Augsburg. In this chapter all monitoring sites and the measured data are described.

3.1 Locations of sampling sites

Figure 3-1 shows the location of the measurement sites where the particulate matter was sampled or the particulate/air pollutants were measured. Data were obtained in total from nine measurement sites spreading in city Augsburg. The red area in this figure indicates the urban area with heavy building density. The most extensive data set was collected at the monitoring site set up in 2004 on the campus of the University of Applied Sciences (UAS), Augsburg by Helmholtz Zentrum München, German Research Center for Environmental Health in cooperation with the Environmental Science Center, University of Augsburg. It is located about 1 kilometer south-east of the city center and is considered as an urban background site (Cyrys et al., 2008). The site is surrounded by campus buildings, a tram depot and a small company within a radius of 100 meters. The nearest main road is in the north-east at a distance of around 120 m. In 200 meters, this site is almost surrounded by residential area and a small park (Pitz et al., 2008b).

Furthermore, I used data collected at three monitoring sites operated by Bavarian Environment Agency as part of the Bavarian Air Quality Monitoring Network LÜB (Lufthygienisches Landesüberwachungssystem Bayern). The first one is located in the city centre at Königsplatz (KP) next to roads with high traffic density. The traffic density monitored in the year 2000 was 30500 cars per day. It is also located next to several tram lines, and near to the central tram station where all trams running in Augsburg pass through. According to the criteria of the classification of environmental monitoring sites in the project "Traffic-Related Air Pollution on Childhood Asthma", urban background sites are defined as those having no more than 3000 vehicles per day passing within the

radius of 50 meters, KP site is classified as a urban traffic site (Hoek et al., 2002b; Cyrys et al., 2008).

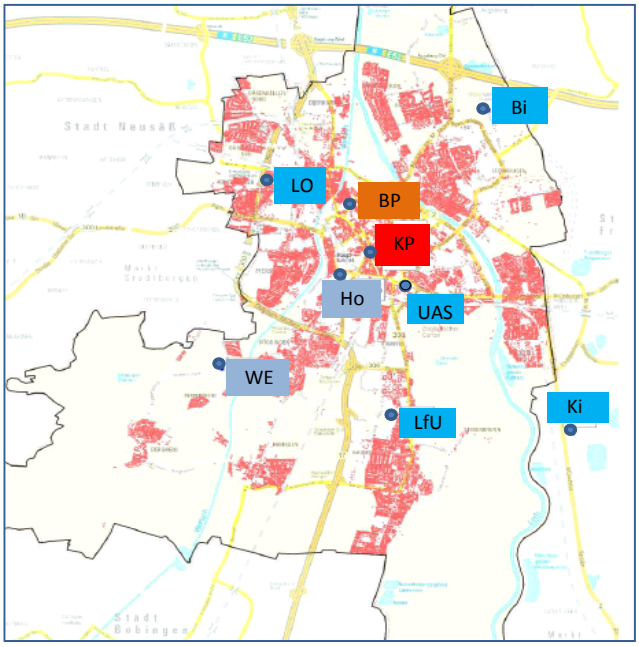

Figure 3-1: Locations of measurement sites in Augsburg (modified from (LfU, 2009)).

The monitoring site at Bourgesplatz (BP) is located in a small park in the city and is about 1 kilometer north of KP site. The third LÜB monitoring site is located within the place of residence of the Bavarian Environment Agency (LfU) approximately 4 kilometers south of the city centre.

Within the framework of a spatial variability study particles were sampled temporally at five further locations. Kriegshaber (LO) site is located in a residential area where home heating is expected to have a great impact in winter season. Hotel tower (Ho) site is located about 1 km southwest of KP site, and on the top of the hotel tower, which is about 100 meters above the ground. Bifa (Bi) site is in the Bifa environmental institute, within an industrial area at the outskirts of Augsburg. The industry area is located in the northeast of Augsburg, the downwind of prevailing wind direction. Kissing (Ki) site is about 1 kilometer north of the town Kissing, which is next to, but not belonging to city Augsburg. Note that between Ki site and LfU site, there is an area of forest. BP, LfU, LO, Bi and Ki are considered as urban background sites. Ho site is a tower site, which is

different from other sites. Wellenburg (We) is a site in the southwest of Augsburg. It is next to the large natural park locates in the southwest-west of Augsburg. WE site is less influenced by the city emissions and is considered as a suburban background site.

3.2 Measurements at University of Applied Science (UAS) site

The University of Applied Science (UAS) site was measuring particle size distribution (PSD) and online particulate chemical composition continuously since 2004. The measurement and data collection were performed by Dr. Mike Pitz and colleagues (Pitz et al., 2008a; 2008b).

Figure 3-2: UAS measurement site.

Table 3-1 shows the particulate pollutants measured at UAS sites in four winter seasons, winter 2004/05, winter 2005/06, winter 2006/07 and winter 2007/08. I defined winter period from November 1 to March 31 the next year. A descriptive analysis focusing on the variations of meteorology and particulate pollutants in the four winter seasons is presented in chapter 3.

Table 3-1: Particulate parameters measured at UAS site during four winter periods from 2004-2008

Parameters	Instruments
$PM_{2.5}$ and PM_{10}	TEOM
TNC	Condensation Particle Counter
PAHs [a]	Photoelectric Sensor
BC	Aethalometer
Sulfate	Sulfate Particulate Monitor
Nitrate	Ambient Particulate Nitrate Monitor
T, RH, radiation	Meteorological sensors

[a] PAS signal was converted to PAH sum mass concentration using HPLC results of 22 filter samples for Benzo(b)fluoranthene, Indeno(1,2,3-c,d)pyrene, Benz(a)anthracene, Chrysen, Benzo(a)pyrene, Benzo(k)fluoranthene, Dibenz(a,h)anthracene and Benzo(g,h,i)perylene (PAH[ng m^{-3}]=0.12×PAS-signal[fA]+3.18, R^2=0.82).

Table 3-2 shows the available particulate pollutants and meteorological parameters in winter 2006/07 and year 2007-2008. I carried out source apportionment analyses for the above two periods, respectively. Source apportionment in winter 2006/07 is to validate the method and to compare it with the other method (source apportionment with PCC data). The longer period analysis in 2007-2008 is to find out further characteristics of PSD sources including weekday-weekends variation, seasonal variation, and potential source locations etc. These results are shown in chapter 7.

The term "particle size distribution (PSD)" is determined by measuring the particle number concentration in a number of particle size bins (67 size bins from 3 nm to 10 µm in this case). The particle size distribution is often presented in a plot with the particle number concentration on the Y-axis and the corresponding sizes on the X-axis (see Figure 2-2).

Table 3-2: Summary of PSD, particulate pollutants and meteorological parameters measured at UAS site

Parameters	Instruments	Winter 2006/07	Year 2007-2008 [a]
PSD (3-800 nm)	(U)-DMA/ (U)-CPC	12.21.2006 - 03.23.2007	03.14.2007-12.17.2008
PSD (3-800nm)_after Thermo Denuder	(U)-DMA/ (U)-CPC & Thermo Denuder	Not used	03.14.2007-12.17.2008
PSD (800 nm-10 µm)	APS	01.17.2007 - 03.23.2007	03.14.2007-12.17.2008 [b]
TNC (3 nm-3 µm)	CPC	12.21.2006 - 03.23.2007	03.14.2007-12.17.2008 [c]
Total and (non)-volatile PM <2.5 µm and <10 µm	TEOM/FDMS	12.21.2006 - 03.23.2007	03.14.2007-12.17.2008
Sulfate	Sulfate Particulate Monitor	Not measured	04.24.2007-12.17.2008
Nitrate	Ambient Particulate *Nitrate* Monitor	12.21.2006 - 03.23.2007	03.14.2007-05.21.2008
BC	Aethalometer	12.21.2006 - 03.23.2007	03.14.2007-12.17.2008 [d]
PAHs [d]	Photoelectric Sensor	12.21.2006 - 03.23.2007	03.14.2007-12.17.2008 [e]
LC (10 nm-1 µm)	Electrical Aerosol Detector	12.21.2006 - 03.23.2007	03.14.2007-12.17.2008
ASC (10 nm-1 µm)	Diffusion Charging Particle Sensor	12.21.2006 - 03.23.2007	03.14.2007-12.17.2008
T, RH, radiation	-	12.21.2006 - 03.23.2007	03.14.2007-12.17.2008

[a] Data from March 14, 2007 – December 17, 2008 were also used in the cluster analysis (see Chapter 0); [b] PSD between 800 nm and 10 µm were missing during 10.16.2008 - 12.03.2008; [c] TNC were missing during 07.25.2008 - 11.25.2008; [d] BC were missing during 07.03.2008 - 09.08.2008; [e] PAHs were missing during 01.20.2008 - 04.07.2008 and 07.05.2008 - 08.19.2008.

Particles number concentrations with diameters between 3 nm and 10 µm were measured using a combination of three different subsystems covering a total of 67 size bins. An ultrafine differential mobility analyzer (UDMA) in combination with an ultrafine condensation particle counter (UCPC, Model 3025, TSI Inc., U.S.) was used for the measurement of particles with diameter between 3 and 23 nm; a differential mobility analyzer (DMA) and a CPC (Model 3010, TSI Inc., U.S.) for the particles with diameter ranges from 18 to 800 nm; and an aerodynamic particle sizer (APS, model 3321, TSI Inc., U.S.) for the measurement of particles between 800 nm and 10 µm. Additionally, PSD after removing the volatile species were measured in the size range from 3 to 800 nm. Particles were forced to pass through a thermodenuder (TD) which was heated up to 300 ˚C (Birmili et al., 2010) before being measured. A condensation particle counter (CPC, model 3025A, TSI Inc., U.S.) measured total number concentration (TNC) in the size range 3 nm to 3 µm.

Continuous measurements of $PM_{2.5}$, PM_{10} (particulate matter with diameter less than 2.5 µm and 10 µm, respectively), particulate sulfate, particulate nitrate, black carbon (BC) and polycyclic aromatic hydrocarbons (PAHs) were conducted at UAS location. Two independent Tapered Element Oscillating Microbalances (TEOM, model 1400ab, Thermo Fisher Scientific Inc., U.S.) were used to measure particle mass concentration of $PM_{2.5}$ and PM_{10}. To correct the loss of the volatile fractions of particulate mass, both TEOMs were equipped with a Filter Dynamics Measurement System (FDMS model 8500b, Thermo Fisher Scientific Inc., U.S.). Volatile, non-volatile and total mass concentrations of $PM_{2.5}$ and PM_{10} were obtained.

Particulate sulfate was measured using a Sulfate Particulate Monitor (SPA, model 5020, Thermo Fisher Scientific Inc., U.S.). Continuous nitrate measurement was conducted by an ambient particulate nitrate monitor (APNM, model 8400N, Thermo Fisher Scientific Inc., U.S.). Black carbon (BC) was measured with an Aethalometer (model series 8100, Thermo Fisher Scientific Inc., U.S.). Particulate PAHs were measured by Photoelectric Aerosol Sensor (PAS, model 2000, EcoChem analytics, U.S.). An electrical aerosol detector (EAD, model 3070A, TSI Inc., U.S.) measured total particle length concentration (LC) in the size range 10 nm to 1 µm. Length concentration is defined as the length of all particles from 1 cm^3 when lined up side by side on a chain. A Diffusion

Charging Particle Sensor (DCPS, model LQ1, Matter AG, Switzerland) measured the total active or Fuchs SC (ASC) of the particles in the size range of 10 nm to 1 µm. Meteorological parameters including temperature, relative humidity and radiation were measured at UAS site.

3.3 Measurements at Königsplatz (KP) site

This monitoring site is operated by LFU and it belongs to the official Bavarian network LÜB (Figure 3-3). Following parameters are measured there on a continuously basis: PM_{10} mass concentration measured by beta- attenuation (FH 62 C14 Series, Thermo Scientific., U.S.) and gaseous pollutants including NO, NO_2, CO and SO_2 measured by commercial gas monitors.

PM_{10} filter samples were collected at this site in winter 2006/07 (December-March) and winter 2007/08 (November-March). The samples were collected and analyzed for chemical composition including OC/EC, trace elements and water-soluble ions and particulate organic compounds (POC) by Dr. Jürgen Diemer, Dr. Jürgen Schnelle-Kreis and colleagues (LfU, 2009; Schnelle-Kreis et al., 2010). The samples were collected on quartz fiber filters (Whatmann) with a high volume sampler (HVS, DigitelDHA 80, Switzerland) at a flow rate of 500 L min^{-1} for 24 hours from 0:00 to 24:00 each day.

Figure 3-3: KP sampling site (left) and High volume sampler (HVS) (right).

Table 3-3 shows the measured particulate and gaseous pollutants at KP site. Elemental composition, water soluble ions, elemental carbon (EC) and organic carbon (OC), as well as the particulate organic compounds were analyzed using subsamples of the original quartz fiber filters. Elemental composition of PM_{10} was analyzed after decomposition of filter subsamples with nitric acid/ hydrogen peroxide using the closed vessel microwave procedure according to DIN EN 14902. Subsequently, As, Ca, Cd, Ce, Co, Cr, Cu, Fe, K, La, Mg, Mn, Ni, Pb, Sb, Ti, Tl and Zn were measured by inductively coupled plasma-mass spectrometry (ICP-MS) using Rhodium and Lutetium as internal standards. The concentrations of water-soluble ions in PM_{10} including Cl^-, SO_4^{2-}, NO_3^-, Na^+, K^+, Ca^{2+}, Mg^{2+} and NH_4^+ were analyzed by ion-chromatography (IC) after elution of a filter subsample by vigorous agitation with water and subsequent treatment in an ultrasonic bath. EC and OC were determined according to VDI 2465 by combustion of filter subsamples in an oxygen atmosphere and coulometric detection of the emerging carbon dioxide. POC were analyzed by direct thermal desorption (DTD) gas chromatography-time-of flight mass spectrometry (DTD-GC-MS) (Schnelle-Kreis et al., 2007; 2010) equipped with a newly implemented special derivatization method (MSTFA-silylation on filter with gaseous derivatization reagent supply in the carrier gas during the DTD step). Among all POCs only levoglucosan (LEV) was used to reveal the association between sources and wood combustion. LEV is a product of cellulose pyrolysis, and is considered as a molecular marker for biomass burning (Simoneit, 1999).

Table 3-3: Summary of measured particulate and gaseous pollutants at KP site

Parameters	Instruments	Winter 2006/07 [c]	Winter 2007/08
PM_{10}	beta attenuation	12.21.06-03.23.07	11.14.07-03.31.08
OC/ EC	Thermal combustion	12.21.06-03.23.07	11.14.07-03.31.08
Trace elements	ICP/MS [a]	12.21.06-03.23.07	11.14.07-03.31.08
Water-soluble ions	Ion-chromatography	12.21.06-03.23.07	11.14.07-03.31.08
Levoglucosan (LEV)	DTD-GC-MS [b]	02.14.07-03.20.07	11.14.07-03.31.08
CO;NO, NO_2; SO_2	gas monitors	12.21.06-03.23.07	11.14.07-03.31.08

[a] Inductively-coupled plasma mass spectrometry; [b] Direct thermal desorption (DTD) gas chromatography-time-of flight mass spectrometry. [c] Date format: mm.dd.yy.

Note that PM_{10} mass concentration and gaseous pollutants data (collected by LfU on a routine basis) were measured with a high time resolution (every minute), whereas the particulate chemical composition samples were 24 average samples. In the correlation analysis with factor contributions, PM_{10} and gaseous pollutants were averaged to 24-hour mean values.

3.4 Measurements at other monitoring stations

3.4.1 PM measurement for spatial variability study in 2008

Particulate matter was sampled by high volume samplers (HVS) at the following seven sites including BP, LO, LfU, Ho, We, Bi and Ki, between February 13 and March 12, 2008, in parallel to KP site. The sampling and chemical analyses were carried out by Dr. Jürgen, Diemer, Dr. Jürgen Schnelle-Kreis and colleagues (LfU 2009; Schnelle-Kreis et al., 2010). With data from the one-month intensive campaign, I carried out source apportionment of PCC data from eight sites, aimed to study the spatial variability of particulate sources.

Table 3-4 shows the data measured at the seven sites. Particulate chemical composition was analyzed using sub-samples of HVS filters. The analyzed chemical components include OC/EC, trace elements and water-soluble ions. PM_{10} mass concentrations were measured by beta-attenuation at BP, LfU, We, Bi and Ki. Gaseous pollutants were measured at some of the sites. Detailed analytical methods were described in section 3.3.

Table 3-4: Summary of available data at other sites in this study [a]

Sampling sites	Parameters	Start time	End time
BourgesPlatz (BP)	PM_{10}, HVS [b], NO, NO_2	02.13.2008	03.12.2008
Kriegshaber (LO) [c]	HVS	02.13.2008	03.12.2008
Bavaian Environment Agency (LfU)	PM_{10}, HVS	02.13.2008	03.12.2008
	T, RH, WS, WD, NO, NO_2, CO, SO_2, O_3	11.14.2007	03.31.2008
Hotel tower (Ho)	HVS	02.13.2008	03.12.2008
Wellenburg (We)	PM_{10}, HVS, NO, NO_2, SO_2, O_3	02.14.2008	03.12.2008
Bifa (Bi)	PM_{10}, HVS	02.13.2008	03.12.2008
Kissing (Ki) [d]	PM_{10}, HVS, NO, NO_2, SO_2, O_3	02.14.2008	03.12.2008

[a] Table modified from LfU (2009). [b] HVS: high volume sampler; Analyzed chemical components include trace elements As, Ca, Cd, Ce, Co, Cr, Cu, Fe, K, La, Mg, Mn, Ni, Pb, Sb, Ti, Tl and Zn; Water-soluble ions Cl^-, SO_4^{2-}, NO_3^-, Na^+, K^+, Ca^{2+}, Mg^{2+} and NH_4^+. [c] HVS instrument error at LO site between 02.17.2008 and 02.20.2008. [d] HVS instrument error at Ki site between 03.01.2008 and 03.05.2008.

3.4.2 Gaseous pollutants and meteorology at urban backgrounds sites

In studying the sources of PSD at UAS site, additional gaseous pollutants and meteorological parameters are needed to help identify the source types. However, there is no gaseous pollutant measured at UAS site. Among the air quality monitoring stations across Augsburg, BP and LfU are urban background stations operated by the Bavarian Environment Agency (LfU) measuring long term gaseous pollutants. Because UAS site is also an urban background site, the gaseous pollutants at BP and LfU may be used to represent the concentrations at UAS site. I made a correlation analysis (Table 3-5) and found that NO, NO_2 had good correlations between two urban background sites, LfU and BP, and between two traffic related sites, KP and Karlstraße (KS), respectively. As a result mean values of NO and NO_2 at LfU and BP were taken to represent the concentrations at UAS. CO was only measured at LfU site, thus CO at LfU was used. Wind speed (WS) and wind direction (WD) were measured at LfU to represent the

regional meteorology. Table 3-6 shows the gaseous pollutants and meteorology parameters from BP and/or LfU site, which are used to represent the concentrations at UAS site.

Table 3-5: Spearman correlations of NO and NO_2 at four monitoring stations in from January 1, 2007 to March 31, 2007

	NO_KP	NO_LfU	NO_BP	NO_KS
NO_KP	1			
NO_LfU	0.60	1		
NO_BP	0.68	0.79	1	
NO_KS	0.84	0.57	0.76	1

	NO_2_KP	NO_2_LfU	NO_2_BP	NO_2_KS
NO_2_KP	1			
NO_2_LfU	0.71	1		
NO_2_BP	0.78	0.92	1	
NO_2_KS	0.92	0.62	0.73	1

Table 3-6: Gaseous pollutants and wind measured at BP and/or LfU sites to represent concentrations at UAS site for interpreting the PSD sources

Species	Site	Winter 2006/07	Year 2007-2008
CO	LfU	12.21.2006-03.23.2007	03.14.2007-12.17.2008
NO, NO_2 [a]	mean of (BP and LfU)	12.21.2006-03.23.2007	03.14.2007-12.17.2008
WS, WD	LfU	12.21.2006-03.23.2007	03.14.2007-12.17.2008

[a] NO and NO_2 are the mean values of BP and LfU sites;

3.5 Overview of the analysis

Table 3-7 gives an overview of the analyses and the sampling sites where data were used. Not listed in the table is chapter 5 (an overview of source apportionment) and chapter 10 (personal measurement).

Table 3-7: Overview of analyses and the data used

	UAS	KP	BP, LfU	WE, Ho, LO, Bi, Ki
Analysis of the pollutants in winter seasons (Chapter 4)	×			
Source apportionment of PCC data (chapter 6)		×		
Source apportionment of PSD data (chapter 7)	×		×	
Comparison of the PCC and PSD sources (chapter 7)	×	×		
Spatial variability of PCC sources (chapter 8)		×	×	×
Cluster analysis of particulate parameters (chapter 9)	×			

4 General descriptions of the particulate pollution and meteorology in winter seasons in Augsburg

In general winter seasons were found to have higher particulate mass concentrations than summer seasons in many cities around the world (Marcazzan et al., 2001; Duan et al., 2006). Due to adverse meteorological conditions such as more frequent stagnant air condition and temperature inversion, particulate matter tends to accumulate and air pollution episodes are more likely to happen in winter. This is evidenced by the frequencies of exceedance of PM_{10} over EU limit in Augsburg in past winter seasons (59, 36 and 41 over the winters 2005/06, 2006/07 and 2007/08, respectively at an urban traffic site). In addition, residential heating was considered to have a big impact on air quality in winter.

The analysis in this chapter is presented as a general introduction to the air pollution conditions in winter seasons in Augsburg. I focused on the year to year variation and/or diurnal variation of meteorology and online particulate pollutants. The relationship between meteorology and air pollution levels was briefly discussed. Four winter seasons including winter 2004/05, winter 2005/06, winter 2006/07 and winter 2007/08 were studied.

4.1 Results and discussion

4.1.1 Meteorological parameters

Table 4-1 shows the descriptive statistics of meteorological parameters in four winters, winter 2004/05, winter 2005/06, winter 2006/07 and winter 2007/08. Average temperature ranged from 0.17 - 4.85 °C in the four winters. The highest average temperature was found in winter 2006/07 while the lowest temperature was in winter 2005/06. The relative humidity (RH) ranged from 81.1% - 87.5%. Average wind speed was in the range of 2.70 - 3.49 m s^{-1}, and average global radiation was in the range of 42.23 - 53.18 W m^{-2}. Overall, winter 2004/05 and 2005/06 showed lower temperature, higher RH, lower wind speed, and lower global radiation strength. It indicated that winter 2004/05 and 2005/06 were colder, moister, and cloudier compared with winter 2006/07 and 2007/08.

Table 4-1: Statistics of meteorological parameters in four winter seasons

	Winter	Mean	Median	95 percentile	5 percentile	stdev	Data coverage
T (°C)	2004/05	1.13	0.85	10.22	-6.96	5.12	1.00
	2005/06	0.17	-0.24	8.33	-6.52	4.53	1.00
	2006/07	4.85	5.28	10.07	-0.91	3.52	1.00
	2007/08	2.89	2.65	9.19	-3.43	4.03	1.00
RH (%)	2004/05	85.07	87.08	98.26	66.49	9.98	1.00
	2005/06	87.45	88.33	97.42	72.99	7.54	1.00
	2006/07	82.33	82.56	97.28	68.48	9.11	1.00
	2007/08	81.08	82.81	97.68	60.87	12.08	1.00
WS (m s^{-1}) [a]	2004/05	2.99	2.05	8.29	0.39	2.58	1.00
	2005/06	2.70	2.16	6.55	0.57	1.97	1.00
	2006/07	3.41	2.63	8.31	0.53	2.65	1.00
	2007/08	3.49	2.72	9.28	0.55	2.68	1.00
GR (W m^{-2})	2004/05	42.23	32.16	117.39	10.28	32.12	1.00
	2005/06	44.48	36.13	116.58	10.58	32.62	1.00
	2006/07	52.12	39.96	143.35	12.18	40.59	1.00
	2007/08	53.18	42.31	134.61	12.48	39.72	1.00

[a] Wind speed and wind direction were obtained from LfU site, other meteorological parameters were obtained from UAS site. The table was prepared based on daily average data. Winter season was defined from November to March.

Wind

Figure 4-1 shows the wind frequencies plotted with wind direction in four winter seasons. The wind speed and direction were measured at LfU site. The prevailing wind direction in winter in Augsburg was southwest (wind direction: 180 - 270°) and account for 47-59% of total wind frequencies. The northeasterly wind (wind direction: 0 - 90°) ranked the second abundant and accounted for 15-28% of total wind frequencies. As shown in Figure 4-1, the frequencies of northeast wind were significantly higher in winter 2005/06 (28%) than other winters (22%, 15%, and 21% for winter 2004/05, winter 2006/07 and winter 2007/08, respectively). In contrast, in winter 2006/07, higher southwest wind frequencies and lower northeast wind were observed. As shown in Table 4-1, average wind speed in winter 2006/07 and 2007/08 were higher than winter 2004/05 and 2005/06.

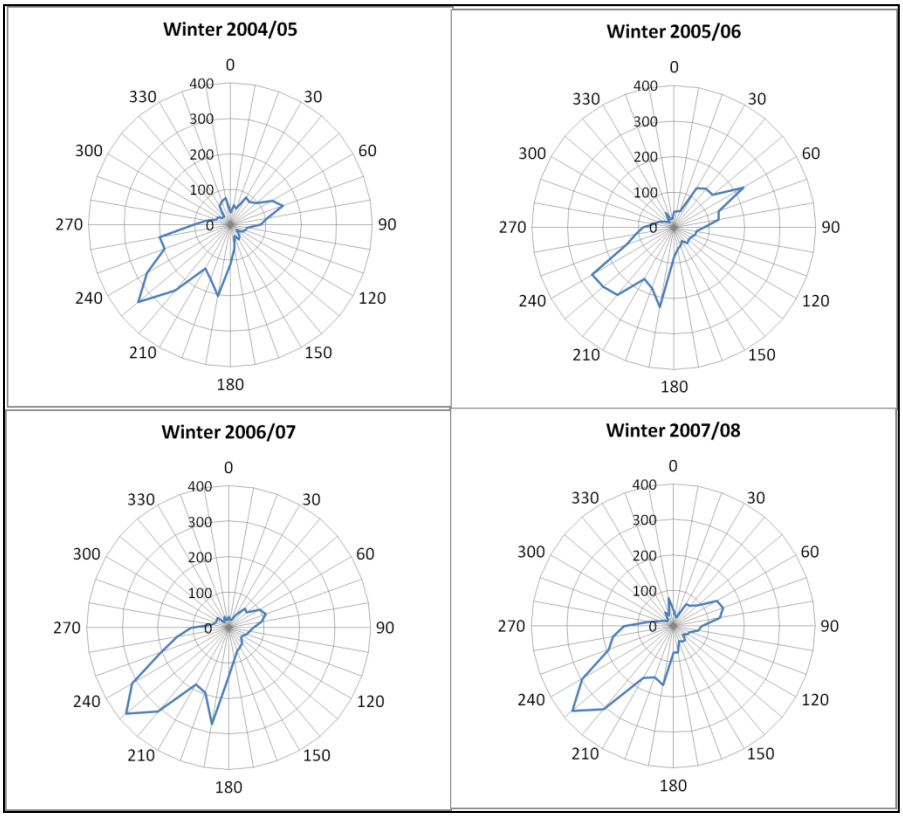

Figure 4-1: Wind frequencies plotted with wind direction in four winter seasons in Augsburg (hourly wind speed and wind direction measured at LfU site were used). There are 3624 data set in winter 2004/05, winter 2005/06, winter 2006/07; and 3648 data set in winter 2007/08.

Temperature

The box-plot of temperature is shown for each month in Figure 4-2. Winter 2006/07 was the warmest winter among the four winters, with an average temperature of 4.85 °C. The median temperature in each month in winter 2006/07 was above the four-winter average (red line shown in Figure 4-2). Winter 2005/06 was the coldest winter with an average of 0.17 °C. The coldest month of each year was not fixed, i.e., February in winter 2004/05, January in winter 2005/06, and December in winter 2006/07 and 2007/08.

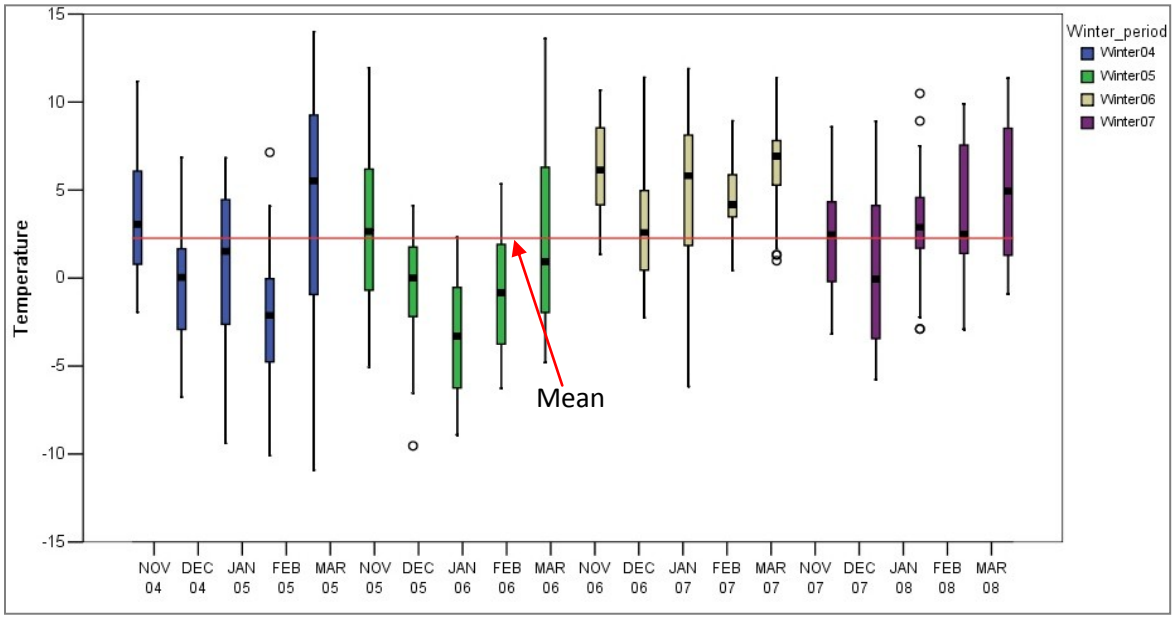

Figure 4-2: Box plot of daily temperature for each Month in four winters (red line represents the mean temperature of all winters).

It is found that the coldest winter (winter 2005/06) was accompanied with the highest northeast wind frequencies, while the warmest winter (winter 2006/07) was accompanied with the lowest northeast wind frequencies. Although direct causal relationship between northeast wind and average temperature cannot be obtained from the four years' data, it is probable that in certain degree the cold current from north led to the low temperature in winter 2005/06.

According to average temperature, relative humidity and radiation, the four winters can be roughly divided into two groups. Winter 2004/05 and 2005/06 are colder winters while winter 2006/07 and 2007/08 are warmer winters. Colder winters were associated with higher RH (85.07% and 87.45% vs. 82.33% and 81.08%) and lower global radiation (42.23 and 44.48 vs. 52.12 and 53.18 W m^{-2}), as well as lower wind speed (2.99 and 2.70 vs. 3.41 and 3.49 m s^{-1}). It indicated that colder winters were moister and cloudier compared with warmer winters.

4.1.2 Particulate pollutants

Table 4-2 shows a summary of particulate pollutants measured at UAS site in four winters. Mean $PM_{2.5}$ mass concentrations were in the range of 16.36 - 27.76 μg m^{-3}. Mean PM_{10} mass concentrations were in the range of 18.91 - 29.94 μg m^{-3}. Mean nitrate concentrations ranged from 2.90 to 5.31 μg m^{-3}. It was found that $PM_{2.5}$, PM_{10} and nitrate concentrations were well classified into two groups. One was the first two winters and the other was the second two winters. $PM_{2.5}$, PM_{10} and nitrate mean concentrations were significantly higher in colder winters (2004/05 and 2005/06) than in warmer winters (2006/07 and 2007/08). $PM_{2.5}$ and PM_{10} were decreased on average by 39% and 32% respectively in warmer winters. Sulfate also showed higher concentration in winter 2004/05 and 2005/06 than in winter 2007/08, however, data in winter 2006/07 was missing, thus making the trend plausible. The same plausible trend was found for BC, which had missing data in winter 2004/05.

Mean NC in four winters ranged from 14142-19632 cm^{-3}. Mean PAHs concentrations were in the range of 4.85-8.88 ng m^{-3}. Lower NC and PAHs concentrations were observed in winter 2007/08 than the other three winters. The winter-to-winter trend of NC and PAHs was different from $PM_{2.5}$, PM_{10} and nitrate. PM mass concentration consists of a large portion of secondary aerosol, which came from long range transport from distant areas, or considered as regional background (Viana et al., 2008a), and is sensitive to meteorological condition (e.g., wind, temperature and RH) (Ansari and Pandis, 1998). So I observed higher $PM_{2.5}$, PM_{10} and nitrate concentrations in cold

winters. NC and PAHs are mainly emitted from combustion process locally, thus shows a different year to year variation.

Table 4-2: Statistics of particulate pollutants in four winter seasons

Pollutants [a]	Winter	Mean	Median	95 percentile	5 percentile	stdev	Data coverage
$PM_{2.5}$	2004/05	26.28	23.05	55.59	8.84	14.87	1.00
	2005/06	27.76	22.04	63.68	5.67	22.08	0.99
	2006/07	16.36	14.81	36.55	2.79	11.77	0.99
	2007/08	16.62	12.71	44.87	1.07	14.12	1.00
PM_{10}	2004/05	29.94	27.22	63.12	9.49	16.51	0.79
	2005/06	26.77	21.03	61.85	4.64	22.61	0.99
	2006/07	18.91	15.32	43.18	2.57	14.00	0.99
	2007/08	19.67	15.86	49.59	2.39	15.33	1.00
NC (cm^{-3})	2004/05	17116	15778	35387	6966	8581	0.84
	2005/06	19632	18448	34002	9256	7951	1.00
	2006/07	18056	16287	35109	7016	8404	1.00
	2007/08	14142	12673	25563	6496	6127	1.00
BC	2004/05	-	-	-	-	-	0.25
	2005/06	2.62	2.18	5.16	0.88	1.73	0.99
	2006/07	1.73	1.46	4.23	0.52	1.21	0.94
	2007/08	1.82	1.39	4.70	0.54	1.33	0.99
Nitrate	2004/05	4.88	4.34	10.82	1.15	3.32	0.83
	2005/06	5.31	4.42	11.81	1.07	3.45	0.98
	2006/07	2.90	2.43	6.52	0.43	2.51	1.00
	2007/08	3.06	2.68	6.65	0.51	2.03	1.00
Sulfate	2004/05	4.35	3.54	10.96	0.99	3.20	0.83
	2005/06	3.16	2.54	7.68	0.71	2.30	0.99
	2006/07	-	-	-	-	-	0
	2007/08	1.87	1.00	6.48	0.15	2.12	1.00
PAHs	2004/05	8.88	7.15	22.12	3.65	5.80	0.85
($ng\ m^{-3}$)	2005/06	6.31	5.10	11.64	4.04	2.74	1.00
	2006/07	7.08	5.91	15.18	3.79	3.94	1.00
	2007/08	4.85	4.50	6.882	3.50	1.17	0.53

[a] Particulate pollutants are in $\mu g\ m^{-3}$ except NC in cm^{-3} and PAHs in $ng\ m^{-3}$.

4.1.3 Diurnal variation of particulate pollutants

Figure 4-3 shows the diurnal variation of NC, PAHs and BC in each winter on weekdays and in weekends, respectively. NC exhibited a major peak at 7:00-8:00 in the morning and a broader but weaker peak around 18:00 in the afternoon on weekdays. The morning peak is much pronounced than the afternoon peak. In weekends no morning peak was observed while an evening peak appeared at 18:00-21:00. Despite of the different NC levels in different winters, the four winters showed consistent diurnal variations.

PAHs showed a pronounced morning peak on weekdays except in winter 2007/08. An evening peak with the similar magnitude as morning peak was observed. In weekends, PAHs concentration was steady during the day time, and no increment in concentration was observed in the morning. High concentrations in the night were observed both on weekdays and weekends.

BC showed similar in diurnal variation as NC and PAHs. On weekdays BC also showed a double-peak diurnal variation, with a morning peak appeared at 8:00 and a night peak around 20:00. In weekends the morning peak was less pronounced or even disappeared, while the night peak existed.

PAHs are considered to be produced by the incomplete combustion of organic materials (Ravindra et al., 2008). It might be an indicator of domestic wood combustion for heating. However, the PAHs in the warmest winter (winter 2006/07) was higher than the coldest winter (winter 2005/06). Furthermore, the morning peak of PAHs was observed on weekdays while absent from weekends, which also indicated that vehicular emission might be the major source of PAHs.

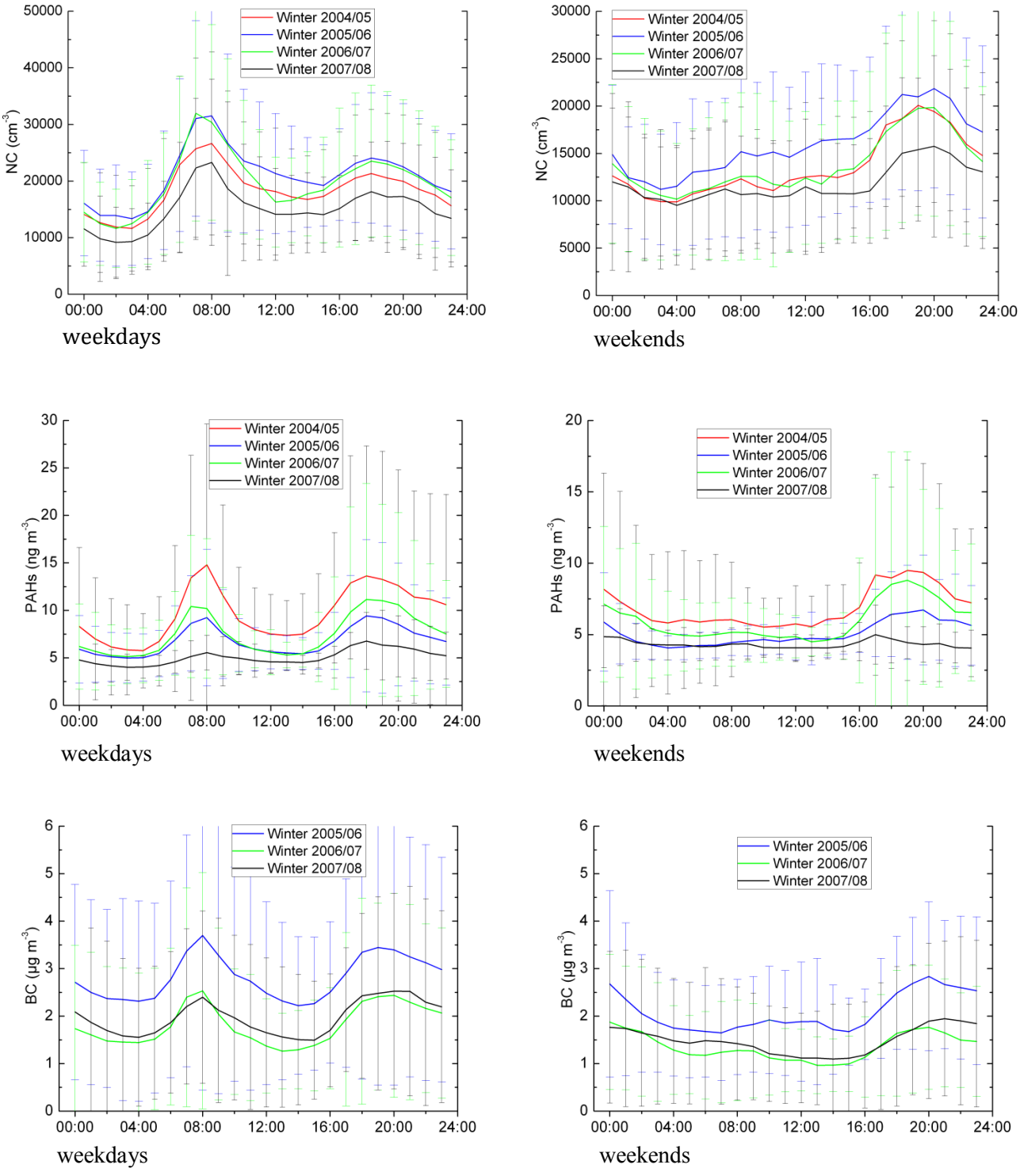

Figure 4-3: Diurnal variation of mean NC, PAHs and BC concentrations on weekdays (from Monday to Friday) and weekends (Saturday and Sunday) in four winters. The error bars are the standard deviation.

The morning peaks of NC, PAHs and BC were attributed to the vehicular emission. Firstly because the morning peaks were only observed on weekdays but absent in weekends. This is because traffic flow rate in weekends will be much smaller, so as the related vehicular emissions. Secondary, NC, PAHs and BC were found to be emitted from vehicles by many previous studies (Ravindra et al., 2006; Schneider et al., 2008; Aatmeeyata and Sharma, 2010; Klems et al., 2011). The morning peak was caused by the meteorology and emission together. In the early morning, atmospheric boundary layer is usually low and temperature inversion can often happen in winter to prevent the air pollutants from dispersion. Gaseous and particulate pollutants emitted from vehicles in morning rush hour greatly increased pollutant concentrations including NC, PAHs and BC. Under same winter condition but with much less vehicles on weekends, no morning peak can be observed. The evening peak, in contrast, occurred both on weekdays and weekends, which may be caused by meteorological conditions and emissions other than traffic like combustion sources.

Figure 4-4 shows the diurnal variation of $PM_{2.5}$ and PM_{10} on weekdays and in weekends. $PM_{2.5}$ exhibited weaker diurnal variation compared with NC, PAHs and BC. On weekdays, it had higher concentrations in the morning and in the night, but the peaks were much smaller. In weekends, the morning peak no longer existed and higher concentrations were observed in the night while lowest concentrations were in the afternoon. The diurnal variation of PM_{10} was similar with $PM_{2.5}$. One thing should be pointed out that in weekends in winter 2005/06, $PM_{2.5}$ and PM_{10} showed a small peak around midday, while for other winters, $PM_{2.5}$ and PM_{10} gradually decreased from early morning till afternoon.

The minor morning peak of $PM_{2.5}$ and PM_{10} on weekdays may be caused by the emissions from traffic. Because the traffic emission only accounted for a small portion of $PM_{2.5}$ and PM_{10} at urban background site, the morning peak was not significant as NC, PAHs and BC.

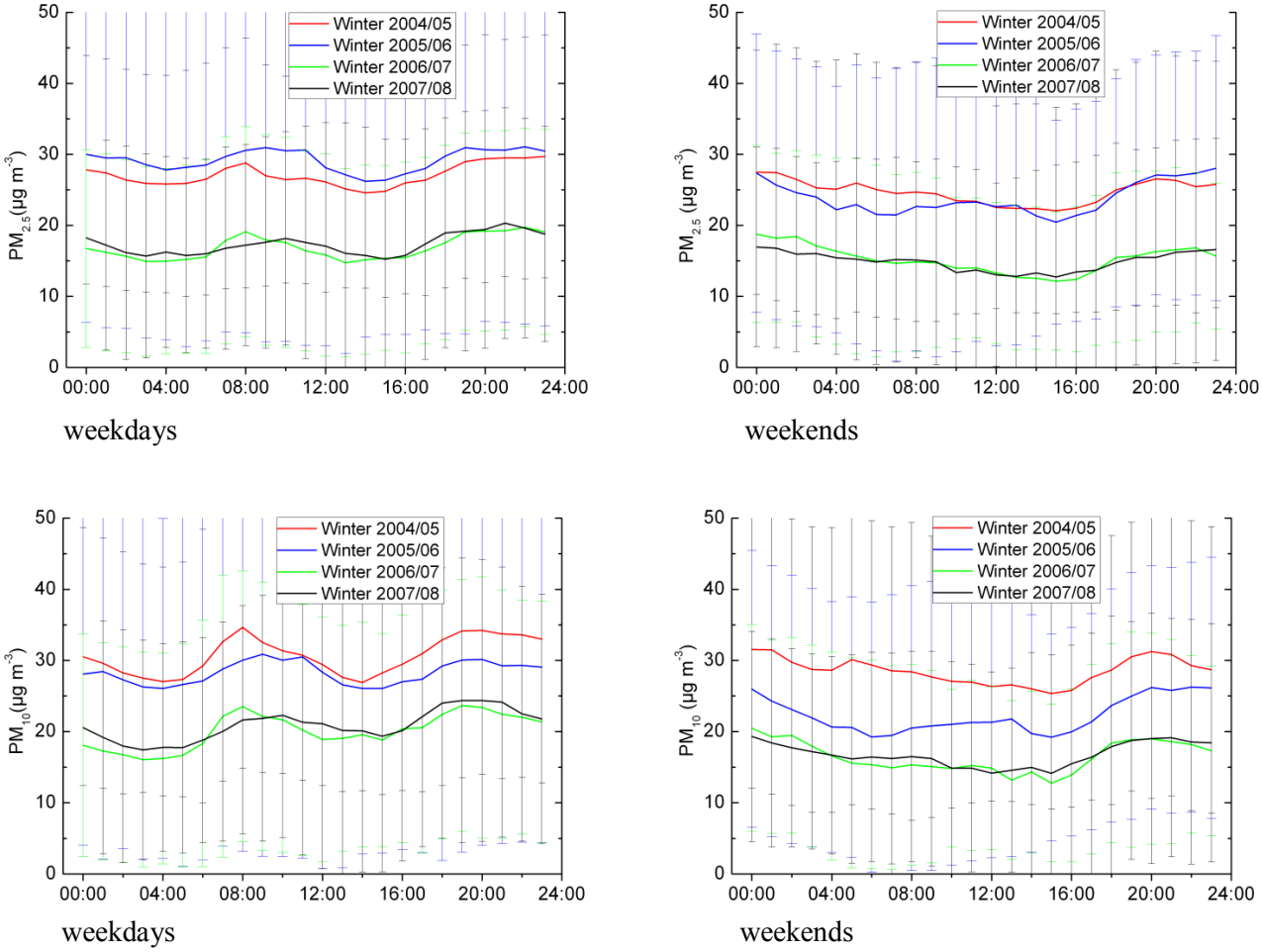

Figure 4-4: Diurnal variation of mean PM_{10} and $PM_{2.5}$ mass concentrations on weekdays (from Monday to Friday) and weekends (Saturday and Sunday) in four winters. The error bar is the standard deviation.

Figure 4-5 illustrates the diurnal variation of sulfate and nitrate on weekdays and in weekends. Sulfate was available in three winters except winter 2006/07. Weak diurnal variations were observed both for weekdays and weekends. Sulfate was formed in the atmosphere through the oxidation of SO_2, which is mainly emitted from power plants or other facilities utilizing coal as energy source. The conversion from SO_2 to sulfate was slow compared with gaseous photochemical reaction (O_3), thus sulfate was considered to mainly come from long range transported. Nitrate also displayed weak diurnal variation, but with a weak peak in the morning, followed by a decrease around midday, and the

lowest values were observed in the afternoon. Nitrate showed similar diurnal variations on weekdays and in weekends.

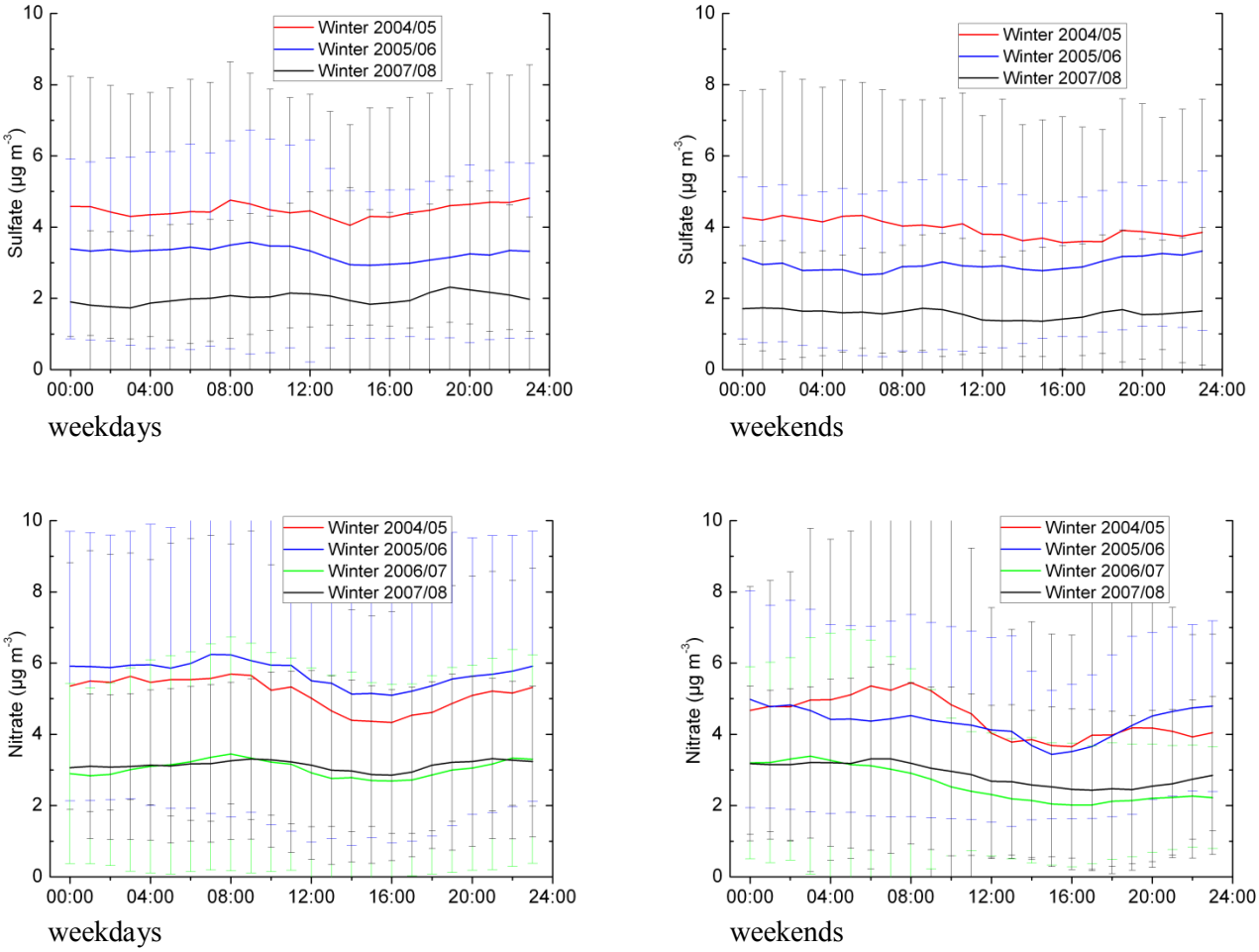

Figure 4-5: Diurnal variation of mean sulfate and nitrate mass concentrations on weekdays (from Monday to Friday) and weekends (Saturday and Sunday) in four winters. The error bar is the standard deviation.

4.2 Conclusions

According to the meteorology parameters, the four winters can be classified into two groups, the cold winters (2004/05 and 2005/06) and warm winters (2006/07 and 2007/08). Cold winters were associated with lower temperature, higher relative humidity and lower global radiation. Warm winters showed higher temperature, lower relative humidity and higher radiation.

$PM_{2.5}$ and PM_{10} mass concentrations, nitrate, sulfate and BC showed higher concentrations in cold winters, while lower concentrations were found in warm winters. NC and PAHs showed lower concentrations in winter 2007/08, which was different from the winter-to-winter trends of PM mass concentration and nitrate etc.

NC, PAHs and BC had different diurnal variations on weekdays and in weekends. Significant morning peaks were observed on weekdays indicating the great impact of vehicular emissions in morning rush hour. In weekends, when morning traffic flow rate was much less than on weekdays, no peak was observed in the morning. $PM_{2.5}$, PM_{10} and nitrate showed weak diurnal variations with high concentrations in the morning and in the night. Sulfate showed very weak diurnal variations. Apart from sulfate, all particulate pollutants showed high concentrations in the night, which may be caused partly by the meteorology and home heating combustions.

5 Source apportionment – an overview

Ambient particulate matter has been found to be associated with adverse health effects. While particulate matter is a complex mixture of components from a variety of sources, studies have been undertaken to better understand the relationship between source-specific PM and health effects. Detailed information on the sources is needed for policy makers of regulative purpose and for epidemiologists to study the health effect of source-specific particulate matter.

This chapter presents some theoretical background for better understanding of the conducted source apportionment analyses. The results of the numerous source apportionment analyses are presented in the following chapters 6 - 8.

At first I applied the source apportionment analysis using PMF method on PCC data obtained in winter 2006/07 and winter 2007/08 at a traffic monitoring site located at Königsplatz (KP) in Augsburg. By comparison of the results obtained from both winter seasons I could track the temporal changes of the source profiles of particulate matter in Augsburg. The trajectory cluster analysis was used to explore the origin and location of the sources. The results of this analysis are described in chapter 6.

Secondly, I conducted an additional analysis for the winter 2006/07 using PSD data obtained at the UAS site. The comparison of the results obtained by the two methods was already published (Gu et al., 2011) and is presented in chapter 7.

Finally, I studied the spatial variability of the sources of particulate matter during a one-month intensive campaign in 2008 at eight measurement sites across Augsburg (chapter 8).

5.1 Overview of source apportionment methods

One of the most important issues with regard to the air quality management is to apportioning the particulate matter to responsible sources. Source apportionment is the technique to resolve sources of particulates. There are two major groups of source apportionment models, dispersion model and receptor model. Dispersion model uses specific gas and particle emission inventories, coupled with meteorology, simulates the aerosol formation, transport and deposition, so as to calculate the concentrations at various locations (Holmes and Morawska, 2006). It requires detailed information on the emission inventory and is beyond the scope of the thesis.

Receptor model, by contrast, is a method of identifying sources based on the particulate concentrations at receptor site. The principle in receptor model is the mass conservation between emission sources and receptor site (or ambient conditions). It is assumed that the concentrations of particulate matter at receptor site are a linear combination of all responsible sources. The approach to solving the receptor model is mass balance analysis and can be expressed in

$$x_{ij} = \sum_{p=1}^{p} g_{ip} f_{pj}, \quad 5.1$$

where x_{ij} is the receptor concentration of jth species in ith sample, g_{ip} is the contribution of pth source to sample i, and f_{pj} is the concentration of jth species emitted by source p.

There exist many methods solving Equation 5.1. Depending on whether the source profiles (f_{pj}) are known, receptor models can be roughly divided into two groups (Hopke et al., 2006). When source profiles are known in prior, the only unknown in Equation 5.1 is g_{ip}, and the values can be estimated by regression analysis (Watson et al., 1984). This method, named chemical mass balance (CMB) (Watson et al., 1990), has been used in solving source apportionment problems when source profiles were known (Watson et al., 1994; Vega et al., 2000; Chen et al., 2010). However, in most cases, a full knowledge of source profiles (f_{pj}) cannot be obtained. In this case, another group of models, which is similar to factor analysis, is used to solve this kind of problem. It includes principal component analysis (PCA), positive matrix factorization (PMF) and Unmix etc. Among these models, PMF is a widely used method (Paatero and Tapper, 1994). Compared with

traditional method like PCA, PMF constrains the source profiles and source contributions to be non-negative and can weigh the data separately by granting respective uncertainties to them (Paatero, 1997; 1999). Such treatments can largely reduce the rotational ambiguity and make the results more physically realistic than previously used PCA. The detailed description of PMF is present in Section 5.2.

It should be noted that the sources obtained from receptor models (without prior factor profiles) are often called factors. Factors are not real sources but only represent real sources in certain degree, and also can be influenced by data error and atmospheric chemistry. The resolved factors need to be related to the real source types. However, here factor and sources are used interchangeably.

5.2 Positive matrix factorization method

PMF is a multivariate tool that decomposes a matrix of data sample into two sub-matrices, the factor profiles and factor contributions. It has been developed by Paatero (Paatero and Tapper, 1994; Paatero, 1997) and was used to resolve dominant positive factors on the basis of observation without detailed prior knowledge of the sources and source profiles. The method of PMF is shown in Equation 5.2,

$$X_{ij} = \sum_{k=1}^{p} g_{ik} f_{kj} + e_{ij}, \quad 5.2$$

where X is a matrix of i by j dimensions, in which i is the number of the sample and j is the number of measured species. f_{kj} is the concentration of the j^{th} species emitted from the k^{th} source; g_{ik} is the contribution of the k^{th} source to the i^{th} sample. e_{ij} is the residual, defined as the sum of differences between observed and modeled concentrations. Equation 5.2 is solved by finding out the minimum Q values, shown in Equation 5.3,

$$Q = \sum_{i=1}^{n} \sum_{j=1}^{m} \left[\frac{x_{ij} - \sum_{k=1}^{p} g_{ik} f_{kj}}{u_{ij}} \right]^2, \quad 5.3$$

where u_{ij} is the uncertainty of x_{ij}.

PMF aims to find a global minimum Q value. The factor profiles (F) and factor contribution (G) obtained at the minimum Q value are considered to represent the real

physical situation. Up till now, there have been several algorithms developed to solve the Q equation including Alternating Least Squares (ALS), PMF2, PMF3 and Multilinear Engine (ME).

ALS is developed in the very beginning to solve PMF problem. It supposes one of F or G is known and determine the other sub-matrix as a least square problem by minimizing Q value. Then the role of F and G reverses and the matrix calculated from last iteration is taken as known and the other matrix is calculated. The iteration continues until reaching convergence. The ALS algorithm can be slow (Hopke, 2000). PMF2 algorithm is improved by modifying the G and F matrix at the same time in each iteration step simultaneously. In each step the increment g and f to the preceding resolved G and F are determined by the minimum Q with respect to g and f (Paatero, 1997).

PMF2 and PMF3 were designated to solve bilinear and trilinear problem. Paatero (1999) developed an algorithm named Multilinear Engine to solve more flexible problems. ME algorithm performs the iteration using the conjugate gradient algorithm to reach the convergence, when the decrease in Q values reach a criteria, say, 0.01.

The U.S. EPA PMF 3.0 software was developed based on the second version of ME algorithm, ME-2 (http://www.epa.gov/heasd/products/pmf/pmf.html, accessed in January, 2009). It has a public license and is freely available. The US EPA PMF 3.0 incorporates the Graphical User Interface (GUI) and contains some data pre-analysis tools, as well as F-peak and bootstrap functions etc.

There are some comparisons between source apportionment using PMF2 and ME-2. Both methods generated similar results, however, the uncertainty in PMF2 was found larger than ME-2 (Ramadan et al., 2003).

5.3 Source apportionment of PCC data

With regard to the application of PMF analyses to particulate matter, a great many studies have been conducted. Most of these applications were based on particulate chemical composition (PCC) data.

Table 5-1 and Table 5-2 give a selected review of source apportionment analyses, which focuses on the resolved factors at different types of monitoring sites.

As shown in Table 5-1, four source apportionment studies conducted in rural areas are presented, and they generally found that secondary aerosols, particularly secondary sulfate factor, were the major components in $PM_{2.5}$ mass concentration. Secondary sulfate factor can account for 40%-62.6% of $PM_{2.5}$. One exception is at a remote site in mid-west of Canada (Jeong et al., 2008), where the wood burning and winter heating were dominant sources, which accounted for 31% and 26% of the $PM_{2.5}$ mass concentration. It also showed that sulfate was more abundant than nitrate at rural sites. Traffic emission factors were not important at rural areas. It was even not resolved in rural sites in New York state (Liu et al., 2003). The contributions of traffic to $PM_{2.5}$ were between 2.5% and 13% in other studies.

In coast areas secondary aerosols were the major PM sources, accounting for a big part of $PM_{2.5}$ mass. Vegetative burning and vehicular emissions have also been found as the major source in some cases. Lee et al. (1999) characterized 10 factors in Hong Kong and were associated with secondary sulfate, chloride depleted marine aerosols, marine aerosols, crustal emission, vehicular emission, nonferrous metal smelter, particulate copper and fuel oil burning. Kim et al. (2010) found 8 factors in coast area in California including secondary sulfate, secondary nitrate, gasoline powered vehicles, diesel powered vehicles, biomass burning, soil, sea salt, aged sea salt. Similarly, fuel oil combustion and sea salt (and/or aged sea salt) have been found by Amato et al. (2009) in Barcelona and by Maykut et al. (2003) in Seattle. Fuel oil combustion factor was typically characterized by Vanadium (V) and Nickel (Ni), which were associated with the emission from oil combustion from ships at coastal cities. Sea salt was characterized by Na and Cl, while aged sea salt was characterized by Na but less Cl. Chloride was depleted by HNO_3 acid through the reaction $NaCl + HNO_3 \rightarrow NaNO_3 + HCl$.

Table 5-1: Overview of selected source apportionment analyses using PMF in rural and coast sites

References	Location	Major factors	PM	Time period	Methods
Rural sites					
(Kim et al., 2007)	Ohio	secondary sulfate (62.6%); secondary organic (19.9%); secondary nitrate (6.5%); steel production (3.1%); traffic (2.5%)	$PM_{2.5}$	04.2004 - 11.2005	PMF2
(Jeong et al., 2008)	British Colombia	wood burning (31%) ; winter heating (26%); wood processing (13%); traffic (13%); sulfate (9%); crustal (8%)	$PM_{2.5}$	11.2004 - 08.2006	PMF2
(Liu et al., 2003)	Potsdam, NY	secondary sulfate (56%); soil (14.6%); nitrate (9.2%); wood smoke (8.8%)	$PM_{2.5}$	Summer 2000, 2001	PMF2
(Liu et al., 2003)	Stockton, NY	secondary sulfate (56.2%); soil (23.9%); Cu smelter (11.6%)	$PM_{2.5}$	Summer 2000, 2001	PMF2
(Kim et al., 2005a)	Illinois	secondary sulfate (40%); secondary nitrate (32%); gasoline vehicles (9%)	$PM_{2.5}$	03.2001- 05.2003	PMF2
Coast sites					
(Lee et al., 1999)	Hong Kong	secondary sulfate (37.8%); aged marine aerosol (14.3%); marine aerosol (6.9%); soil dust (6.1%)	PM_{10}	1992-1994	PMF2
(Kim et al., 2010) *	Los Angeles	secondary sulfate (30%); secondary nitrate (24.6%); diesel emission (10.4%); biomass burning (10.2%); soil (10.2%)	$PM_{2.5}$	2003-2005	PMF2 & EPA PMF
(Kim et al., 2010) *	Rubidoux, CA	secondary nitrate (49.8%); gasoline vehicles (10%); secondary sulfate (9.2%); soil (6.5%)	$PM_{2.5}$	2003-2005	PMF2 & EPA PMF
(Amato et al., 2009)*	Barcelona	mineral (31%); vehicles (18%); secondary nitrate (15%); aged sea salt (11%); secondary sulfate (10%); brake ware (10%)	PM_{10}	2003-2007	PMF & ME2
(Amato et al., 2009)*	Barcelona	vehicles (25%); secondary sulfate (25%); secondary nitrate (20%); mineral (14%)	$PM_{2.5}$	2003-2007	PMF & ME2
(Amato et al., 2009)*	Barcelona	secondary sulfate (33%); vehicles (30%); secondary nitrate (20%); fuel oil combustion (7%)	PM_1	2003-2007	PMF & ME2
(Maykut et al., 2003)	Seattle	vegetative burning (28%), diesel (18%); secondary sulfate (18%); soil (14%); fuel oil combustion (10%)	$PM_{2.5}$	1996-1999	PMF2

* Both PMF2 and ME2 were used and results from PMF2 were presented.

Table 5-2: Overview of selected source apportionment analyses using PMF at urban sites, traffic sites, and industrial sites

References	Location	Major factors	PM	Time period	Methods
Urban sites					
(Baumann et al., 2008)	Birmingham	secondary sulfate (35.2%); vehicles (24.6%); Secondary organics (11.9%); road dust (5.9%); secondary nitrate (4.4%)	$PM_{2.5}$	2002-2004	EPA PMF
(Brown et al., 2007)	Phoenix	Motor vehicles (26%); dust (25%); power generation (13%); diesel	$PM_{2.5}$	2001-2003	EPA PMF
(Heo et al., 2009)	Seoul	Secondary nitrate (20.9%); secondary sulfate (20.5%); gasoline vehicles (17.2%); biomass burning (12.1%); diesel (8.8%)	$PM_{2.5}$	03.2003-12.2006	PMF2
(Martello et al., 2008)	Pittsburgh	Secondary sulfate (47.4%); secondary semi-volatile mass (19.0%); diesel (10.4%); gasoline (8.0%); wood smoke (4.0%);	$PM_{2.5}$	10.1999-09.2001	PMF2
Traffic sites					
(Mooibroek et al., 2011)	Rotterdam	secondary nitrate (41%); secondary sulfate (20%); vehicles (21%); industry (9%)	$PM_{2.5}$	08.2007-09.2008	EPA PMF
(Furusjo et al., 2007)	street, Stockholm	long range transport (26%); vehicles (36%); re-suspension (23%); regional combustion (14%)	PM_{10}	2003-2004	PMF2
(Furusjo et al., 2007)	highway, Stockholm	long range transport (34%); vehicles (13%); re-suspension (23%); regional combustion (19%)	PM_{10}	2003-2004	PMF2

Table 5-2 (continued): Overview of selected source apportionment analyses using PMF at urban sites, traffic sites, and industrial sites

Industrial sites					
(Viana et al., 2008b)	Spain	regional sulfate (25%); regional marine (23%); clay (16%); industry (16%); vehicles (10%)	PM_{10}	2002-2005	PMF2
(Alleman et al., 2010)	France	crustal dust (11%); marine aerosols (12%); petro-chemistry (9.2%); metallurgical sintering plant (8.6%); metallurgical coke (12.6%); ferromanganese (6.6%); road transport (15%)	PM_{10}	06.2003-03.2005	PMF2
(Lim et al., 2010)	Korea	secondary aerosol (20%); cement/construction (20%); soil dust (16%); road dust (12%);	PM_{10}	04.2000-21.2002	PMF2

At urban sites, secondary aerosols (sulfate and/or nitrate) have been found as the major sources to PM mass concentration. Compared with the rural sites, traffic related sources had much higher contributions to PM mass. Brown et al. (2007) observed vehicular sources (motor vehicles & diesel) accounted for 35% of $PM_{2.5}$ in Phoenix in a traffic influenced urban site. Contributions of vehicular sources to $PM_{2.5}$ by 24.6%, 26%, and 18.4% were reported by Baumann et al. (2008), Heo et al. (2009) and Martello et al. (2008), respectively.

Traffic sites are those sites very close to roads, or locate at the road sides, which are influenced greatly by vehicles. Furusjo et al. (2007) studied sources of PM_{10} at two traffic sites, a city center road site and a highway site in Norway. Traffic related sources (vehicles+ re-suspension) accounted for 59% and 36% of PM_{10} mass concentration at city center road site and highway site, respectively. Although Mooibroek et al. (2011) reported vehicular sources accounting for 21% of $PM_{2.5}$ in Rotterdam, similar with those found in urban sites, this fraction is much higher than at an urban background site in Rotterdam (9%).

Table 5-2 also shows the source apportionment of PM at industrial sites using PMF method. Viana et al. (2008b) reported two industry related sources: clay and industrial sources in an industrial site in Castello, Spain. Together they contributed to 16% of PM_{10} mass concentration. A cement/construction source was found in an industrial area in South Korea and accounted for 20% of PM_{10} (Lim et al., 2010). Alleman et al. (2010) resolved four industry related sources in an industrial area in France. In another study in a coastal industrial urban area in southern Texas, which is not shown in Table 5-2, one industrial emission factor was characterized and contributed to 6% of $PM_{2.5}$ mass concentration (Karnae and John, 2011). It seems that the number of industrial factors, as well as their contributions to PM mass concentrations varies greatly from one site to another. It is assumed that industrial types (and emitted elements), as well as the emission strength can explain the different results in different studies.

In addition to chemical composition data, methods that can deal with different kinds of data have also been attempted. Kim et al. (2004a) and Jeong et al. (2008) included the temperature resolved carbon fractions to improve the source identification. Particulate

composition with high time resolution is easier to obtain due to more widely use of continuous measurement devices. In order to take full advantage of the high resolution data, Zhou et al. (2004a) and Pere-Trepat et al. (2007) incorporated multiple time resolution aerosol composition data (with time resolution ranges from 30 minutes to 24 hours) in PMF. Chemical composition data combined with particle size distribution in PMF analysis has also been reported, and will be discussed in the following.

Normally PMF utilize the inherent non-negative constrains, studies have been taken to apply extra constrains on PMF to reduce rotational ambiguity and for better source separation. Kim et al. (2003b) incorporated the time resolved wind parameter into Multilinear Engine (ME2) model. Lately Amato and Hopke (2012) added extra constrains on ME2 in order to improve the model performance on multi-sites data.

How to choose the right number of factors? As stated by Paatero (2007), there seems no mathematical criteria that is able to predict the "true" number of factors. In fact, there may exist no "correct" number of factors. The question becomes rather to find out the most useful or meaningful method. Lee et al. (1999) and Heo et al. (2009) showed the increase of the rotational uncertainties at a critical number of factors and indicated the increase can be used as a indicator of the best number of factors. However, this approach hasn't been widely accepted. Most of the papers select the number of factors with most plausible meanings.

PMF has been extensively used to characterize particulate sources (Kim et al., 2003a; Song et al., 2006; Kim and Hopke, 2008; Amato et al., 2009). In spite of this, such applications are limited in Germany (Quass et al., 2004; Schnelle-Kreis et al., 2007). The study location is Augsburg, a median sized city in southern Germany. The numbers of exceedance of EU PM_{10} standard in Augsburg (monitoring site: Königsplatz) were 59, 36 and 41 over the past winters 2005/06, 2006/07 and 2007/08, respectively. As estimated by the government of Swabia (RVS, 2009) for the year 2005 (PM_{10}: 37 µg m^{-3}), the regional aerosols accounted for a part of 55% in PM_{10} in Augsburg. The contribution of the urban background to PM_{10} was 22%, and the local traffic contributed 24% to the PM_{10}. Schnelle-Kreis et al. (2007) resolved five sources of organic compounds using positive matrix factorization (PMF) based on concentrations of semi-volatile organic

compounds (SVOC) in $PM_{2.5}$. They found strong seasonality for combustion related sources with highest values in winter. Despite of these studies, more information on the PM sources is needed, especially in winter when higher PM levels occur.

5.4 Source apportionment of PSD data

Unlike particulate chemical composition, particle size distribution was far less applied to multivariate models. This is partly because the measurement of PSD is relatively complicate and the instrument is expensive. Furthermore, particle numbers are mainly dominated by ultrafine particles (< 100 nm) and they have a short life time due to nucleation and coagulation. The fundamental assumption of mass conservation between sources and receptor site in multivariate models that worked for mass based chemical composition data, faces some challenges when applied to number based particle size distribution data.

In early factor analysis of PSD data (Wahlin et al., 2001; Zhou et al., 2004b; Kim et al., 2004b), it was assumed that the after the dynamic processes right after the sources, the particle number concentrations dropped, and in a proper distance from the sources the condensation, coagulation and deposition processes slow down. The particle size distribution becomes relatively stable and a quasi-stationary profile can be assumed. Thereafter, principal component analysis (PCA) and PMF have been applied to PSD data, assuming a linear combination of the impact of sources at the receptor site.

Table 5-3 gives a summary of source apportionment analyses (with FA, PCA or PMF methods) using PSD data. Among all the studies listed in Table 5-3, two were carried out at traffic sites in London (Charron and Harrison, 2003; Harrison et al., 2011), while the others were conducted at (traffic influenced) urban or urban background sites. The measurement site types matter much, due to the dynamic physical processes from vehicular tail pipe emission to downwind of road, and to urban background site. The particle size as well as particle number and composition will change dramatically from source to receptor site. Because of this, a few factors obtained from road site PSD source apportionment were difficult to attribute (Harrison et al., 2011). Indoor source

apportionment using PSD data carried out by Ogulei et al. (2006a) resolved nine sources, of which seven were related to indoor activities (cooking, candle burning and vacuuming etc.) while only two factors were associated with outdoor sources: the traffic emission and wood smoke.

Some factors were repeatedly resolved in source apportionment analyses using PSD data. Nucleation particles/diesel emission factor typically had the number size distribution peaked below or around 10 nm, thus only studies measuring particles of diameter at about 10 nm or smaller can resolve this factor. Wahlin et al. (2001) found this factor related to traffic but not correlated with the general diurnal pattern of traffic. Similar factors have been reported by Zhou et al. (2004b), Ogulei et al. (2007a; 2007b) and Costabile et al. (2009). In above studies, this factor was attributed to fresh tail pipe emission from diesel or nucleation particles.

Traffic emission factors have been identified in all listed studies. Generally, two or more traffic factors were resolved, depending on the study location. Indeed, traffic is considered as the main source of particle number concentration. A two-traffic factor result has been commonly reported and was characterized as local traffic and remote traffic, or as diesel vehicles and motor vehicles. The two traffic factors differed in size mode. Local traffic factor consists of smaller particles in Aitken mode, while remote traffic was in larger size ranges. Kim et al. (2004b) characterized a diesel emission factor and a motor vehicle factor in Seattle. Zhou et al. (2004b) reported two traffic related factors with one peaked at 15 nm and the other peaked at 40 nm. Two traffic factors have been also reported by some other studies (Ogulei et al., 2007a; Yue et al., 2008). In traffic site and traffic influenced site, more traffic related factors have been identified (Ogulei et al., 2007b; Harrison et al., 2011).

The mineral dust /airborne soil factor generally consists of super-micron particles and thus only studies measuring PSD above 1 μm were able to characterize this factor. Yue et al. (2008) attributed a coarse particle factor to airborne soil. Harrison et al., (2011) resolved three coarse particle factors which were associated with brake dust, re-suspension of vehicles, and a nighttime local source.

Secondary aerosols were typically in the accumulation mode between 0.1 and 1 μm. The secondary aerosol factor has been reported by most of the studies list in Table 5-3.

Industrial related sources were rarely reported from source apportionment analyses using PSD data only. This is because the lack of tracer in PSD data for industrial sources. As shown in the lower part of Table 5-3, a combination of PCC and PSD could resolve industrial related factor. In Table 5-3, four studies used a combination of PCC and PSD data as PMF input. Zhou et al. (2005) combined particle number size distribution (33 size bins), 13 chemical composition and 5 gaseous pollutants with a time resolution of 30 minutes in PMF and obtained 11 factors. The inclusion of particle size distribution and gaseous pollutants aided the separation of certain factors. The secondary sulfate factor and coal-fired power plant emission, both dominated by chemical composition sulfate, were separated due to different size distribution and dominant gaseous pollutants. In addition, two nitrate factors were separated and peaked at 0.08 μm and 0.01 μm, respectively. Other factors, however, were identified primarily with either chemical composition data, including diesel traffic, lead, steel mill, coke plant, secondary sulfate and secondary nitrate factors, or with particle size distribution data including nucleation particles, local traffic emission and remote traffic emission. Ogulei et al. (2006b) combined high time resolution (1 hour) particle number size distribution, chemical composition and gaseous pollutants in PMF similarly with Zhou et al. (2005), and identified factors mainly based on chemical composition. A long term application of combined chemical composition and particle volume size distribution data to PMF was carried out by Larson et al. (2006) for a period of 3.5 years. In this study, the volume size distribution data were down weighted for a factor of 10 to reduce their importance relative to chemical composition data. Likewise, most of the factors were determined by chemical composition.

It appears that combining PCC and PSD (and/or gaseous pollutants) in PMF obtain relatively more factors (11, 12 and 11 from above three studies) than using PSD data only. However, in what extent the combination of PCC and PSD improves the source separation is not certain, as most of the factors from combined PCC and PSD method have been identified by other studies using either PCC or PSD data alone.

As UFP dominate the particle number concentration, the approach based on PSD data provides insight into the sources of very small particles which may be inadequately addressed by source apportionment based on PCC data. Source profiles based on PSD provide the source information from the physical aspect, which differs from the chemical aspect of PCC method. There is an urgent need to know the consistency or discrepancy of sources obtained from PCC and PSD data, respectively. However, currently there is only few paper published on the relationship of the source apportionment results from the two kinds of data set. Zhou et al. (2005) found linear associations of three latent variables between PCC and PSD. In spite of this, it is still not clear whether the two data sets can give comparable results or not if run separately by a multivariate model. Because the time and effort of the analytical determination of PCC is much higher than the measurement of PSD with online methods, it is particularly important for long-term studies to know the differences or consistencies between both methods.

Table 5-3: Literature review of source apportionment of PSD data

Reference	Data	Model	Study time period	Size range	Site type	Location	factors
(Wahlin et al., 2001)	PSD	FA*	winter/spring, 1999	6–700 nm	urban	Denmark	3
(Charron and Harrison, 2003)	PSD	PCA	07.1998 - 08.2001	11–452 nm	Traffic	London	4
(Kim et al., 2004b)	PSD	PMF2	12.2000 - 02.2001	20–400 nm	Urban	Seattle	4
(Zhou et al., 2004b)	PSD	PMF2	30.06.2001 - 04.08.2001	3 nm–2.5 µm	Urban background	Pittsburgh	5
(Ogulei et al., 2006a)	PSD	PMF2	11.1999 - 03.2000	10 nm – 20 µm	indoor	Reston, VA	9
(Ogulei et al., 2007b)	PSD	PMF2	23 - 24, June, 2004	6 – 500 nm	5 sites, downwind of roads	Buffalo	7
(Yue et al., 2008)	PSD	PMF2	09.1997 - 08.2001	10 nm – 2.8 µm	Urban background	Erfurt	5
(Costabile et al., 2009)	PSD	PCA	2005 - 2006	3 - 800 nm	8 sites	Leipzig	6-14
(Ogulei et al., 2007a)	PSD & gas	PMF2	12.2004 - 11.2005	11 - 470 nm	Suburban & traffic	Rochester	7-9
(Thimmaiah et al., 2009)	PSD & gas	PMF2	7 - 23 Jan, 2008	19 - 720 nm	Urban background	Prague	4
(Harrison et al., 2011) **	PSD & gas	PMF2	19.10 – 08.11, 2007	15 nm- 10 µm	Traffic	London	10
(Zhou et al., 2005)	PSD & PCC	PMF2	16 - 24 July, 2001	3 nm – 2.5 µm	Urban background	Pittsburgh	11
(Ogulei et al., 2006b)	PSD & PCC	PMF2	6 days in summer 2002	9.6 nm – 2.5 µm	traffic influenced urban	Baltimore	12
(Larson et al., 2006)	PSD & PCC	ME2	02.2000 - 06.2003	20 nm - 5 µm	Urban background	Seattle	11
(Pey et al., 2009) ***	PSD & PCC	PCA	11.2003 – 12.2004	13 - 800 nm	Traffic influenced urban	Barcelona	7

*FA: factor analysis; ** in addition to PSD and gaseous pollutants, meteorology parameters and traffic density and speed related information were also included; ***PSD data were summarized in 6 groups.

6 Source apportionment of PCC data

Ambient particulate matter (PM) has been found to be associated with adverse health effects by many studies. While PM is a complex mixture of components from a variety of sources, and every component is not equally important in terms of causing adverse health effects. Studies have been undertaken to better understand the relationship between source-specific PM and health effects. Detailed information on the PM sources is needed for policy makers of regulative purpose and for epidemiologists to study the health effect of source-specific PM.

In this chapter, particulate sources in winter 2006/07 from source apportionment analysis based on PCC data were presented. Trajectory cluster analysis was employed to indicate the possible source locations. In addition, sources of PCC data in winter 2007/08 was obtained and a comparison was made between both winter seasons, so as to track the temporal changes of the source structure in Augsburg.

6.1 Methods

6.1.1 Data treatment (winter 2006/07)

The available particulate composition include As, Ca, Cd, Ce, Co, Cr, Cu, Fe, K, La, Mg, Mn, Ni, Pb, Sb, Ti, Tl, Zn (trace elements); Cl^-, SO_4^{2-}, NO_3^-, Na^+, K^+, Ca^{2+}, Mg^{2+}, NH_4^+ (Water-soluble ions), OC, EC and PM_{10}. A summary of particulate chemical composition is shown in Table 6-1.

Table 6-1: Summary of measured particulate species concentrations in winter 2006/07 (ng m^{-3})

Species	mean	median	min	max	S/N[a]	<LOQ[b]	(%)
Ca	822	726	201	1793	3.31	13	14
Cd	0.19	0.15	0.02	0.65	7.51	0	0
Ce	0.39	0.35	0.1	1.18	6.35	0	0
Co	0.23	0.19	0.1	1.34	1.79	25	26.9
Cr	9.4	8.6	3.1	22.8	2.39	9	9.7
Cu	43.9	39.2	10.9	124.4	6.80	0	0
Fe	1261	1112	183	3675	8.57	0	0
K	238	183	54	2112	3.58	2	2.2
La	0.18	0.16	0.04	0.61	4.52	0	0
Mg	187	162	50	491	3.08	6	6.5
Mn	15.7	13.6	2.8	38.5	9.30	0	0
Ni	3.9	3.4	1.2	9.5	3.13	12	12.9
Pb	8.8	7.9	3.2	27	2.21	20	21.5
Sb	6	5.2	1.3	14.8	8.28	0	0
Ti	4	3.4	1	12	3.40	0	0
Zn	47.4	33.1	11.1	401.7	3.90	3	3.2
Cl^-	811	446	129	5043	6.15	15	16.1
NO_3^-	5453	4259	208	28020	8.03	0	0
SO_4^{2-}	2263	1929	362	6926	7.61	0	0
Na^+	613	412	71	2969	2.15	34	36.6
NH_4^+	2131	1692	25	10173	7.71	5	5.4
EC	4359	3763	1617	11154	10.07	0	0
OC	3499	2964	1313	10363	9.62	0	0
PM_{10}	31775	26646	8708	93229	11.33	0	0

[a] S/N, ratio of signal to noise; [b] <LOQ, number of samples below the Limit of Quantification; n=93 samples.

I excluded two species, thallium (Tl) and arsenic (As) from the analysis. Tl has very low data coverage and signal to noise ratio. Though As shows pronounced temporal variations, it has high concentration on February 21, 2007, a unique temporal variation and was found in a separate factor in a set of trail model runs. As a factor mainly composed of arsenic was not considered as an important source for PM_{10} in Augsburg, this element was not included in the model either. Some elements were measured by IC

and ICP-MS. I chose only the data from ICP-MS, because IC represented water-soluble fraction and the non water-soluble part e.g. from crustal particles could be underestimated. Data lower than the Limit of Quantification (LOQ) were replaced by half of the LOQ and their uncertainties were set to five-sixths of the LOQ (Polissar et al., 1998). Missing data were replaced by the mean value of the respective species and their uncertainties were set to 3 times of the mean value. The uncertainties for the other values were calculated according to Equation 6.1(Norris et al., 2008),

$$u = [(Error\ Fraction \times concentration)^2 + LOQ^2]^{0.5}, \quad 6.1$$

where error fraction is the percentage of uncertainty. They are estimated from sampling error and analytical errors. The errors for trace elements are about 2/3 of water soluble ions and they are assumed 8% for trace elements (from ICP/MS) and 12% for water soluble ions (from IC).

Five samples were excluded in this work, in which two were excluded for potassium high spikes due to the New Year's celebrating fire works on Dec 31, 2006 and January 1, 2007, and the other two were for zinc with an increase of 10 times to the vicinity on December 25 and 28, 2006, and the last one for titanium on January 24, 2007. They may come from the occasional emissions or analytical errors and the model cannot simulate these events. As a result, 88 daily samples were used in the analysis.

A variety of source numbers were tested. First, all species were set to strong. Later in the analysis certain species were re-characterized as "weak" by tripling the uncertainties if the signal to noise is too low to provide enough variability. The six factor method, with the Q value of 950, provided the most physical meaningful results.

The comparison of modeled and measured species showed that PMF is able to well reproduce measured values. For modeled and measured PM_{10}, the regression slope is 0.96 with r^2=0.99. In EPA PMF, bootstrap is a solution to test the stability and uncertainty of the method. It is performed by creating a new data set with the same dimensions by randomly selecting non-overlapping blocks of samples. Each factor from bootstrap is then compared with base run factor. If the correlation between bootstrap factor and base run factor is above a threshold (r^2, usually choose 0.6), then the factor is treated as mapped, otherwise, unmapped. A 100-bootstrap was run for six factor method. Of the

100 bootstraps, factor 5 had seven bootstraps unmapped. However, the main species of this factor remains the same. Factor 6 had one bootstrap unmapped while the remaining four factors had all the bootstrap runs mapped. Hence the six factor method provided a stable result.

6.1.2 Backward trajectory cluster analysis

1) Method introduction

Trajectory is defined as the path that a moving object follows through space as a function of time. The forward trajectory is the path that the object reaches the designated position from the original position. The backward trajectory is the path history before the object reaching the designated position. The backward trajectory is often used in atmospheric environmental researches to determine the path of the air parcel before reaching the studied location.

I used the Hybrid Single-Particle Lagrangian Integrated Trajectory (HYSPLIT) model (version 4.8, http://ready.arl.noaa.gov/HYSPLIT_hytrial.php) to compute the simple parcel trajectories. The HYSPLIT was jointly developed by US National Oceanic and Atmospheric Administration (NOAA) and Australia's Bureau of Meteorology. For the calculation of trajectory, it utilizes a Lagrangian approach which uses a moving frame of air parcel as it moves from its initial position (Draxler and Hess, 1997). Both forward and backward trajectories can be calculated by the model.

To identify the possible source locations, especially for long range transported sources, I carried out the cluster analysis of backward trajectories. The Trajectory cluster analysis tool integrated in the NOAA-HYSPLIT model was used. Initially it assumes that each trajectory is a cluster and for k trajectories there are k clusters. In the first iteration two clusters are paired and the model calculates the cluster spatial variance (SPVAR) for all possible clustering methods. SPAVR is the sum of the squared distances between the endpoints of the cluster's component trajectories and cluster-mean (Draxler et al., 2009). Here the endpoints are a series of points that comprising the trajectory.

$$SPVAR = \sum_{j=1}^{m} \sum_{i=1}^{n} D \times D, \quad 6.2$$

where D is the distance between a trajectory endpoint and the corresponding cluster-mean endpoint. n is the number of trajectory endpoints. m is the number of trajectory numbers contained in a cluster. i is the i^{th} endpoint in j^{th} trajectory in a cluster.

The sum of total cluster spatial variance (TSV) is calculated by summarizing SPVAR values for all clusters (Draxler et al., 2009).

$$TSV = \sum_{p=1}^{k} SPVAR, \quad 6.3$$

where p is the p^{th} cluster of all k clusters.

In each step two clusters are combined as one and the pair of clusters combined is the clustering with the lowest increase in TSV. The iteration continues until reaching one cluster. For cluster analysis of k trajectories, there will be $k-1$ iterations.

2) Backward trajectories reaching Augsburg

I made the backward trajectory analysis in winter 2006/07 and winter 2007/08, respectively, the same time period as the sampling period carried out at KP site. I chose the Global Data Assimilation System (GDAS) meteorological archives as the input meteorology. It was computed by National Weather Service's National Centers for Environmental Prediction (NCEP) (Kanamitsu, 1989). The meteorological archives are freely available on NOAA website. The backward trajectories were calculated daily in the past 72 hours before reaching Augsburg at 13:00 local time. The trajectory height was set to 300 meters above ground when arriving at Augsburg. In total 93 trajectories were obtained in winter 2006/07 and 138 trajectories were obtained in winter 2007/08.

3) Trajectory cluster analysis

I made the cluster analysis of trajectories in winter 2006/07 and winter 2007/08, respectively. The “Change in TSV” figure (Figure 6-1) is used to determine the possible number of clusters. Normally TSV will increase with the decrease of the number clusters, however, when similar trajectories are combined into the same cluster, the TSV will

increase slowly, or occasionally decrease. A sharp increase in TSV usually indicates that different clusters have been merged. Thus number before the sharp TSV increase indicates the possible number of clusters (Draxler et al., 2009). In this figure, four clusters have been chosen.

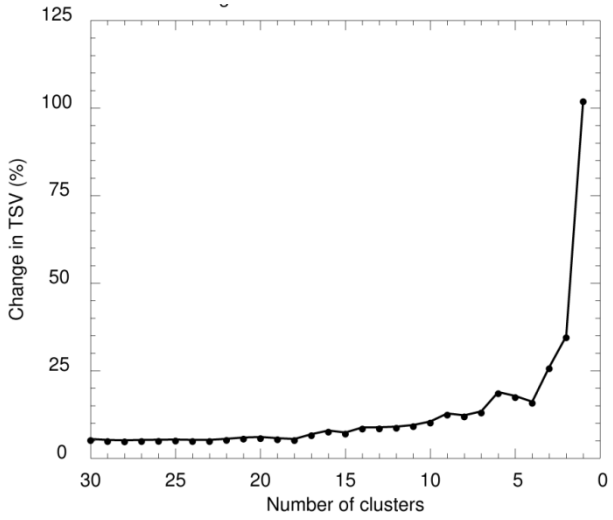

Figure 6-1: An example of the changes of TSV (%) when trajectory clusters are combined.

6.2 Results and discussion

6.2.1 Source apportionment of PCC data in winter 2006/07

6.2.1.1 Temporal variation and chemical composition of PM_{10} in winter 2006/07

In winter 2006/07 between December 21, 2006 and March 23, 2007, the temperature was on average 3.4 °C (-7.2 - 10.9 °C) and the mean relative humidity was 80% (59% - 95%), indicating humid and cold weather conditions. An average wind speed of 3.9 m s^{-1} (0.3 - 15.2 m s^{-1}) was observed. The average daily PM_{10} concentration measured at KP site during study period was 32 µg m^{-3} (9 - 93 µg m^{-3}). There were 15 days with PM_{10} values exceeding the daily EU PM_{10} limit (50 µg m^{-3}).

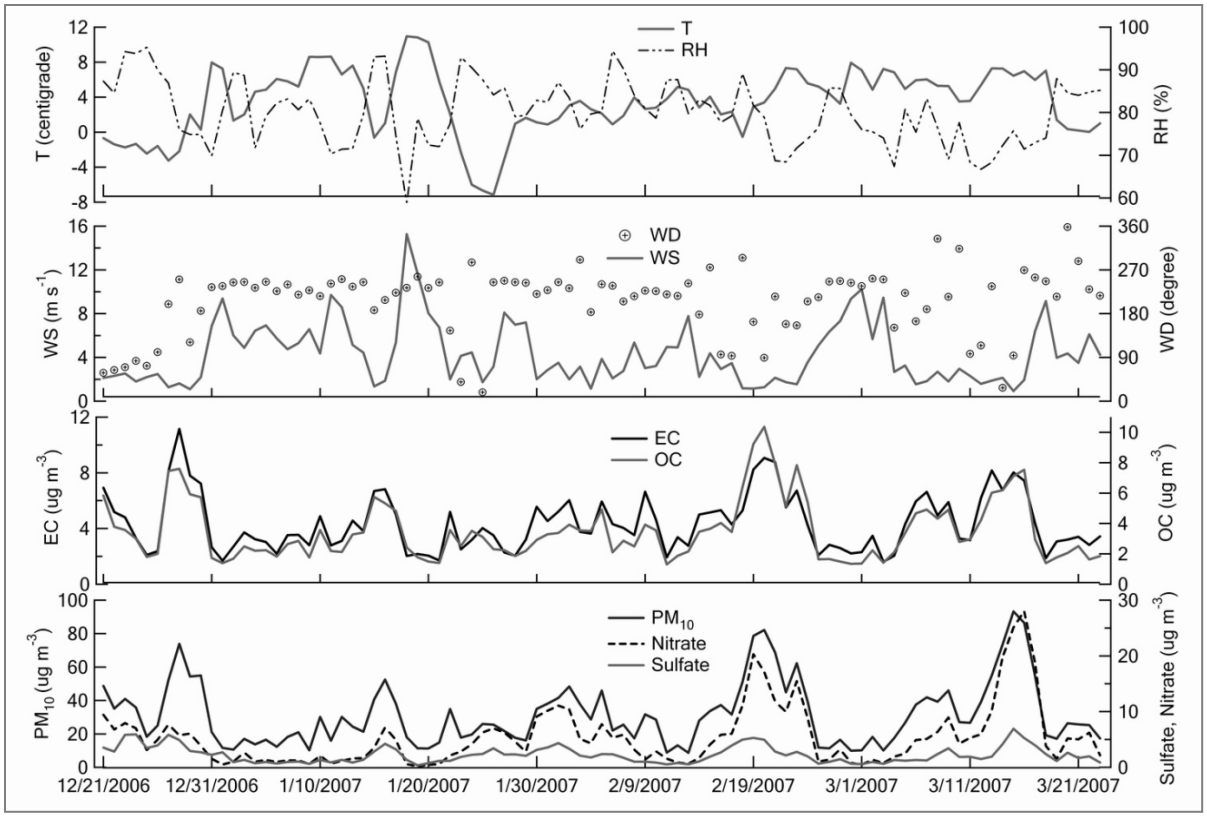

Figure 6-2: Temporal variations of PM_{10}, nitrate, sulfate, EC, OC and meteorology in winter 2006/07. The meteorological parameters (T, RH, WD and WS) were obtained at LfU site.

As shown in Figure 6-2, three visible PM_{10} episodes were observed: around December 28, 2006, February 20, 2007 and March 15, 2007, respectively. Daily PM_{10} value could reach over 80 μg m^{-3} in the episodes. The temporal variations of EC and OC were very similar with each other, and their major peaks were in coincidence with PM_{10}. Nitrate and sulfate showed similar temporal variations with PM_{10} except in the first episode around December 28, 2006, when only limited increase was observed for nitrate and sulfate compared with EC and OC, indicating this episode was mainly caused by local traffic or combustion sources. Meteorology played an important role in the PM_{10} concentration levels, as shown in Figure 6-2, PM_{10} mass concentration was negatively associated with the wind speed.

Figure 6-3 shows the mass contribution of major chemical components to PM_{10}. Water soluble inorganic species including sulfate, nitrate and ammonium altogether accounted for 31% of PM_{10}. Nitrate concentration was 2.4 times of sulfate. The value is much higher than the ratio observed by Quass et al. (2004) in Duisburg, Germany in one year period (nitrate/sulfate=1.1). The high nitrate/sulfate ratio is probably caused by the elevated nitrate concentrations in cold season (Park et al., 2005). EC and OM contributed 13% and 15% to PM_{10}, respectively. EC accounted for 46% of TC (EC+OM), which is comparable to the results from Leipzig in winter seasons between 1999 and 2002 (Spindler et al., 2004). Trace metals contributed to 8% of the PM_{10} mass concentration.

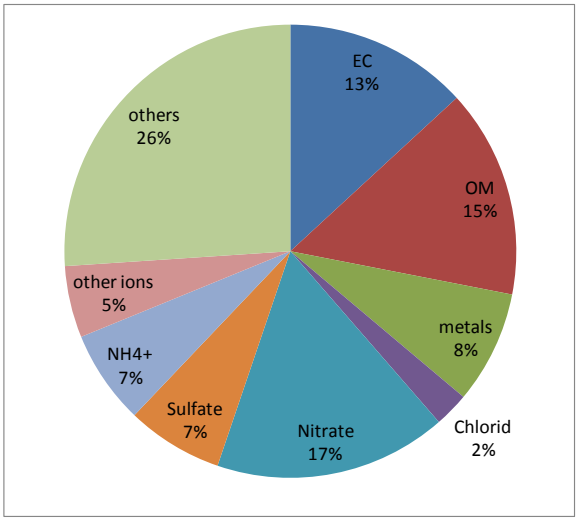

Figure 6-3: Mass contributions of chemical components to PM_{10} in winter 2006/07 (OM is calculated as 1.4×OC).

6.2.1.2 Factor characterization of PCC data (KP) in winter 2006/07

PMF was applied to PCC data in winter 2006/07 and six factors have been characterized. They are associated with NaCl, secondary sulfate, residential and commercial combustion, secondary nitrate, traffic emissions and re-suspended dust. Figure 6-4 illustrates the factor profiles by concentrations (g g^{-1}) and percentage of species mass (%). Percentage of species mass (%) is the concentration contained in one factor divided by total concentration of the species. The temporal variation for each factor can be seen in Figure 6-5. Table 6-2 shows the factor mass contributions to PM_{10}, as well as spearman correlation coefficients between factors and gaseous pollutants and levoglucosan (LEV).

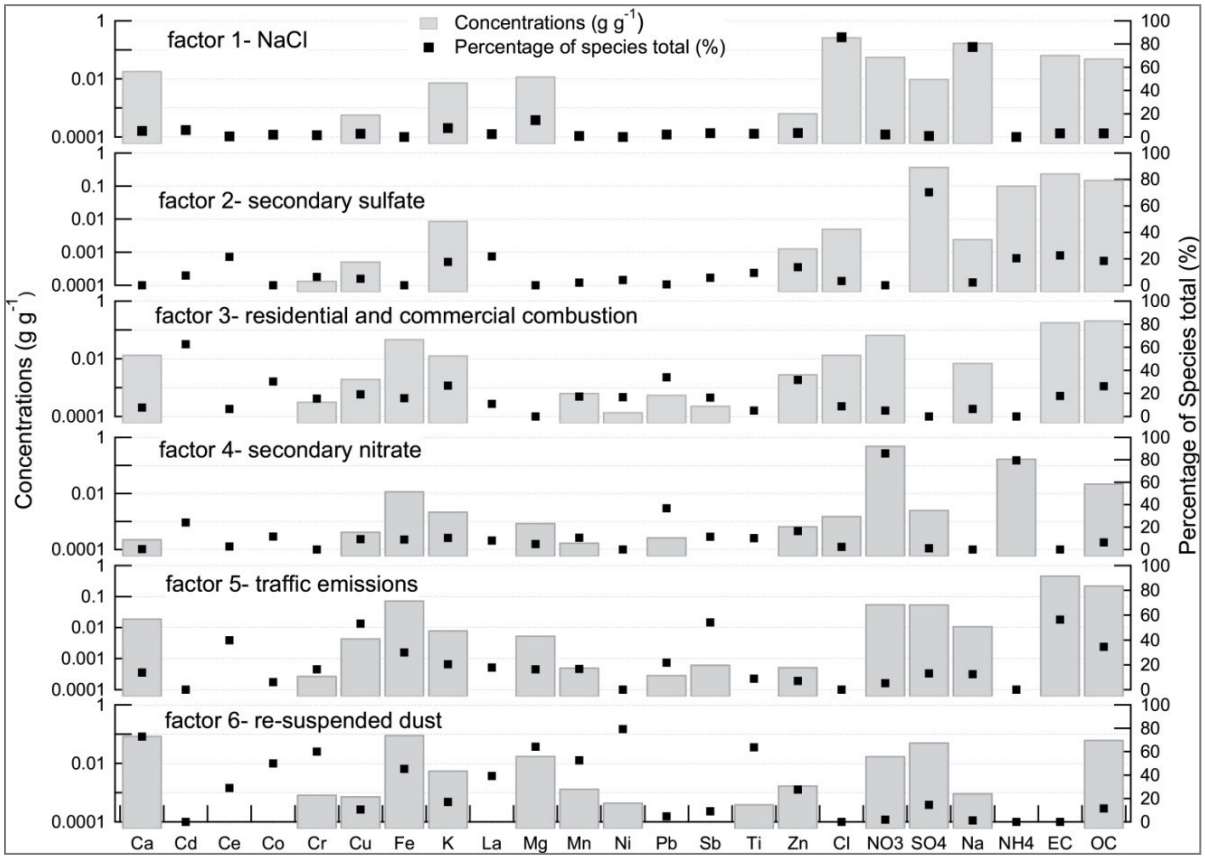

Figure 6-4: PMF factor profiles from chemical composition data in winter 2006/07.

Table 6-2: Spearman correlation coefficients between daily factor contributions and daily means of gaseous pollutants, LEV and PM_{10}, as well as factor mass contribution to PM_{10}

Species	N	NaCl	sulfate	combustion	nitrate	traffic	dust
NO	91	0.01	0.17	0.65	0.45	0.75	0.46
NO_2	91	0.10	0.24	0.65	0.60	0.75	0.52
CO	91	0.13	0.31	0.36	0.64	0.52	0.24
SO_2	91	0.02	0.47	0.39	0.62	0.22	0.29
LEV	35	-0.13	0.53	0.76	0.84	0.55	0.53
PM_{10}	91	0.04	0.56	0.61	0.80	0.53	0.52
Contribution to PM_{10} mass concentration (%)							
	-	6.7	13.0	13.3	30.5	16.5	20.0

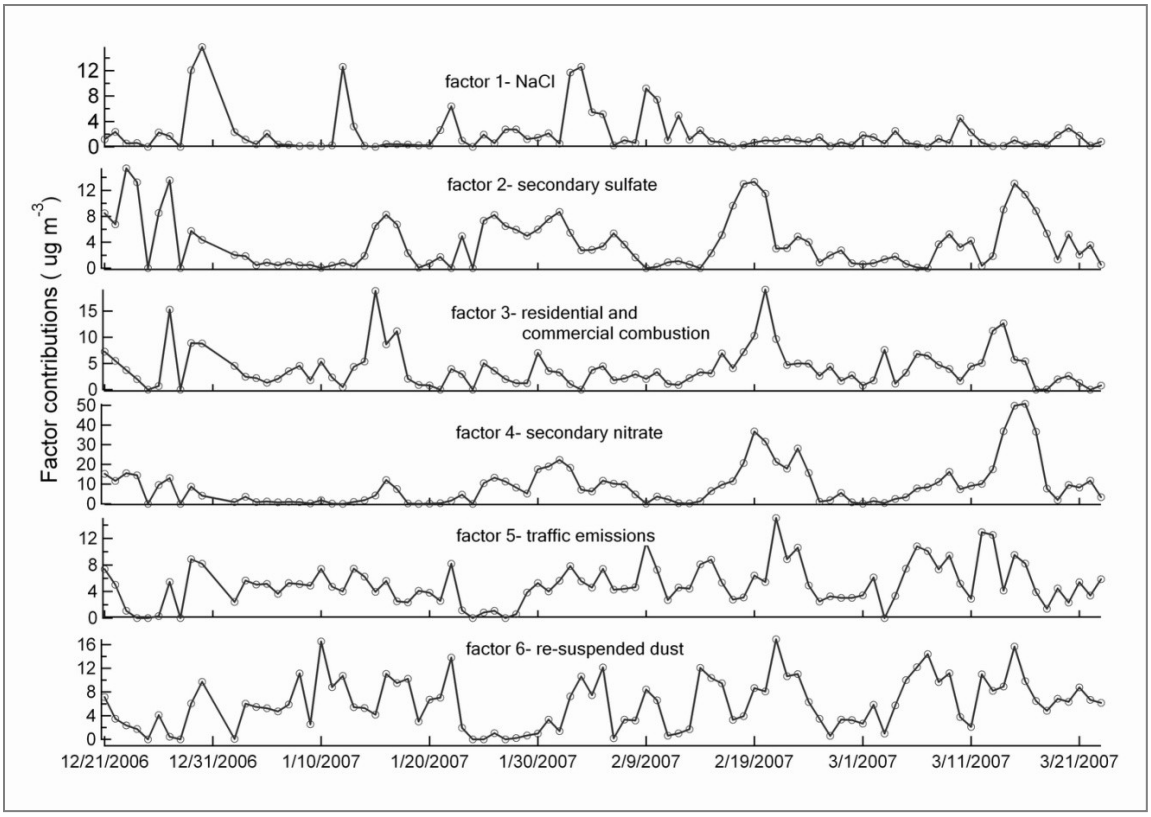

Figure 6-5: Daily factor contributions in winter 2006/07.

Factor 1- NaCl

Factor 1 was characterized by high concentrations of Na^+ and Cl^- (Figure 6-4), and could explain 77% of Na^+ and 86% of Cl^-. It contributed on average 6.7% (2.1 µg m^{-3}) to PM_{10} mass concentration (Table 6-2). As can be seen in Table 6-2, this factor was weakly correlated with gaseous pollutants and PM_{10}. A molar ratio of 0.99 was observed for Na^+ to Cl^-, which indicated the salt was fresh emitted. Some incidences with high NaCl loadings were observed. On December 29 and 30, 2006 NaCl was extraordinarily increased and was associated with low temperatures, low wind speeds and showers of sleet. It is probably because of the de-icing agents used in the vicinity of the measurement site. Under some conditions, elevated NaCl concentrations were also observed when air masses came from the Atlantic and we could not exclude the possibility of the sea salt impacting on receptor site under favorable meteorology.

Factor 2- Secondary sulfate

Factor 2 was dominated by SO_4^{2-}. It also contained high concentrations of EC (22.5%), OC (18.4%) and NH_4^+ (20.5%). It was considered as secondary sulfate and contributed on average 13% (4.1 μg m^{-3}) to PM_{10}. The apportioned molar ratio of SO_4^{2-} to NH_4^+ is 1.45, lower than 2, indicating that the sulfate may not be fully neutralized by NH_4^+. However, the lower SO_4^{2-} to NH_4^+ ratio may also be caused by model uncertainty. As shown in Table 6-2, secondary sulfate factor was weakly correlated with gaseous pollutants and the strongest correlation was observed for SO_2 (r=0.47). This factor was most likely from long range transport. The temporal variation frequency of this factor was low and low concentrations have lasted for several days, as well as high concentrations.

Factor 3- Residential and commercial combustion

Factor 3 was characterized by OC and EC. The factor contributed on average 13.5% (4.2 μg m^{-3}) to PM_{10}. It was highly correlated with particulate levoglucosan (r=0.76), an organic tracer for biomass burning. Although the correlation coefficient was lower compared with factor 4, secondary nitrate (r=0.84), based on the factor profiles, factor 3 was considered to represent residential and commercial combustion, especially wood combustion. However, K was found evenly distributed in several factors. This result differs from what had been found using levoglucosan and K as tracers of wood combustion, which assumed almost all K was emitted from wood combustion (Schnelle-Kreis et al., 2010). A sensitivity analysis of K was then carried out to see the cause of the difference, and could be found in appendix A, from which concluded that due to the low signal/noise (S/N) ratio, the importance of K as an inorganic biomass burning tracer was weakened in the PMF analysis. This factor, therefore, is considered not only influenced by biomass burning, but also partly by other combustion sources, like residential and commercial combustion. High loading of Cd (62.6 %) was observed in this factor. Previous studies showed that wood combustion is also a significant source for Cd (Narodoslawsky and Obernberger, 1996; Hansen et al., 2001).

Factor 4- Secondary nitrate

Factor 4 was characterized by high concentrations of nitrate and ammonium and was considered as secondary nitrate. It contributed 30.4% to PM_{10}. A molar ratio of 1.17 was observed between apportioned NH_4^+ and NO_3^-. The value is a little higher than 1, which may be caused partly by mixture of sulfate and chloride and partly by model uncertainty.

Factor 5- Traffic emission

This factor was characterized by EC, OC, Cu, Sb, Ce and Fe et al. (Figure 6-4), and can explain 56%, 34%, 53%, 54%, 40% and 30% of the above species, respectively. Factor 5 contributed 16.6% to PM_{10} and correlated well with NO and NO_2, both markers of traffic emissions. This factor had dominant contributing sources from vehicular tail pipe emission and brake ware. The tail pipe emission was characterized by EC and OC. In this work the concentration and fraction of EC were higher than OC, which is likely due to the wide use of diesel-powered vehicles. Diesel-powered vehicles are quite popular in Germany because of lower fuel costs in comparison to gasoline-powered vehicles. Diesel-powered vehicles accounted for 28% of registered cars in January 2009 in Bavaria, Germany (KBA, 2009). Brake ware was characterized by Cu and Sb. Cu and Sb were commonly used in vehicle brake linings and were considered as inorganic tracers for brake ware (Weckwerth, 2001; Westerlund, 2001; Iijima et al., 2007). The presence of Cu and Sb in this factor was due to the fact that the monitoring site is located next to busy streets, as well as several traffic lights where vehicles start and stop constantly, and the braking processes always take place. As a result, elements such as Cu and Sb were released to the air mixed with the tail pipe emission.

Factor 6- Re-suspended dust

Factor 6 was considered as re-suspended dust, a combination of natural dust and road dust and contributed 20% to PM_{10}. It contained high concentrations of Ca, Mg and Fe, which are mainly of crustal origin. Besides, high contents of trace elements such as Ni, Mn, Cr, Ti and Co were also observed in this factor. These elements and a part of Fe were believed to come from tram lines.

The sampling site is located next to tram lines and close to the city central public transportation station, known as Königsplatz, where all the trams running in city Augsburg will pass through. Metals including Fe, Cr, Ni and Mn are components of steel, were likely to come from the frictions between the tram wheels and rails or the pantograph and the catenary. These particles, usually in the coarse particle mode, can be re-suspended into the air by passing vehicles. A study in Cologne, Germany also demonstrated that the rails had a high potential of metal emissions (Weckwerth, 2001). These particles, usually in the coarse particle mode, will be re-suspended into the air by passing vehicles. As a result, road dust was mixed with natural dust in the factor.

6.2.1.3 Trajectory cluster of PMF factors in winter 2006/07

Figure 6-6 shows the mean trajectory clusters in winter 2006/07. Four clusters were obtained. Cluster 1 was composed of air masses originating from eastern regions, and most of the trajectories in this cluster came from Austria and Czech Republic. Cluster 2 contained trajectories coming from western regions, and many of which were originated from Germany and Switzerland. These two clusters were composed of short trajectories, indicating a stagnant atmospheric condition. Cluster 3 represented air coming from southwest continental areas in France, passing through Switzerland or southern Germany. Cluster 4 mainly came from the Atlantic Ocean and passing through France and/or Switzerland.

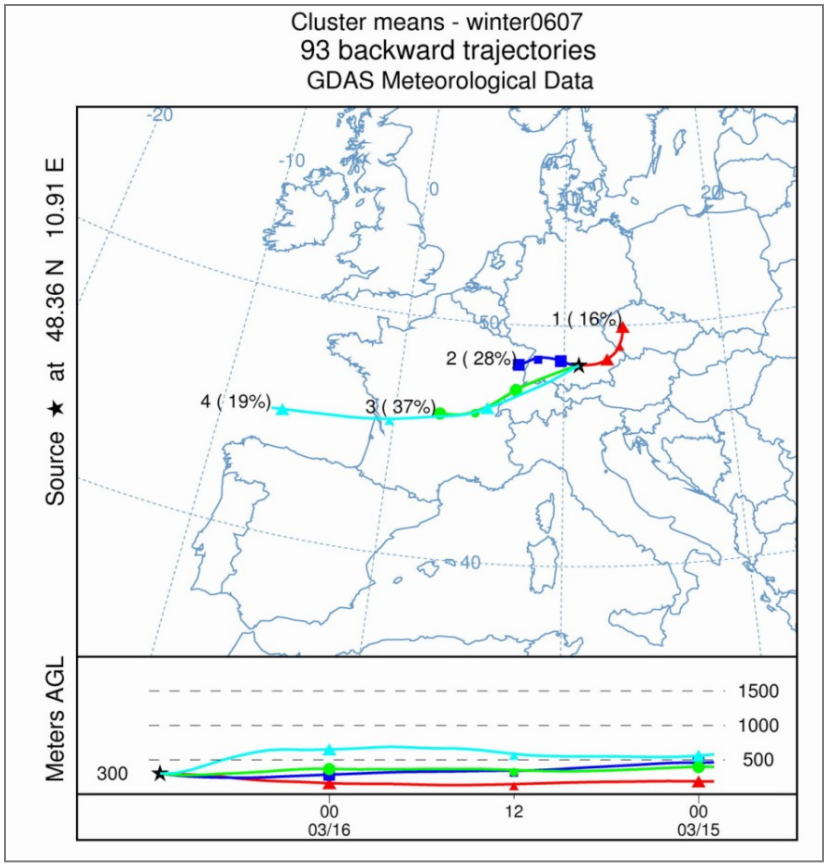

Figure 6-6: Cluster of backward trajectory in winter 2006/07. (The trajectories were calculated 36 hours back before arriving at Augsburg at 13:00 each day at 300 meters above ground level. The trajectories shown in this figure represent the mean trajectory of that cluster.)

All measurement days have been classified according to which cluster of daily 36-hour mean backward trajectories belongs. The trajectories in cluster 1 (east) and 2 (west) were rather short and showed near-ground courses. This is an indication of weather situation with rather limited exchange of air masses. Thus highest PM_{10} MC were found in cluster 1 (east) and 2 (west) (40.9 and 45.0 µg m^{-3} respectively), followed by cluster 3 (southwest), while PM_{10} concentration was the lowest in cluster 4 (the Atlantic) (14.9 µg m^{-3}), the trajectories with the highest wind speeds and altitudes. A summary of trajectory clusters can be seen in Table 6-3.

Table 6-3: Summary of four trajectory clusters and factor concentrations of each cluster in winter 2006/07

N.	direction	N	T	WS	PM_{10}	NaCl	sulfate	combustion	nitrate	traffic	dust
			°C	m s^{-1}		mass concentration [µg m^{-3}] (mass fraction in PM_{10}, [%])					
1	East	15	0.1	2.4	40.9	1.1 (2.8%)	8.6 (21.0%)	4.3 (10.4%)	17.4 (42.5%)	4.1 (10.0%)	4.9 (12.0%)
2	West	26	2.6	2.5	45.0	2.6 (5.8%)	6.1 (13.5%)	6.5 (14.5%)	16.0 (35.5%)	6.2 (13.8%)	6.7 (14.8%)
3	South-west	34	4.0	4.7	27.1	2.4 (9.0%)	2.4 (8.8%)	3.5 (12.8%)	5.8 (21.3%)	5.5 (20.2%)	7.2 (26.6%)
4	Atlantic	18	6.5	7.4	14.9	1.4 (9.6%)	1.0 (6.7%)	2.3 (15.2%)	1.2 (7.9%)	4.2 (27.9%)	5.0 (33.3%)

NaCl

As shown in Table 6-3, lowest NaCl concentration was observed in cluster 1, the eastern region, while higher concentrations were found in cluster 2 and 3, the western and southwestern regions, respectively.

Secondary sulfate

Aerosol concentrations are always affected by the sources and atmospheric conditions, however, in this work cluster analysis of backward trajectory revealed that secondary sulfate factor concentrations were highly related to the sources and courses of air masses. As indicated in Table 6-3, a factor of 8.6 was observed for secondary sulfate concentration between the cluster 1 and cluster 4. When air masses came from the east (cluster 1), a maximum mean value of 8.6 µg m^{-3} was observed (peak values were observed on e.g. December 22 to December 26, 2006), followed by 6.1 µg m^{-3} in cluster 2 (e.g. February 15 to February 20, 2007). Minimum sulfate factor concentration (1.0 µg m^{-3}) was observed in cluster 4 when air masses came from the Atlantic Ocean.

Residential and commercial combustion

There are some differences in the concentration levels among four trajectory clusters. The maximum mean factor concentration of 6.5 µg m^{-3} was found in cluster 2, followed by cluster 1 and 3 (4.3 and 3.5 µg m^{-3}), while lowest concentration was observed in cluster 4

(2.3 µg m^{-3}). The mass fraction of this factor to PM_{10} was more even, in the range of 10.4% to 15.2% for four clusters.

Secondary nitrate

Similar with secondary sulfate, this factor had the highest concentrations in cluster 1 (east), followed by cluster 2 (west), both were short in trajectory length. The lowest concentration was observed in cluster 4 (Atlantic). There is a factor of 14.5 in nitrate factor concentration between cluster 1 and cluster 4. The cluster analysis for secondary sulfate and nitrate factor revealed that secondary aerosols, both the mass concentration and the mass fraction in PM_{10}, increased greatly when air mass came from east or west region together under stagnant atmospheric conditions. These secondary aerosols, considered as long range transported, were the major components of PM_{10} in cluster 1 and 2, in which the mass contribution to PM_{10} reach 63.5% and 49%, respectively. In contrast, in cluster 4 when air mass came from the Atlantic, secondary sulfate and nitrate contributed 6.7% and 7.9% to PM_{10}, respectively.

Traffic emission

The traffic factor concentrations showed little variation among different trajectory clusters, indicating the sources of air masses have limited influence on this factor. This is in accordance with the fact that traffic emission is mainly of local source.

Re-suspended dust

Smaller differences in concentrations among four clusters were observed compared with secondary sulfate and nitrate factors concentrations. The highest concentration was found in cluster 3, where air masses came from southwest. When looking at the mass fraction in PM_{10}, re-suspended dust in cluster 4 can explain 1/3 of PM_{10} in Augsburg, indicating that under windy air conditions from Atlantic, re-suspended dust became the major contributor to PM_{10} mass concentration.

6.2.2 Factor comparison: winter 2006/07 vs. winter 2007/08 at KP site

In winter 2007/08, source apportionment analysis was carried out with data from KP site (November 2007 - March 2008) with the same method as in winter 2006/07. In this section, comparison of factors between winter 2006/07 and winter 2007/08 using data at KP site was made.

Figure 6-7 shows the differences in the source profiles between winter 2006/07 and winter 2007/08 using data at KP site. Although the analyses from both winters resulted in the same number of factors and same factor types, there exist some differences in factor profiles. The factor profiles of NaCl and re-suspended dust showed minor differences between two winters. In contrast, the other four factors exhibited larger differences regarding their source profiles (i.e. concentration and contribution of certain species to specific factors).

In winter 2007/08, 11% of sulfate was mixed in the secondary nitrate factor, and 20% of nitrate was mixed in the secondary sulfate factor, while in winter 2006/07 few mixture was observed, which makes the differences in the source profiles of the two factors between two winters.

OC and EC contributions in the traffic emission factor were lower in winter 2007/08. They are more distributed in the residential and commercial combustion factor. It is found that OC and EC in winter 2007/08 were strong correlated with K and Cd (combustion tracers), but less strong correlated with traffic tracers (mainly Sb and Cu). On the other hand, in winter 2006/07, OC and EC were strong correlated with K, Cd, Sb and Cu, as well as some other trace elements. It seems that the OC and EC in winter 2007/08 are less related to traffic, but more to combustion sources. This may in part explain the differences in traffic factor profiles between two winters.

The residential and commercial combustion factor in winter 2007/08 was characterized by OC, EC, K, Cd and Pb, and can explain 48%, 46%, 60%, 57% and 43% of above species. The factor was strongly correlated with levoglucosan (r=0.84). In winter 2006/07, similar characteristic species including OC, EC, Cd, Pb and K were observed, however, the concentrations and the percentage of species mass were different. OC, EC and K in this factor accounted for 26%, 18% and 27% of total species in winter 2006/07, lower

than in winter 2007/08. Potassium, normally considered as an inorganic tracer of biomass burning, was found evenly distributed in several factors in winter 2006/07. Moreover, correlations of this factor with levoglucosan and K were 0.76 and 0.70, respectively, not as strong as correlation with Cd (r=0.85).

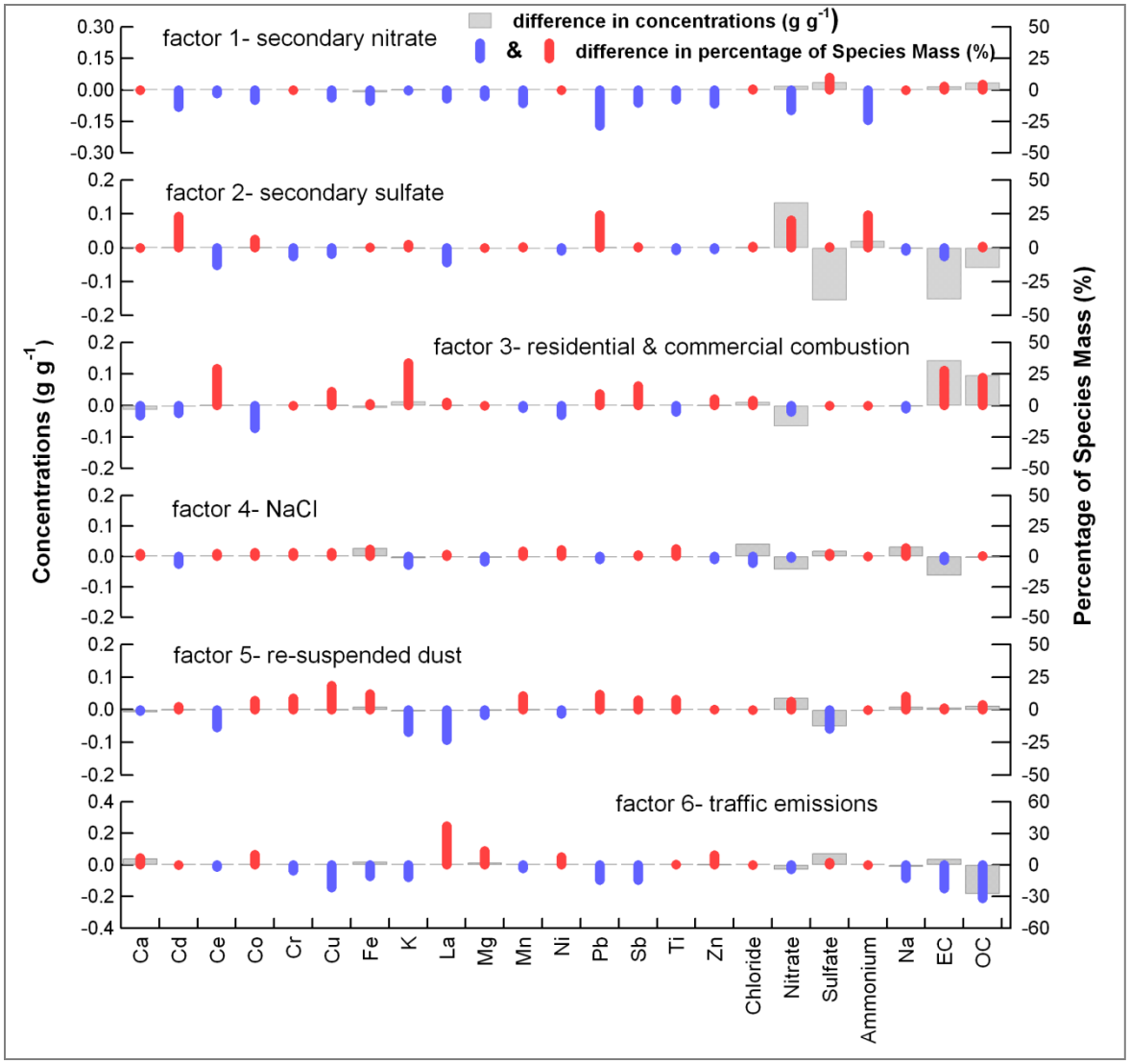

Figure 6-7: Comparison of factor profiles between two winters at KP site (winter 2007/08 minus winter 2006/07). Grey bars are the differences in concentrations (g g^{-1}). Red and blue bars are differences in the percentage of species mass (%). Red ones represent the positive values (i.e. increase in winter 2007/08) and blue ones represent negative values (i.e. decrease in winter 2007/08).

A sensitivity study of K was carried out to test the influence of signal/noise (s/n) ratio on the model result in winter 2006/07. In parallel to the base PMF run, the s/n ratio was increased from 3.6 to 9.8 (High_K method), and in another scenario K was excluded in PMF analysis (No_K method). PMF analyses were performed for the High_K and No_K method, respectively while keeping other settings the same with the base run. The residential and commercial combustion factor had a near perfect correlation (r=0.99) between the No_K method and base run. For High_K method, a higher K fraction of 41% was observed in this factor. The correlation with levoglucosan was improved (r=0.89). The analysis showed the s/n of K in winter 2006/07 was underestimated and the importance of K as a biomass burning tracer was weakened. Details of the K sensitivity analysis in winter 2006/07 can be found in the Appendix A. The same sensitivity analysis was made in winter 2007/08 and the residential and commercial combustion factor was not sensitive to the s/n ratio of K.

Table 6-4: Factor concentrations and contribution to PM_{10} at KP site in winter 2006/07 and winter 2007/08

	nitrate	sulfate	combustion	NaCl	dust	traffic
winter 2006/07_KP_analysis						
concentration (μg m^{-3})	9.6	4.1	4.2	2.1	6.3	5.2
% in PM_{10}	30.4	13.0	13.5	6.6	19.8	16.6
winter 2007/08_KP_analysis						
concentration (μg m^{-3})	7.2	8.2	6.2	3.0	8.0	3.0
% in PM_{10}	20.3	23.1	17.3	8.5	22.6	8.3

Note: winter 2006/07_KP_analysis is short for PMF analysis in winter 2007/08 with data from KP site only, the same for winter 2007/08_KP_analysis.

As shown in Table 6-4, secondary sulfate factor concentrations and the contribution to PM_{10} increased in winter 2007/08 compared with winter 2006/07. However, the measured concentrations of nitrate, sulfate and ammonium at KP site in both winters had much smaller differences in the mean values (5.5 vs. 5.4 μg m^{-3} for nitrate, 2.3 vs. 2.6 μg m^{-3} for sulfate and 2.1 vs. 2.3 μg m^{-3} for ammonium between winter 2006/07 and winter 2007/08). The secondary sulfate factor concentration increased in winter 2007/08 partly because of the mixture of nitrate and ammonium. This also explains the lower

concentrations of secondary nitrate in winter 2007/08. Residential and commercial combustion factor and NaCl factors were about 30% higher in winter 2007/08 than in winter 2006/07. Traffic emission was lower in winter 2007/08, which is in accordance with the decrease of OC and EC contributions in winter 2007/08 shown in Figure 6-7. Mean concentrations of OC and EC in two winters were also close to each other (3.5 vs. 4.0 μg m^{-3} for OC and 4.4 vs. 4.5 μg m^{-3} for EC in winter 2006/07 and winter 2007/08).

6.3 Conclusions

Source apportionment with particulate chemical composition data using PMF method were carried out in Augsburg, Germany for winter 2006/07 and winter 2007/08. In both winters six factors were obtained. In winter 2006/07, aerosols from long range transport: the secondary sulfate and nitrate, were major contributors to PM_{10} in Augsburg. On average they accounted for 44% of PM_{10}. Traffic emission accounted for 16.6% of PM_{10}. The re-suspended dust factor was a mixture of natural dust and road dust, representing 20% of PM_{10} mass. The residential and commercial combustion factor accounted for 13% of PM_{10} mass. NaCl-factor was associated with de-icing agent on roads, and contributed 8.7% to PM_{10} mass.

Four backward trajectories clusters have been separated in winter 2006/07. Highest PM_{10} mass were found in cluster 1 and 2, representing air masses coming with low wind speeds from the east and from the west, respectively. Lowest PM_{10} values were found in cluster 4, which was characterized by air masses coming from the Atlantic under high wind speeds. In general factors dominated by local sources (traffic emission, residential and commercial combustion, re-suspended dust and NaCl) are influenced by origin of back trajectories to a minor degree. On the other hand long range transported secondary aerosols were the major components in PM_{10} in cluster 1 and 2. Though re-suspended dust concentration changed not much among four trajectory clusters, the contribution to PM_{10} increased to 33% in cluster 4, showing that under the highest wind speed and with decreased anthropogenic influence, the re-suspended dust factor became the main PM_{10} source.

PMF analyses in both winters yield similar results (number of sources and factor profiles), however, the source structures are not stable between both winters, especially for residential and commercial combustion factor and traffic emission factor. The factor specific contributions to PM_{10} were also different between two winters, and are caused mainly by the change of factor profiles (secondary sulfate, secondary nitrate, traffic emission factor and residential and commercial combustion).

The cause of differences in factor profiles is explored by comparing the chemical composition (as well as correlations). The signal/noise ratio of potassium played an important role in combustion factor. Weaker correlations of OC and EC with traffic tracers (Cu and Sb) probably caused a shift of OC and EC from traffic factor to combustion factor in winter 2007/08. However, it is still not clear whether the differences of factors are due to changes of actual/real-world source profiles, or due to errors and uncertainties in data.

7 Source apportionment of PSD data

Particle number concentration is dominated by ultrafine particles (UFP). Because of their low contribution to PM mass concentration, UFP can hardly be represented in currently widely monitored $PM_{2.5}$ and PM_{10} mass concentration. In contrast, UFP is related to many adverse health effects, particularly cardiovascular diseases (Peters et al., 1997; Pekkanen et al., 2002; Delfino et al., 2005). As a result, conventional source apportionment analysis utilizing particulate chemical composition (PCC) would inevitably overlook these ultrafine particles, which may pose a crucial threat to human health.

This chapter resolves and characterizes particle sources in terms of particle size distribution (PSD), with which the sources of the smallest particles of several nanometers in diameter can be characterized. Because source apportionment with PSD data is a relatively new method compared to source apportionment based on PCC data, moreover, PSD is more liable to changes in the sizes and concentrations from emission to receptor site, comparison has been made between the sources obtained from PSD data and PCC data. For this reason source apportionment using PSD was conducted separated only for winter 2006/07. In such way the results of the analysis using PCC data for the same time period could be directly compared to the results of source apportionment using PSD data. The results of this PCC vs. PSD comparison are already published (Gu et al., 2011). An analysis for longer time period (2007-2008) is presented in addition. This analysis in a wider time scale is focusing on the seasonal variation, weekday-weekend differences and the potential source locations.

7.1 General data treatment for PSD source apportionment

7.1.1 Data uncertainty

PMF requires a proper estimate of data uncertainty. This is an important feature of PMF aiming to scale the data set individually. However for the particle size distribution data,

there is no measurement error available. And the measurement error should be estimated properly. The uncertainties were calculated according to the empirical equations (Ogulei et al., 2006b; Paatero, 2007; Ogulei et al., 2007b), and shown as follows for different kind of data.

Missing data

Data set containing missing size bins will not be simply removed, as it may lead to a loss of information. Instead, the missing value was replaced with the mean value of the size bin. Because this replaced data is not a real measurement, high uncertainty should be granted to greatly reduce its importance in PMF analysis. Here an uncertainty of 3 times of the mean value was assumed.

Data below detection limit

All the data below detection limit are shown as 'zero'. The uncertainty was assumed as 2 times of the mean values of the respective size bins.

Other data

$$\sigma_{ij} = 0.01(N_{ij} + \bar{N}_j), \quad 7.1$$

where σ is the estimated measurement error for size bin j and sample i. N is the observed number concentration and $\bar{N}$ is mean value of a size bin.

Based on above estimations of measurement error, the heuristic error estimates (S_{ij}) is then calculated based on the data points and their original error estimates.

$$S_{ij}=\sigma_{ij}+C_3\,(N_{ij}), \quad 7.2$$

C_3 should be chosen so that the scaled residuals (e/s) are approximately randomly distributed between -2 and +2. In this study, C_3 was set to 0.05. An extra uncertainty of 25% was added in the model.

7.1.2 Volume concentration

Because the original PSD profiles generated by PMF only provide information on particle number concentration, the volume concentration, on the other hand, cannot be seen. As a result, PSD was converted to volume concentration (VC) assuming spherical shape of the

particles (Zhou et al., 2004b; Ogulei et al., 2006b). Calculation method is shown in equation 7.3,

$$f_j^V = \frac{f_j^{NA} d_j^3 \pi/6}{\sum_{j=1}^{n} f_j^N d_j^3 \pi/6} = \frac{f_j^N d_j^3}{\sum_{j=1}^{n} f_j^N d_j^3}, \quad 7.3$$

where f_j is the fraction for the jth size bin. Superscript V and N represent the volume and number, respectively. d_j is particle diameter.

7.1.3 Potential source location

The directionality of source contribution can be used to determine the type of sources. Conditional probability function (CPF) is used to indicate the major direction of sources (Kim and Hopke, 2004),

$$CPF_{\Delta\theta} = \frac{m_{\Delta\theta}}{n_{\Delta\theta}}, \quad 7.4$$

where $m_{\Delta\theta}$ is the number of occurrences from wind sector $\Delta\theta$ that exceeded a defined a threshold criterion. $n_{\Delta\theta}$ is total number of data points from the same sector. Here the threshold is taken as 75 percentile. In this study each sector was set to 10 degrees, and 36 direction sectors were obtained. Wind speeds below 1 m s^{-1} were excluded from the analysis. For those wind sectors with wind frequencies less than 10, the CPF values were set to null.

7.2 Source apportionment of PSD data in winter 2006/07

1) Data treatment

PSD data between 3 nm and 800 nm were available from December 21, 2006 to March 23, 2007, while PSD between 800 nm and 10 μm were only available from January 17, 2006 to March 23, 2007 due to APS maintenance. The original data resolution was 10 minutes. For PMF input, the data were averaged to 1 hour.

Of the 2228 samples, 171 were missing due to routine maintenance and instrument error, and 19 samples were excluded as outliers. They were often sharp peaks for one or two hours with an increase of about 10 to 100 times, which may be caused by occasional or unknown emissions. The rest 2038 samples accounted for 91.5% of total samples (while

the data coverage is 61.6% for particles with diameter > 800nm). Besides, in this work, particles with diameter of 3 nm, 3.4 nm and 10 μm were eliminated because of high percentage of data below detection limit, which were 92%, 56% and 58%, respectively. As a result, the input data set was 2038 samples by 64 size channels between 3.8 nm and 8836 nm.

There are about 30% APS data (particles with diameter > 800 nm) not measured due to instrument maintenance. These missing data were replaced by the mean value of the respective size bins and the uncertainty was assumed as 3 times of the mean.

The signal to noise (s/n) ratios are much higher for SMPS data (particle size 3-800 nm) than for APS data (particle size > 800 nm). This is partly due to the missing APS data, which coupled with very high uncertainty. The marginal size bins (3.8 nm, 4.3 nm and 4.9 nm) showed lower s/n ratios due to the zero values (higher percentage of data below detection limit) in these size bins.

2) PMF analysis and selecting the factor numbers

Multiple runs with random starting points were operated each time to ensure the Q value is the global minimum. I tested a variety of PMF methods with factor number ranging from 5 to 8 to check the most reliable method. The 7-factor method seems to have the most plausible physical meaning resulting in two traffic emission factors, one secondary inorganic factor, a residential heating factor, a nucleation factor, a coarse dust factor and long range transported dust. If 8-factor method is chosen, the secondary inorganic factor splits into two factors, with one peaked at 300-400 nm and the other peaked at 500-600 nm. The two factors have very similar diurnal variations, correlations with chemical species and directionality. As a result, they should be originated from the same source so that it is confident to combine both factors in one factor. The remaining 6 factors are quite similar with the counterparts in 7-factor method. The 6-factor method, on the other hand, combines the two traffic sources into one, with other factors being similar with the counterparts in 7-factor method. The 5-factor method, compared with 6-factor method, seems to combine the secondary inorganic factor and residential heating into one factor, which accounts for 60% of the total particle volume concentration. As a result of these

preliminary investigations, the 7-factor method is considered to represent the most plausible physical meaning.

3) Bootstrap runs

200 Bootstrap runs were performed and all the factors are mapped except factor 3, aged traffic emission (with 8 bootstraps unmapped, but major species have quite good agreement), indicating a stable result.

4) PSD factor characterization in winter 2006/07

Source apportionment was carried out in winter 2006/07 using PSD data ranging from 3 nm to 10 μm. Seven factors have been characterized. The factors were associated with re-suspended dust, fresh traffic emission, aged traffic emission, stationary combustion, long range transported dust, nucleation particles and secondary aerosols. The source types were identified by the following information, (I) profiles with particle number and volume size distribution (The volume size distribution was calculated from number size distribution assuming spherical shape of the particles (Zhou et al., 2004b; Ogulei et al., 2006b), (II) factor contributions to total number and volume concentration, (III) factor diurnal variation and (IV) daily spearman rank correlation coefficients between each factor and gaseous species as well as online chemical composition data.

Figure 7-1 illustrates the number and volume size distribution of PSD factors. Table 7-1 shows the mean number and volume concentrations of each factor, as well as the proportion in the total number and volume concentration. Figure 7-2 shows the average diurnal variations of factor contribution.

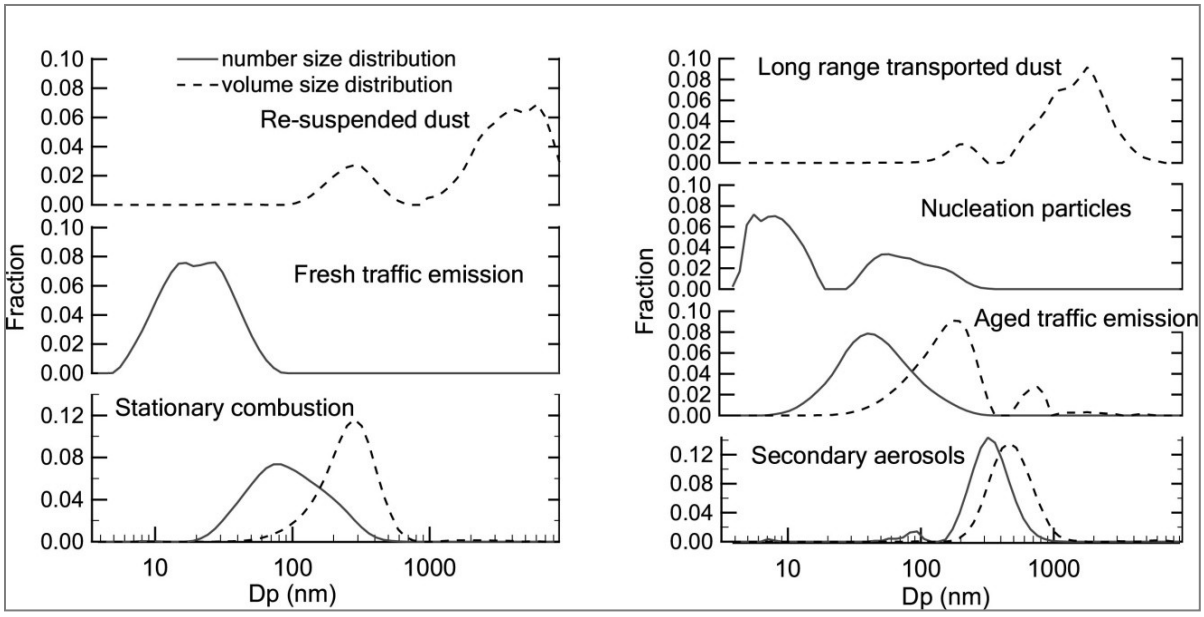

Figure 7-1: Number and volume size distribution of PSD factors in winter 2006/07 (profiles not shown for certain factors if the number/ volume fraction is marginal).

Table 7-1: Average volume and number concentration and proportion of PSD factors in comparison to the total concentration in winter 2006/07

PMF factors	Number	Number ratio	Volume	Volume ratio
	(cm^{-3})	%	($\mu m^3\ cm^{-3}$)	%
re-suspended dust	340	2.6	1.5	8.7
fresh traffic emission	3201	24.9	0.1	0.5
aged traffic emission	5182	40.3	1.7	10.1
stationary combustion	3358	26.1	7.1	41.8
long range transported dust	136	1.1	1.5	8.9
nucleation particles	471	3.7	0.2	0.9
secondary aerosols	157	1.2	4.9	29.1

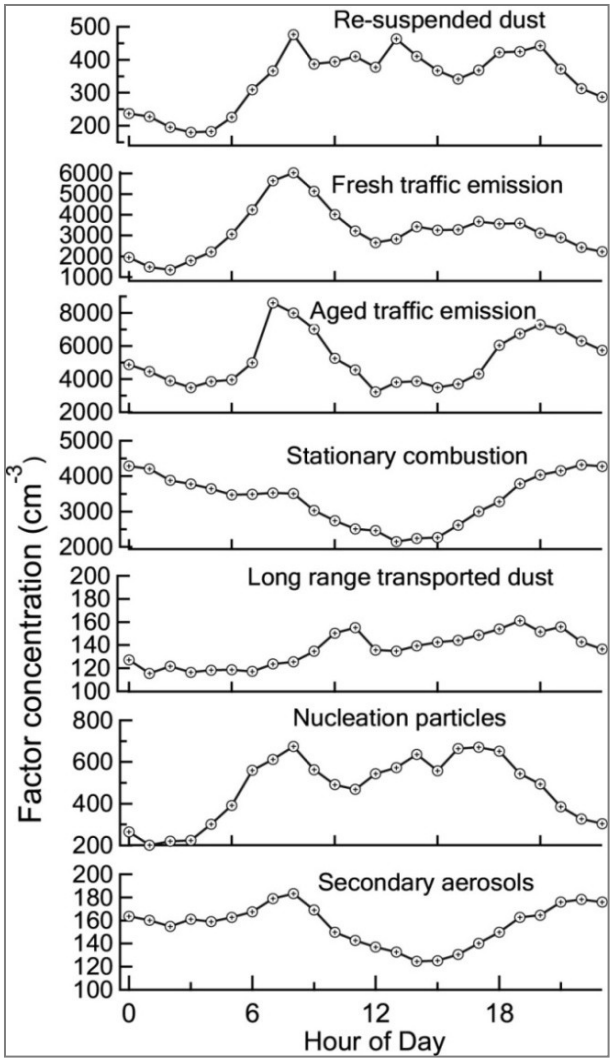

Figure 7-2: Diurnal variation of PSD factors in winter 2006/07.

Factor 1- Re-suspended dust

Factor 1 showed the volume size distribution with a major peak between 2 and 8.8 µm and a minor peak between 0.1 and 0.4 µm. It had low number concentration (NC, 2.6% of total) but higher volume concentration (VC, 1.5 $\mu m^3\ cm^{-3}$), which contributed to 8.7% of total VC. This factor thus represented the coarse mode particles. It showed moderate correlations with NO, NO_2, CO and BC (with r~ 0.5, shown in Table 7-2). As the crustal elements were mainly distributed in the coarse mode (>2 µm) (Cabada et al., 2004; Zhang et al., 2010; Oh et al., 2011; Waheed et al., 2011; Li et al., 2011), this factor was considered to be the re-suspended dust. It was associated with crustal dust, as well as

road dust, which explains why the factor was moderately correlated with gaseous markers of traffic. High concentrations were observed during daytime (Figure 7-2), which coincided with human activities (construction, traffic etc.) and higher wind speed: the favourable conditions for dust re-suspension.

Table 7-2: Spearman rank correlations between PSD factors and gaseous and particulate pollutants in winter 2006/07.

Factors	NO	NO_2	CO	BC	Nitrate	TNC	PM_{10}	$PM_{2.5}$
N	91	91	91	91	91	91	91	91
re-suspended dust	0.48	0.55	0.48	0.50	0.41	0.59	0.54	0.46
fresh traffic	0.53	0.56	0.41	0.40	0.24	0.67	0.25	0.20
aged traffic	0.89	0.88	0.84	0.77	0.54	0.88	0.66	0.63
stationary combustion	0.82	0.85	0.88	0.87	0.88	0.73	0.91	0.92
long range transported dust	0.23	0.24	0.21	0.27	0.18	0.30	0.33	0.30
Nucleation particles	0.00	-0.02	-0.14	-0.09	-0.25	0.15	-0.28	-0.28
secondary aerosols	0.72	0.75	0.81	0.85	0.89	0.58	0.94	0.96

Factor 2 and 3- Fresh and aged traffic emissions

Factor 2 (fresh traffic emission) was considered to probably emit from those vehicles on the nearby roads. As can be seen in Figure 7-1, it consisted of particles mainly in the diameter range from 9 to 40 nm. As shown in

Table 7-1, this factor contributed to 25% of total NC but to only 0.5% of VC. It had moderate correlations with NO, NO_2 and NC (r=0.53, 0.56 and 0.67). A pronounced morning peak was observed which was in accordance with the morning rush hour.

Factor 3 (aged traffic emission) was dominated by UFP between 20 and 100 nm and accounted for 40% of total NC and 10% of VC. It showed stronger correlations with NO, NO_2, CO and BC (r=0.80, 0.80, 0.70 and 0.77, respectively) than fresh traffic emission. The correlation with BC indicated that aged traffic emission is more associated with diesel-powered vehicles. As can be seen in Figure 7-2, a morning peak was also observed for aged traffic emission, which was similar with fresh traffic emissions due to rush hour. In addition, high values were observed in the evening, considering the moderate

correlations with combustion related gases, indicating a mixture of other types of combustion sources in this factor, probably residential heating.

Similar results were reported (Zhou et al., 2004b; Ogulei et al., 2007a; Ogulei et al., 2007b). Zhou et al. (2004) found two traffic factors with very similar size distributions (local traffic factor peaked at 15 nm for NC and remote traffic peaked at 40 nm for NC). However, unlike some other studies, I did not distinguish the two traffic factors into gasoline and diesel vehicles by the fuel types (Ogulei et al., 2007b), as there is no evidence indicating if the dominating contribution came from gasoline or diesel vehicles. Based on the particle size distribution, as well as diurnal variation and correlation analysis, these two factors were related to traffic emission but only distinguished as fresh and aged traffic emissions. Due to particle agglomeration, particles of traffic emission grew bigger with time when reaching UAS site. This means that with the distance from the emission source (in this case traffic) increases, the particle sizes increase in downwind receptor sites (Zhang et al., 2004).

Factor 4- Stationary combustion

The size distribution for factor 4 had one number concentration peak at 70-80 nm and one volume concentration peak at 0.28 μm. This factor contributed significantly to both NC (26%) and VC (41%) and was highly correlated with CO (r=0.88), NO (r=0.82), NO_2 (r=0.85) and BC (r=0.87). The sizes for volume concentration were similar with the particle mass emitted from wood combustion and meat charbroiling (Kleeman et al., 1999; Kleeman et al., 2008), where particle mass, as well as OC and other organic compounds were mainly in the 0.10-0.30 μm range. Raunemaa et al. (1996) found the ambient BC was highly associated with accumulation mode aerosols in the range of 0.10-0.32 μm.

Based on above named information, I attribute this factor to stationary combustion, which may be from local combustion sources including residential and commercial combustion, but it was unlikely from vehicle emissions. Low concentrations were observed in the afternoon and high values during the night and in the morning. It is supposed that this effect resulted from the use of residential heating facilities especially in the morning and evening hours and the formation of a stable, but shallow nocturnal boundary layer (NBL), which traps particle emissions from local sources during the entire night.

Similar results were also observed for source apportionment applied to PSD data. Ogulei et al. (2007a) and Zhou et al. (2004b) resolved residential combustion factor with number concentration peaked around 100 nm.

Factor 5- Long range transported dust (LRT dust)

This factor contributed 8.9% to total VC and showed a bimodal distribution with the major peak between 0.7-3 µm. The proportion of NC to total NC was small (1.1%). In addition, the correlations with gaseous and particulate pollutants were weak. The source of this factor is not clear within the context of winter 2006/2007.

In addition, in an extended analysis for the following years, an increase of factor contribution in parallel to the increased dust concentration between May 27 and May 31, 2008 when Sahara dust event had its impact on southern Germany was observed. The Sahara dust episode has been studied using a combination of meteorological analysis, physical measurements (Light Detection and Ranging system LIDAR, particle size distribution and satellite observation) and ground based PM measurements in Alpine regions (Bruckmann et al., 2008). Also based on the size distribution of this factor, it is assumed as long range transported dust.

Measurement of mineral dust emission typically observed a volume size distribution from sub-micron range up to 20 µm (Kok, 2011). The particle sizes gradually decreased in the long range transport process. Mori et al. (2003) observed particle sizes of Asian dust changed during the long-range transport. The major peak shifted from 4.7 - 7.0 µm in Beijing, China to 3.3 - 4.7 µm in Yamaguchi, Japan. In current study, the re-suspended dust factor was considered to be emitted locally while long range transported dust factor was transported over long distance. This could explain the smaller size distribution of the long range transported dust (0.7-3 µm) compared with re-suspended dust (2-8.8 µm).

Factor 6- Nucleation particles

A bimodal PSD for this factor was observed with a major peak at 5.5 nm and a second one at 40-50 nm. This factor contributed only 3% to NC and 0.9% to VC but almost all of the particles < 7 nm were in this factor. This factor was named as nucleation particles,

which features only the smallest particles (Zhou et al., 2005; Ogulei et al., 2006b). High values were observed in the morning and in the afternoon.

Kittelson et al. (2006) reported that diesel vehicular emissions led to nucleation particles in the size range of 6-11 nm. The peak of smallest PSD was observed in winter morning by Jeong et al (2004; 2006), which may be formed from the dilution of direct emission of motor vehicles. Hence the morning peak of the nucleation particles could be induced by the cooling and condensation of newly emitted gases during rush hours. The afternoon peak can be generated by the photochemical reaction and evening rush hour, which is similar with the measurement by Jeong et al. (2006).

Zhou et al. (2004b; 2005) and Ogulei et al. (2007b) resolved a nucleation mode mainly composed of particles less than 10 nm by receptor model. Other source apportionment studies with lowest measurement size of 10 nm or even 20 nm, resolved nucleation related factors but with size range above 10 nm (Ogulei et al., 2007a; Pey et al., 2009), or did not resolve a nucleation factor (Kim et al., 2003a; Larson et al., 2006; Yue et al., 2008; Thimmaiah et al., 2009).

Factor 7- Secondary aerosols

For this factor a peak in the PSD at 0.32 µm for NC and 0.56 µm for VC was observed. It accounted for 28% of the total VC but only 1% of NC. I assume factor 7 to represent secondary aerosols, mainly the inorganic aerosols including nitrate and sulfate. This factor showed strong correlations with nitrate (r=0.89), CO (r=0.81) and BC (r=0.85). The continuous measurement of sulfate was not available in winter 2006/07 period. However, according to the correlation of other time periods sulfate was well correlated with nitrate, and this fact was assumed valid for winter 2006/07. This factor showed a weak morning peak and high concentrations could be observed during the night. The diurnal pattern was quite similar with $PM_{2.5}$ or PM_{10}. Lower levels in the afternoon can be explained by better atmospheric convection conditions.

Secondary sulfate was found in the accumulation mode by many studies (Zhuang et al., 1999; Hazi et al., 2003; Liu et al., 2008). Secondary nitrate was found both in sub-micro mode and coarse mode ranges (Zhuang et al., 1999). A secondary nitrate factor with number size distribution at 300 nm was observed by Ogulei et al. (2007a), same as in this

study. A secondary aerosol factor peaked at around 0.3 μm was also resolved by Kim et al. (2004b).

7.3 Comparison of factors from PSD and PCC data

The results of factor contributions obtained from PSD and PCC data in winter 2006/07 were compared. In order to make the two methods comparable, the original hourly PSD factor contributions were averaged to 24 hours. PCC data were obtained at KP site and the PSD were measured at UAS site. Figure 7-3 illustrates the comparison of selected factor contributions between the two methods. Note that the two methods used data from two separate measurement sites with different characteristic: UAS is an urban background site, and KP is an urban traffic site. In spite of the different locations and different data sets (PSD vs. PCC) I observed four similar pairs of factors (see Figure 7-3). In the following the pairs of the determined factors from PSD and PCC which have similar sources will be discussed. These pairs are I) aged traffic and traffic emissions, II) stationary combustion and residential and commercial combustion, III) re-suspended dust, and IV) secondary aerosols and the sum of secondary nitrate & sulfate.

Some factors were detected by only one method. For PSD method fresh traffic, nucleation and long range transported dust factors had no counterparts in PCC method. Fresh traffic and nucleation factors consisted of the smallest particles which contributed little to volume mass concentrations. Therefore it is unlikely to detect those factors based on chemical composition data only. Long range transported dust was also not found in PCC method and NaCl factor was found in PCC method, but not in PSD method. Secondary aerosols could be separated into secondary nitrate and sulfate using PCC.

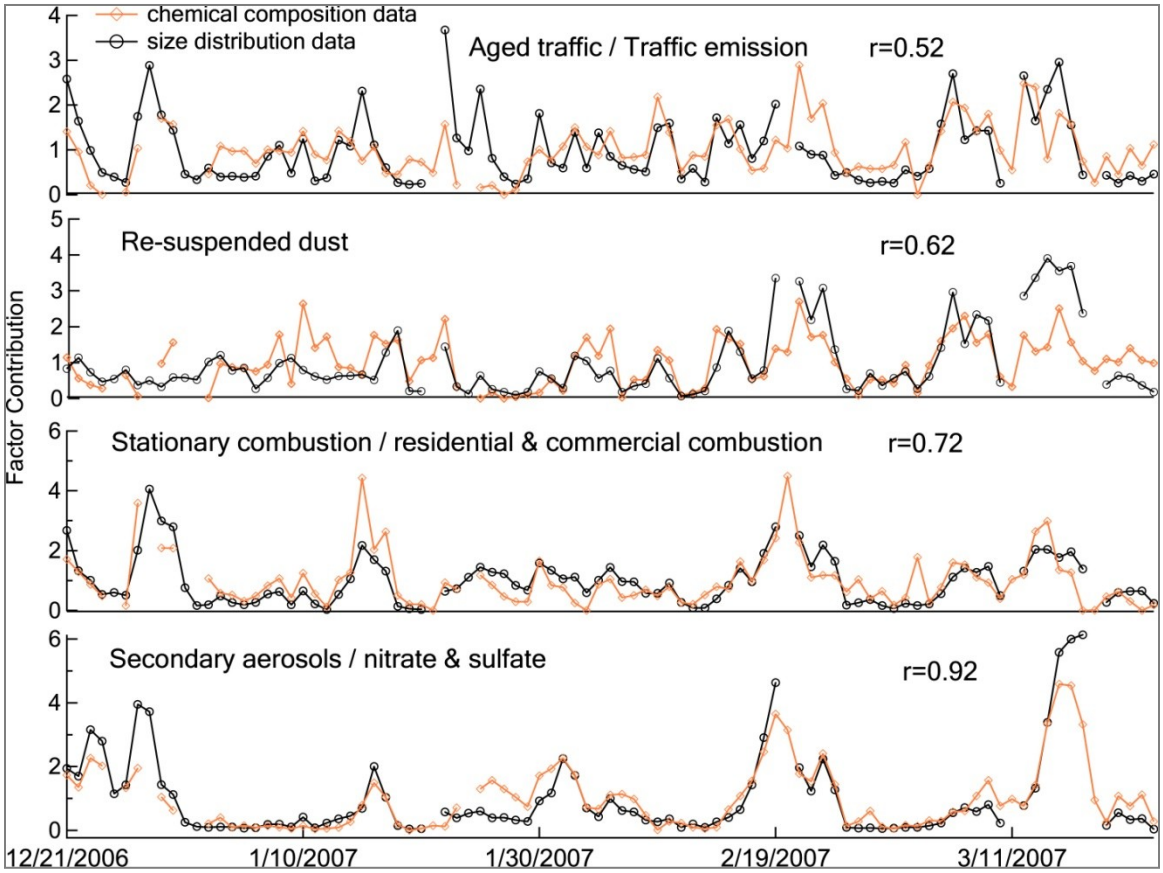

Figure 7-3: Comparison of factor contributions between chemical composition and size distribution data in winter 2006/07 (only factors with significant volume concentration were used in the comparison).

Table 7-3 shows the correlation coefficients between factors from PCC and PSD data. Although the two data sets represented in one case the physical and in the other case the chemical properties of the ambient particles, source apportionment led to moderate to strong correlations for four pairs of factors. Given that the measurement sites of PCC and PSD were classified as urban traffic influenced and urban background site, respectively, the agreement is more remarkable. As shown in Figure 7-3, the best correlation between both methods was observed between the sum of nitrate & sulfate (PCC) and secondary aerosols (PSD) with r=0.92, followed by r=0.72 for residential and commercial combustion (PCC) and stationary combustion (PSD). Re-suspended dust showed weaker but moderate correlations (r=0.62) between PCC and PSD. Weak correlation (r=0.29) was observed between the re-suspended dust (PCC) and long range transported dust

(PSD), indicating in PCC method the transported dust was not resolved and the re-suspended dust was mainly composed of local dust. The traffic factors showed weaker correlation with a correlation coefficient of r=0.52. It's reasonable that the PCC traffic factor assembles PSD fresh and aged traffic factors. But due to the very low volume (and mass) contribution of the fresh traffic factor, the combination of fresh and aged traffic did not change the correlation with the PCC traffic factor. As a result, only aged traffic (PSD) and traffic emissions (PCC) are comparable. With respect to re-suspended dust and traffic emissions, the larger differences were caused by the different surrounding of the two sites, in particular with regard to traffic density and the closeness to roads. The measure of correlation quality of both methods can be ranked by the nature of the sources. For factors with high contribution of background concentrations, e.g. nitrate & sulfate or secondary aerosols, the highest correlation was observed as expected.

Table 7-3: Spearman correlation coefficients between factors from PCC and PSD data (row: PCC factors; column: PSD factors)

	re-suspended dust	fresh traffic	combustion	LRT dust	nucleation	aged traffic	secondary aerosol
NaCl	-0.15	0.03	0.11	0.37	0.14	0.11	-0.08
combustion	0.37	0.18	0.72	0.12	-0.26	0.58	0.36
traffic emission	0.61	0.26	0.43	0.24	-0.10	0.52	0.16
re-suspended dust	0.62	0.15	0.29	0.36	-0.13	0.42	0.18
sulfate & nitrate	0.58	-0.02	0.68	0.33	-0.36	0.35	0.92
secondary sulfate	0.20	-0.03	0.58	0.15	-0.27	0.23	0.79
secondary nitrate	0.68	-0.02	0.66	0.38	-0.36	0.36	0.90

As shown in Table 7-4, the factor contribution to PM_{10} differs. The difference is large only for the two combustion factors. The factor residential and commercial combustion (PCC) and the factor stationary combustion (PSD) account for 13% of PM_{10} mass and 41% of total VC. For all other pairs of comparable factors the difference is smaller; 14% for the secondary aerosols (43% PM_{10}, 29% VC), 11% for re-suspended dust (20% PM_{10}, 9% VC) and 6% for traffic related emission factors (16% PM_{10}, 10% VC).

Table 7-4: Summary of factors used for comparison from two methods

PCC			PSD		
	MC	MC%		VC	VC%
Nitrate & sulfate	13.7	43.5	Secondary aerosols	4.9	29.1
Residential and commercial combustion	4.2	13.3	Stationary combustion	7.1	41.8
Re-suspended dust	6.3	20.0	Re-suspended dust	1.5	8.7
Traffic emission	5.2	16.5	Aged traffic emission	1.7	10.1

There are several possible reasons for these differences. First, both methods could estimate the factor contribution with some uncertainties, although the uncertainties may be as low as a few percentages. Secondly, I estimated the source contribution at two different sites; urban traffic (KP) and urban background site (UAS). Obviously the impact of emissions caused by residential heating is higher at the background site (UAS) than at the traffic site (KP). Finally, the use of different tracers in PCC and PSD is another reason for the differences, because the PSD method only relies on particle sizes and numbers, whereas PCC data can use specific source tracers. Because PCC data use mass concentration of chemical composition, it could offer more reliable results in terms of mass contribution.

With regard to the question which method is superior, there are some criterions one can consider (Table 7-5). The two data sets reflect the chemical and physical characters of ambient particles, respectively. As a result the source types obtained by two methods are different. PSD method separates sources by particle size composed of very small particles with diameter < 50 nm while PCC method can separate sources composed of particles within the similar size range. PSD has the obvious advantage for its automatic data acquisition, while PCC is more labor intensive. Also PSD can provide data of high time resolution, which can reach as high as several minutes. While PCC is restricted by the analytical detection limits, therefore usually sampling times of longer than 1 hour are required. Thus PSD can provide more information on temporal variations. However, the interpretation of sources with PCC data is more clear and concrete as with PSD. This is because PCC itself contains tracers for specific sources or source specific tracer profiles,

like Sb and Cu for brake wear. On the contrary, PSD has no specific tracer. Another reason is that inorganic chemical composition is usually stable in the air thus only limited changes may occur from local sources to receptor site. The PSD, on the other hand, will change more rapidly due to physical and chemical processes, especially for ultrafine particles. The size distribution of particles from a source will change with the distance between the source and receptor site, and then one should carefully compare the results between different studies. However, for a given receptor site, the source profiles would be expected to be stationary in a time period. This will also increase the difficulty of interpretation of PSD results. In summary, PSD requires additional data and the knowledge of measurement location to help determine the source types. In this study we have a full data set including meteorology, gaseous pollutants and online particulate chemical compositions to assist in interpreting the sources.

Table 7-5: Comparison of source apportionment based on PCC and PSD

	PCC	PSD
Data category	Chemical	Physical
Time and effort	time consuming	automatic
Temporal/Diurnal variation	usually daily	hourly
Source interpretation	based on the category of measurement site and factor profile	very dependent on additional data and measurement location

7.4 Source apportionment of PSD data in year 2007 - 2008

1) Data treatment

Hourly particle size distribution in the range 3 nm and 10 μm between March 14, 2007 and December 17, 2008 were used. Of all the 67 size bins, 3 size bins (3 nm, 3.4 nm and 10 μm) were excluded because of high percentage of data below detection limit (87%, 43% and 48%). 53 samples were excluded as outliers. The average data coverage for SMPS data (particle size 3-800 nm) is 94.6%. The APS data (particle size > 800 nm) were missing between October 21, 2008 and December 4, 2008 due to instrument maintenance. As a result, the data coverage for APS data is 87.4%. Totally, 14643 data sets consisting of 64 size bins were applied to PMF.

2) PMF analysis and selecting the factor numbers

Multiple model runs were performed with random starting points. The observed vs. predicated values were studied for each size bin. Seven size bins that were poorly modeled were characterized as 'weak' by tripling the data uncertainty (3.8 nm, 4.3 nm, 4.9 nm, 5.5 nm, 6.9 µm, 7.8 µm and 8.8 µm). A variety of methods with factor numbers ranging from 5 to 8 were tested. The 7-factor method was found to represent the most plausible physical situation.

7.4.1 Factor characterization

Source apportionment analysis using PSD in year 2007-2008 obtained six factors which were associated with re-suspended dust, fresh and aged traffic emission, stationary combustion, long range transported, nucleation particles and secondary aerosols. The factors were similar with the ones in winter 2006/07. Figure 7-4 shows the PSD factor profiles of number size distribution and volume size distribution. The temporal variations of factor contribution in the whole study period are shown in Figure 7-5. Figure 7-6 shows the conditional probability function (CPF) of each factor. As discussed previously, the measurement site is located on the campus of the University of Applied Science Augsburg (UAS). The nearest roads to the measurement site are Friedberger street over 100 meters in the north to northeast, and Nagahama Avenue about 300 meters in the southeast.

The re-suspended dust factor was mainly composed of particles larger than 2.5 µm. It had low number concentration of 42 cm^{-3}, accounting for 0.4% of total NC. The volume concentration was 2.1 μm^3 cm^{-3}, accounting for 8.2% of VC. High values were observed during the daytime. The re-suspended dust factor showed high concentrations in spring in 2007 (shown in Figure 7-5). The CPF plot for re-suspended dust factor showed that these particles mainly came from north and northeast of the site. It is coincident with the nearest road: Friedberger street, which is located in the north to northeast of the measurement site. Thus this factor is probably from the re-suspension of road dust.

The fresh traffic emission factor mainly consisted of particles between 10 nm and 50 nm and peaked at about 27 nm. It is considered to represent local vehicle emissions near to the measurement site. The fresh traffic emission factor contributed to 37.5% of NC and 1% of VC. A pronounced morning peak at 6:00-7:00 am was observed. The fresh traffic emission factor showed major source location from north to northeast and south. Aged traffic emission factor exhibited the number size distribution peaked at 50 nm and volume size distribution peaked at 200 nm. It showed moderate correlations with CO, NO and NO_2, as well as particulate chemical compositions including BC and PAHs. This factor accounted for 41% of NC and 17.4% of VC. High values were observed at night and in the morning. Aged traffic emission factor mainly came from south and southeast, as well as from east and northeast. As shown in Figure 7-5, the fresh traffic emission factor, as well as the aged traffic emission factor had rapid day-to-day variation. The concentrations in cold seasons were slightly higher than in warm seasons.

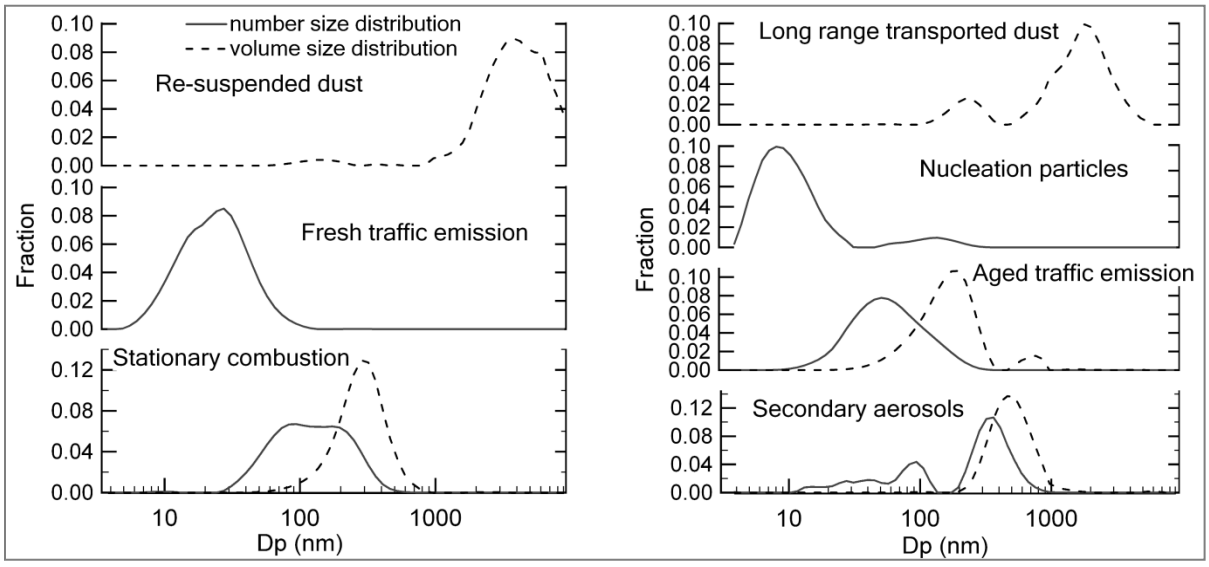

Figure 7-4: Number and volume size distribution of PSD factors in 2007-2008 (profiles not shown for certain factors if the number/ volume fraction is marginal).

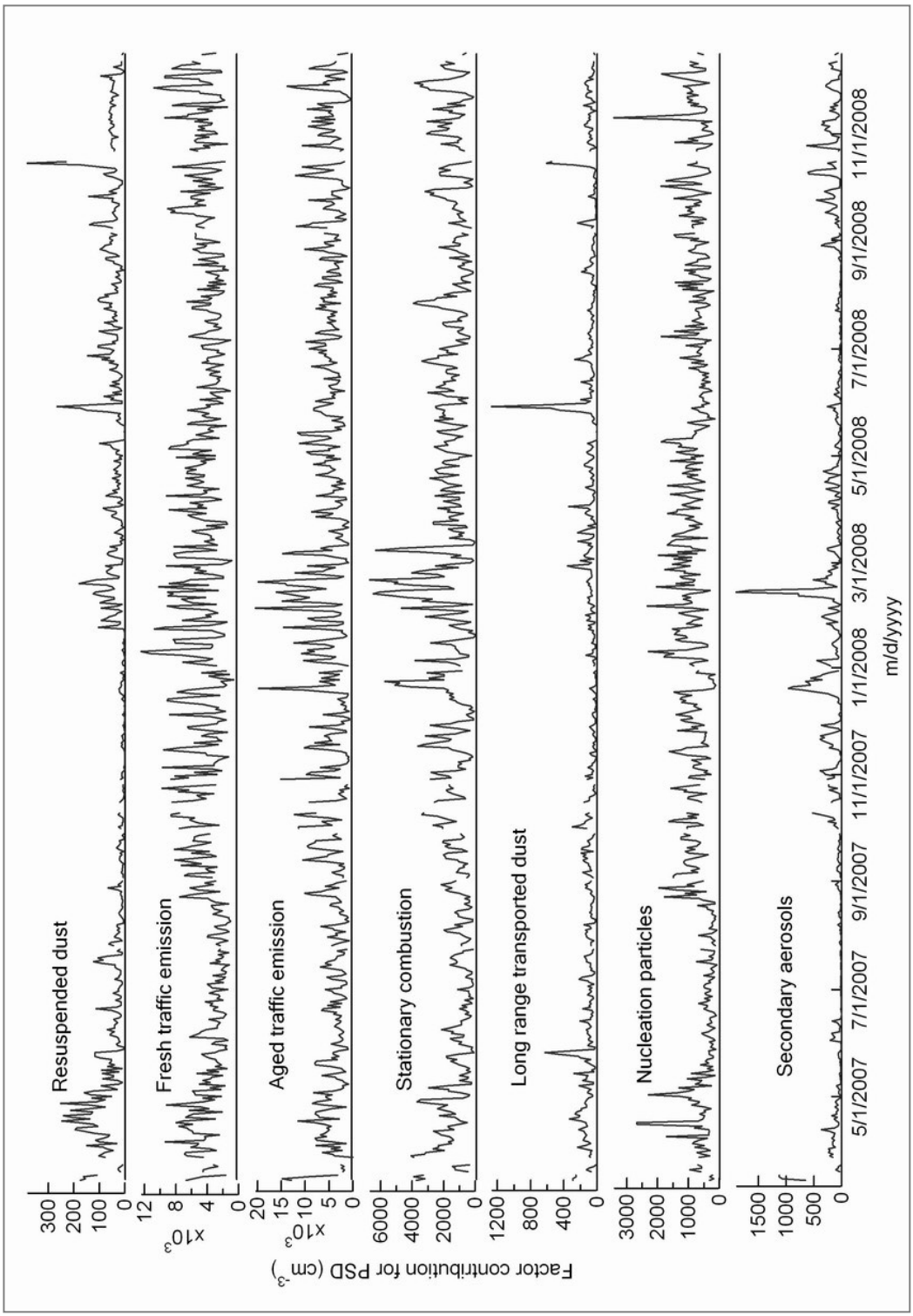

Figure 7-5: Daily averaged temporal variation of PSD factor concentrations in 2007-2008.

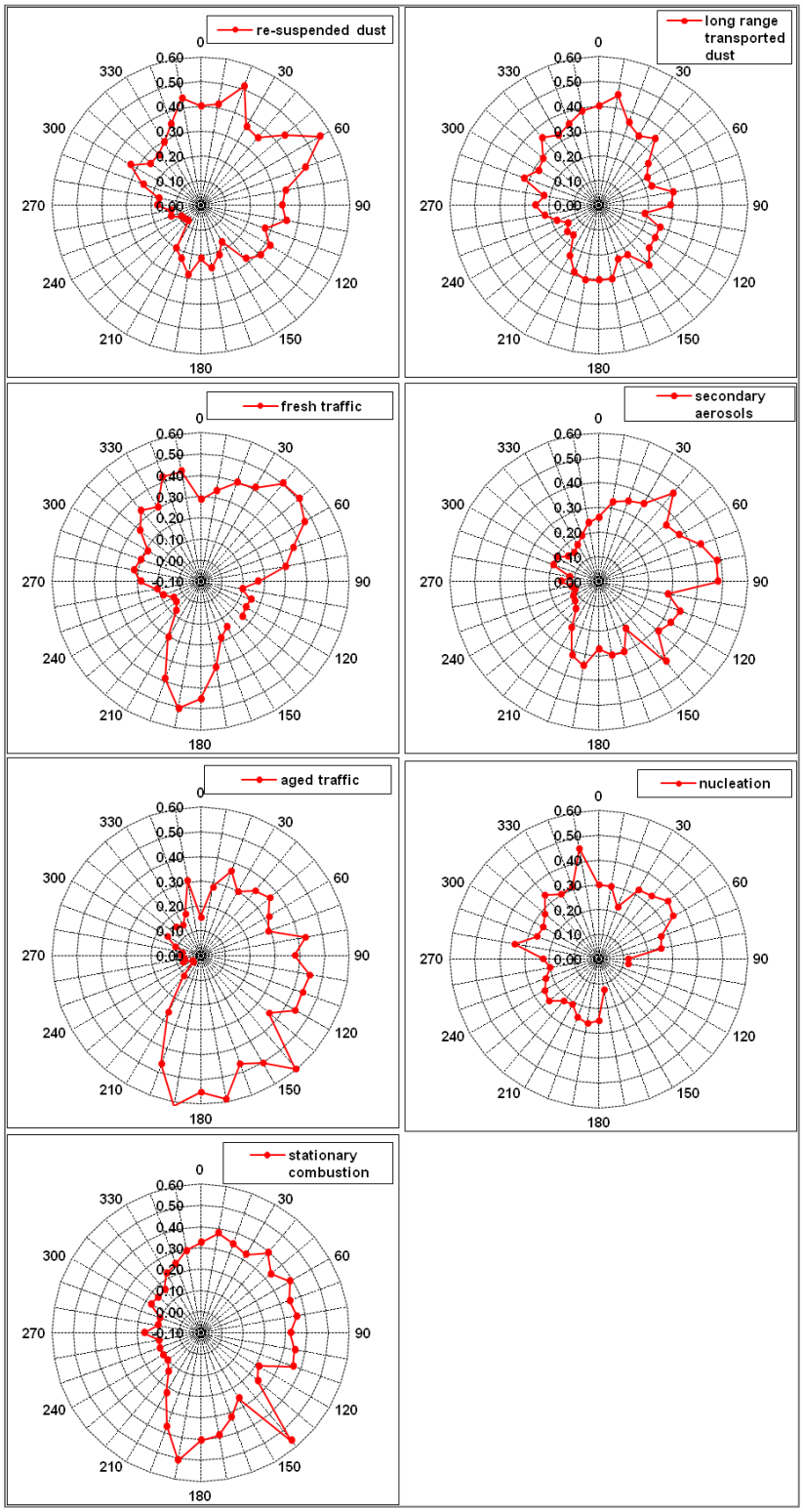

Figure 7-6: The conditional probability function for factor contribution based on hourly data in year 2007-2008.

The nucleation factor mostly consisted of particles smaller than 20 nm and with number size distribution peaked at 7 nm. This factor represented particles from nucleation of gaseous pollutants or fresh particles emitted from vehicles nearby roads. High values were observed during daytime. The CPF plot of nucleation particle factor mainly pointed to north direction, indicating the emission from local streets, as well as traffic plume from city centre might be the source of nucleation particles.

Stationary combustion factor showed a wide number size distribution between 60 nm and 200 nm. The volume size distribution peaked at 300 nm. It had number concentration of 1487 cm^{-3} accounting for 12.7% of NC and volume concentration of 10.3 μm^3 cm^{-3} accounting for 40% of VC. High concentrations were observed in winter periods and low concentrations were observed in summers. In winter season this factor mainly came from residential heating while in summer when there is no heating necessary, this factor are from other combustion sources and from secondary oxidation of volatile organic compounds and other primary organic emissions. Stationary combustion mainly came from the south and north to east.

Secondary aerosols factor was composed of particles in accumulation mode between 100 nm and 1µm. Number size distribution peaked at 220 nm and volume size distribution peaked at about 400 nm. It had high volume concentration (5.7 μm^3 cm^{-3}, 22.4% of VC) but low number concentration (117 cm^{-3}, 1% of NC). The temporal variation frequency is quite low, with stable low concentrations lasted for months in the summer. The CPF plot of secondary aerosols factor mainly pointed to east and north east. The secondary aerosols were considered to come from transported and in previous section (6.2.1.3), the secondary nitrate and secondary sulfate were associated with backward trajectories from eastern countries.

Long range transported dust factor showed major peak of volume size distribution at 2 µm and a minor peak around 200 nm. Weak diurnal variation was observed for this factor. No major direction was observed for this factor.

7.4.2 Seasonal variation

Figure 7-7 shows the monthly average of each factor. The re-suspended dust factor showed the highest concentration in April, 2007 and the lowest in November, 2007. The seasonal trends were not the same for both years.

The fresh traffic emission factor showed lowest concentration in summers in both years. It may be caused by higher atmospheric boundary layer in warm seasons. The aged traffic emission showed less seasonal variation except one high concentration in February 2008. The stationary combustion factor showed a clear trend with high concentrations in winter and low concentrations in summer. For long range transported dust factor, high concentrations were observed in spring, between March and May, and low concentrations were observed in winter 2007 and summer 2008. As shown in Figure 7-5, this factor normally remained at low concentrations except some very high but occasional peaks in May, and less in other months. The high peaks were probably caused by some long range transported dust events. And take the peak in May 2008 for instance: it was found to be well correlated with the Saharan dust event, which was discussed before (Pitz et al., 2011). The nucleation particle factor showed the minimum concentrations in summer.

The secondary aerosols factor showed very large differences in concentration levels in different seasons. Very high concentrations were observed in winter while the lowest concentrations in summer. The secondary aerosols, in this case, were believed to represent mostly the secondary inorganic species including sulfate and nitrate, neutralized by ammonium. Nitrate ammonium is not stable in the atmosphere and will establish a thermodynamic equilibrium between gas and particulate phase. The equilibrium is highly affected by temperature and relative humidity (Ansari and Pandis, 1998). In warmer seasons with higher temperature and lower relative humidity, the equilibrium moves to gas phase, while in cold season it moves toward the particulate phase. In addition, in winter season more frequent adverse meteorological conditions with low boundary layer, stagnant air mass condition can also cause the increase of the secondary aerosol concentration.

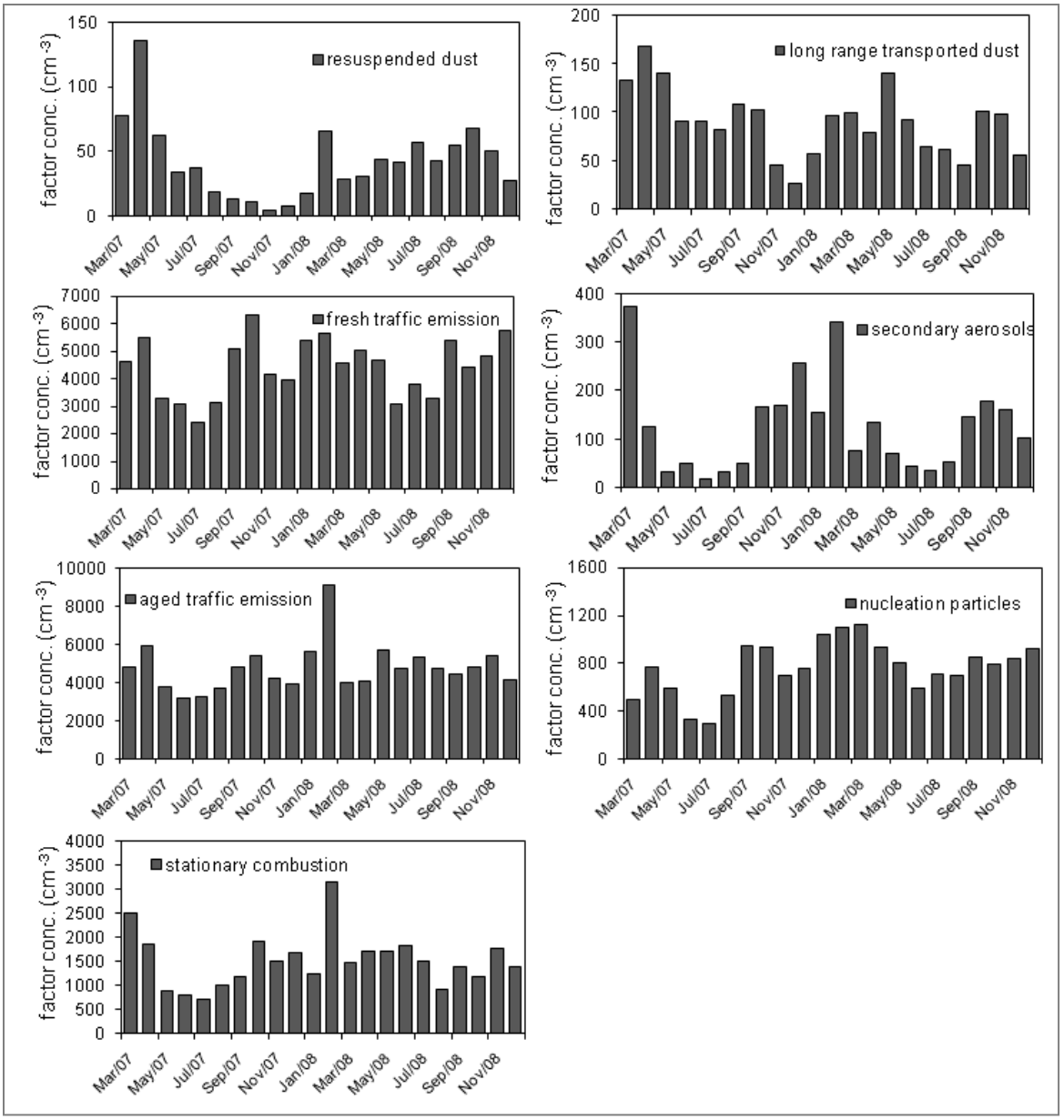

Figure 7-7: Monthly mean temporal variation of factor contribution.

7.4.3 Weekday-weekend variation

Figure 7-8 shows the averaged factor concentrations from Monday to Sunday. In urban areas, the vehicular emission, industrial and construction activities can be very different between weekdays and weekends. Motor vehicles are expected to be much less on weekends, though no measurement was performed. The concentration, as well as the composition of particles can be different on weekdays and weekends.

The concentrations of re-suspended dust, fresh traffic emission and nucleation particle factors were lower in weekends. The above three factors were considered to be related to traffic: re-suspended dust was produced (partially) by the moving vehicles; the nucleation particle was associated with diluted tailpipe pollutants from vehicles; and the fresh traffic was directly emitted from vehicles. In weekends there is lower traffic density compared with on weekdays, which lead to lower concentration of fresh traffic emission. Re-suspended dust and nucleation particles, the traffic related factors, also showed lower concentrations in weekends.

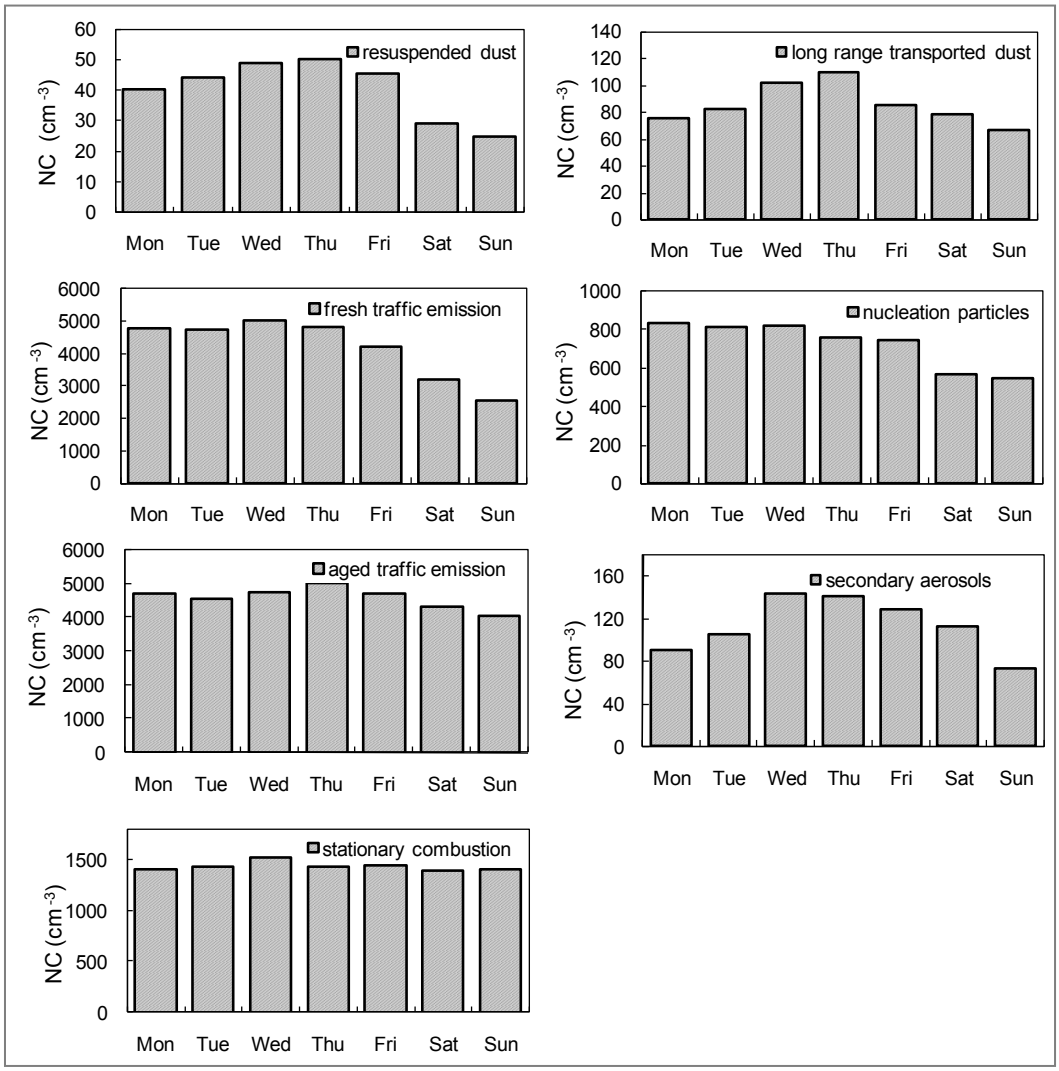

Figure 7-8: Averaged factor concentrations from Monday to Sunday in year 2007-2008.

The aged traffic emission showed only small decrease in concentration level in weekends. This may be explained by the mixture of some stationary combustion related sources in the factor, which have little weekday-weekend differences. Secondary aerosol factor showed low concentration on Sunday, Monday and Tuesday. Nitrate is the main secondary inorganic matter in Augsburg, and it comes from the oxidation of NO_x. The NO_x are expected to have low concentrations in weekends and higher concentrations on weekdays. The low concentration of secondary aerosols on Monday and Tuesday may be an indication of the time required for NO_x to be oxidized to form secondary nitrate and be transported to Augsburg. From the weekday-weekend trends of secondary aerosols, a formation time of 1-2 days from precursors to secondary aerosols is assumed.

Stationary combustion factor showed little differences between weekdays and weekends. The long range transported dust showed weekday-weekend trends similar with secondary aerosol factor. I will not discuss the weekday-weekend trends for the long range transported dust as it may be caused by the irregular "dust episodes".

Figure 7-9 shows the averaged factor concentrations and contributions to total number concentration from Monday to Sunday. The total NC from Monday to Friday was between 11391 and 12410 cm^{-3}, while on Saturday and Sunday, NC was 9703 and 8690 cm^{-3}, respectively. Fresh traffic emission and aged traffic emission were the major contributors to NC. The decrease of NC on weekends was mainly due to the decrease of fresh traffic emission, and to a less extent by the decrease of aged traffic emission.

Regarding the contribution by percentage, the fraction of nucleation particle in NC keeps steady in a week. While the total traffic emission also contributed to NC similarly from Monday to Sunday in the range of 76% to 80%. However, in weekends, the traffic emission showed higher fraction of aged traffic factor, which coincided with the fact of less fresh traffic emission due to fewer vehicles in weekends.

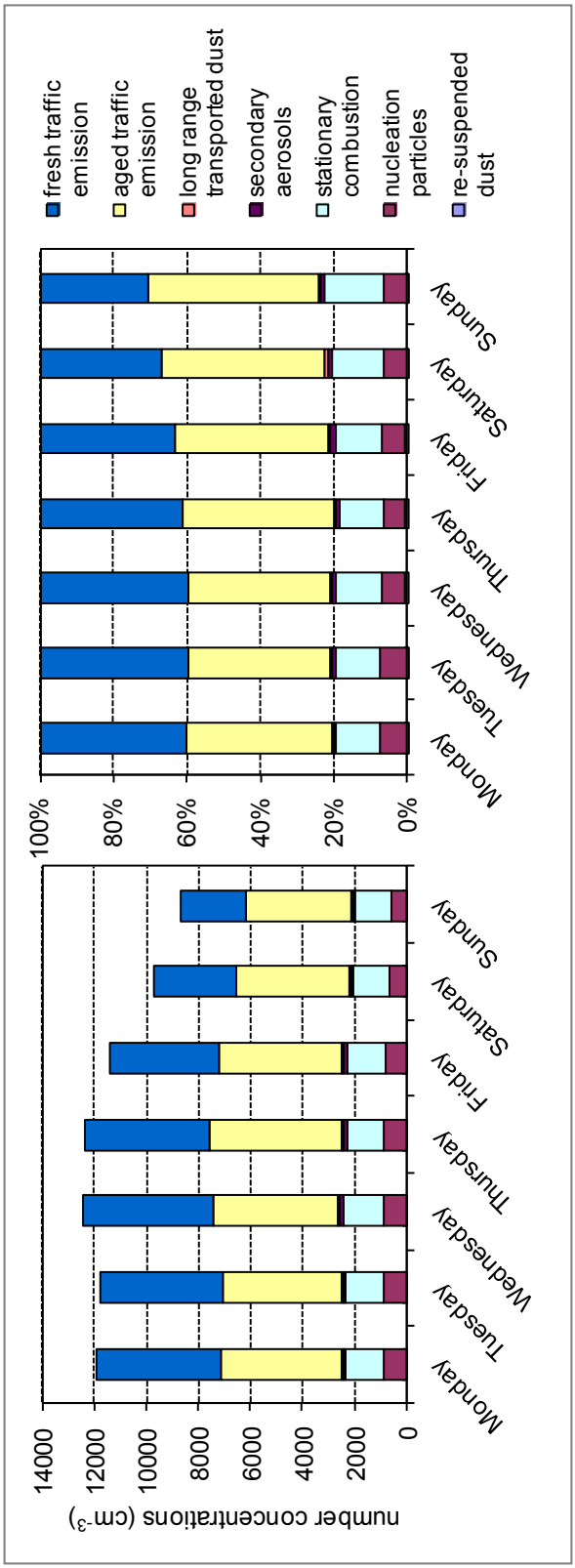

Figure 7-9: Stacked factor concentrations and contributions to number concentration from Monday to Sunday in year 2007-2008.

7.5 Conclusions

Source apportionment of particle size distribution data have been successfully carried out using PMF method. The analyses were done respectively for winter 2006/07 and a two year's period in 2007-2008.

In winter 2006/07 seven factors were characterized using PSD data, which were associated with re-suspended dust, fresh traffic emission, aged traffic emission, stationary combustion, long range transported dust and secondary aerosols. Fresh traffic and aged traffic sources dominated the UFP. Stationary combustion factor accounted for 26% of total NC. The major contributors to VC were stationary combustion (42%), secondary aerosols (30%), followed by aged traffic (10%), long range transported dust (9%) and re-suspended dust (9%).

Source apportionment results with PSD and PCC were compared for similar factors. PSD and PCC method gave 4 similar pairs of factors. The temporal variations of traffic factors and re-suspended dust at two sites showed weak agreement due to the influence of local traffic emissions, whereas secondary aerosols, which mostly originated from long-range transport, showed a better temporal agreement and a minor spatial discrepancy. Because of the regional nature of secondary aerosols, the correlation coefficient of 0.92 revealed the closeness of the two methods.

In year 2007-2008 seven factors were found which were similar with factors observed for winter 2006/07. Nucleation particles, fresh traffic emission showed lowest concentrations in summer. For stationary combustion, lowest concentration was observed in summer 2007. Secondary aerosols exhibited the largest differences between seasons with very low concentrations observed in summer and very high concentrations in winter. The possible cause may be the meteorological condition which is favorable for pollution accumulation, and can affect the gas to particle equilibrium of nitrate ammonium. Fresh traffic emission and two traffic related factors: nucleation particles and re-suspended dust showed decreased concentrations in weekends. Secondary aerosols showed the lowest concentrations on Sunday and Monday, and a formation time of 1-2 days from gaseous precursors to secondary aerosols were proposed to be responsible for the special weekday/weekend variation.

8 Spatial and temporal variation of particulate sources

A one-month intensive campaign was conducted in Augsburg in 2008. During this measurement campaign PCC data were collected at seven additional monitoring sites (in addition to KP site which measured for the whole winter 2007/08) spreading out over the whole city area of Augsburg. By extension of the source apportionment on the seven additional sites we are able to evaluate the spatial variability of PM sources across the urban area.

In this chapter, the spatial and temporal variation of particulate sources was discussed. The factors were obtained from the PMF analysis with combined PCC data from eight sites in winter 2007/08. The results can also provide implications for epidemiological studies conducted in the city of Augsburg.

8.1 Determination of spatial and temporal variation

The temporal variation is normally determined by calculation of correlation coefficients. If correlation coefficients are close to unity it means both variables have the similar or same temporal variation. Spatial variability or uniformity refers to the heterogeneity or homogeneity of particulate matter across an area of interest. Many studies calculated the correlation coefficients to determine the spatial variability of $PM_{2.5}$ or PM_{10}. The correlation coefficient, however, tracks the temporal similarity of paired sites, cannot indicate the differences in absolute concentrations. Pinto et al. (2004) suggested that the correlation coefficient is not sufficient to determine the spatial variability of particulate matter. Instead, the coefficient of divergence (COD) is used to provide a measure of homogeneity (Wongphatarakul et al., 1998; Cyrys et al., 2008).

$$COD = \sqrt{\frac{1}{n}\sum_{i=1}^{n}\left(\frac{x_{ij}-x_{ik}}{x_{ij}+x_{ik}}\right)^2}, \qquad 8.1$$

where x_{ij} and x_{ik} are the i^{th} observations of x at j and h sampling sites, respectively. n is the total observation number.

The COD provides information on the degree of uniformity between monitoring sites. For the spatial distribution, the COD approaches zero if the measured values at two monitoring sites are similar. In contrast, the COD approaches unity if the measured values are quite different.

Table 8-1: Average PM_{10} mass concentration, nitrate, sulfate, EC, OC, calcium, magnesium, iron and potassium ($\mu g\ m^{-3}$) and corresponding standard deviations at eight sampling sites between February 13, 2008 and March 12, 2008

	KP	BP	Lo	LfU	HO	WE	Bi	Ki
PM_{10}	**42.7 ± 23.04**	28.0 ± 18.99	-	24.60 ± 17.53	-	**17.55 ± 11.09**	26.11 ± 18.39	18.98 ± 10.44
Nitrate	**6.77 ± 5.32**	6.65 ± 5.27	6.23 ± 5.26	6.42 ± 4.91	6.73 ± 4.96	**5.63 ± 3.87**	6.68 ± 5.04	6.53 ± 3.73
Sulfate	2.29 ± 2.21	2.22 ± 2.04	**2.45 ± 2.28**	2.25 ± 2.09	1.97 ± 1.80	**1.81 ± 1.42**	2.33 ± 2.14	2.15 ± 1.67
EC	**4.44 ± 2.17**	2.67 ± 1.96	2.28 ± 1.76	2.32 ± 1.72	**1.33 ± 1.13**	1.51 ± 0.95	2.31 ± 1.62	1.92 ± 0.94
OC	**4.18 ± 2.40**	3.24 ± 2.29	3.03 ± 2.21	3.15 ± 2.36	**2.20 ± 1.82**	2.36 ± 1.47	3.16 ± 2.13	2.97 ± 1.45
Ca	**1.11 ± 0.48**	0.54 ± 0.3	0.42 ± 0.21	0.72 ± 0.52	0.35 ± 0.13	**0.34 ± 0.11**	0.47 ± 0.29	0.45 ± 0.23
Mg	**0.27 ± 0.1**	0.14 ± 0.07	0.12 ± 0.05	0.14 ± 0.07	**0.10 ± 0.04**	0.11 ± 0.04	0.12 ± 0.07	0.11 ± 0.06
Fe	**1.82 ± 0.84**	0.58 ± 0.45	0.31 ± 0.21	0.33 ± 0.24	0.17 ± 0.11	**0.16 ± 0.10**	0.37 ± 0.24	0.33 ± 0.23
K	0.25 ± 0.15	0.24 ± 0.15	0.23 ± 0.13	0.23 ± 0.14	**0.17 ± 0.10**	0.20 ± 0.10	0.25 ± 0.12	0.24 ± 0.11

Note: Bold fonts represent the highest and lowest component levels among eight sites. PM_{10} concentrations at Lo and Ho have not been measured.

8.2 Results

8.2.1 Composition of PM_{10} at eight sites

Table 8-1 presents the mean concentrations of PM_{10} and selected chemical composition in the intensive campaign between February 13, 2008 and March 12, 2008. PM_{10} concentrations varied among sites with the highest concentration at KP site (42.7 μg m^{-3}) and the lowest at WE site (17.55 μg m^{-3}). Nitrate, sulfate and K showed smaller differences among sites. The concentration of Fe, on the contrary, differed largely from site to site and a factor of 11 was observed between KP site and WE site.

8.2.2 Source apportionment of PCC data in winter 2007/08

In winter 2007/08, a combination of PCC data from KP site (November 14, 2007 – March 31, 2008) and other seven monitoring sites (February 13, 2008 – March 12, 2008) were used together in PMF. There were 139 samples from KP site and 201 samples from other seven sites. Among them 5 samples were excluded as outliers and 9 samples were removed due to instrument failure, resulting a total of 326 samples in PMF analysis. 24 species including Ca, Cd, Ce, Co, Cr, Cu, Fe, K, La, Mg, Mn, Ni, Pb, Sb, Ti, Tl, Zn, Cl^-, SO_4^{2-}, NO_3^-, Na^+, NH_4^+, EC, OC and PM_{10} were used in PMF analysis. The uncertainties were set according to Equation 6.1.

Error fraction is estimated from sampling error and analytical error. In PMF analysis we assumed 8% for trace elements (from ICP/MS) and 12% for water soluble ions (from IC). Four species Co, Cr, Ni and Tl that have low signal/noise ratio (s/n) were characterized as weak by tripling the uncertainties. PM_{10} were included in PMF but characterized as weak.

A variety of factor numbers between 5 and 9 have been tested and 6 factor method provided the most meaningful results. Bootstrap runs were performed and all factors showed good stability.

8.2.3 Factor characterization in winter 2007/08

In this section, PMF factors using combined data at KP site and 7 satellite sites are present. Similar with in winter 2006/07, six factors were resolved. The factors were

associated with secondary nitrate, secondary sulfate, residential and commercial combustion, NaCl, re-suspended dust and traffic emissions. Figure 8-1 illustrates the factor profiles by concentrations (g g^{-1}) and percentage of species mass (%). Table 8-2 shows the Spearman rank correlation coefficients between factors and gaseous pollutants, as well as levoglucosan.

Factor 1- Secondary nitrate

Factor 1 was characterized by high concentrations of nitrate and ammonium and was considered as secondary nitrate. A molar ratio of 1.06 was observed between apportioned NH_4^+ and NO_3^-.

Factor 2- Secondary sulfate

Factor 2 was dominated by SO_4^{2-}. It also contained high concentrations of NH_4^+ (25%). It was considered as secondary sulfate. As shown in Table 8-2, secondary sulfate factor was weakly correlated with gaseous pollutants. Like secondary nitrate, this factor originated most likely from long range transport. The molar ratio of NH_4^+ to SO_4^{2-} was 1.68, less than 2, which may be caused by model uncertainty.

Factor 3- Residential and commercial combustion

Factor 3 was characterized by OC, EC and K and can explain 56%, 44% and 63% of above species. It was highly correlated with particulate levoglucosan (r=0.92), an organic tracer for biomass burning, and moderately correlated with SO_2 (r=0.56) and CO (r=0.54). Factor 3 was considered to represent residential and commercial combustion, especially wood combustion. High loading of Cd (65%) was observed in this factor which was considered to emit from wood combustion.

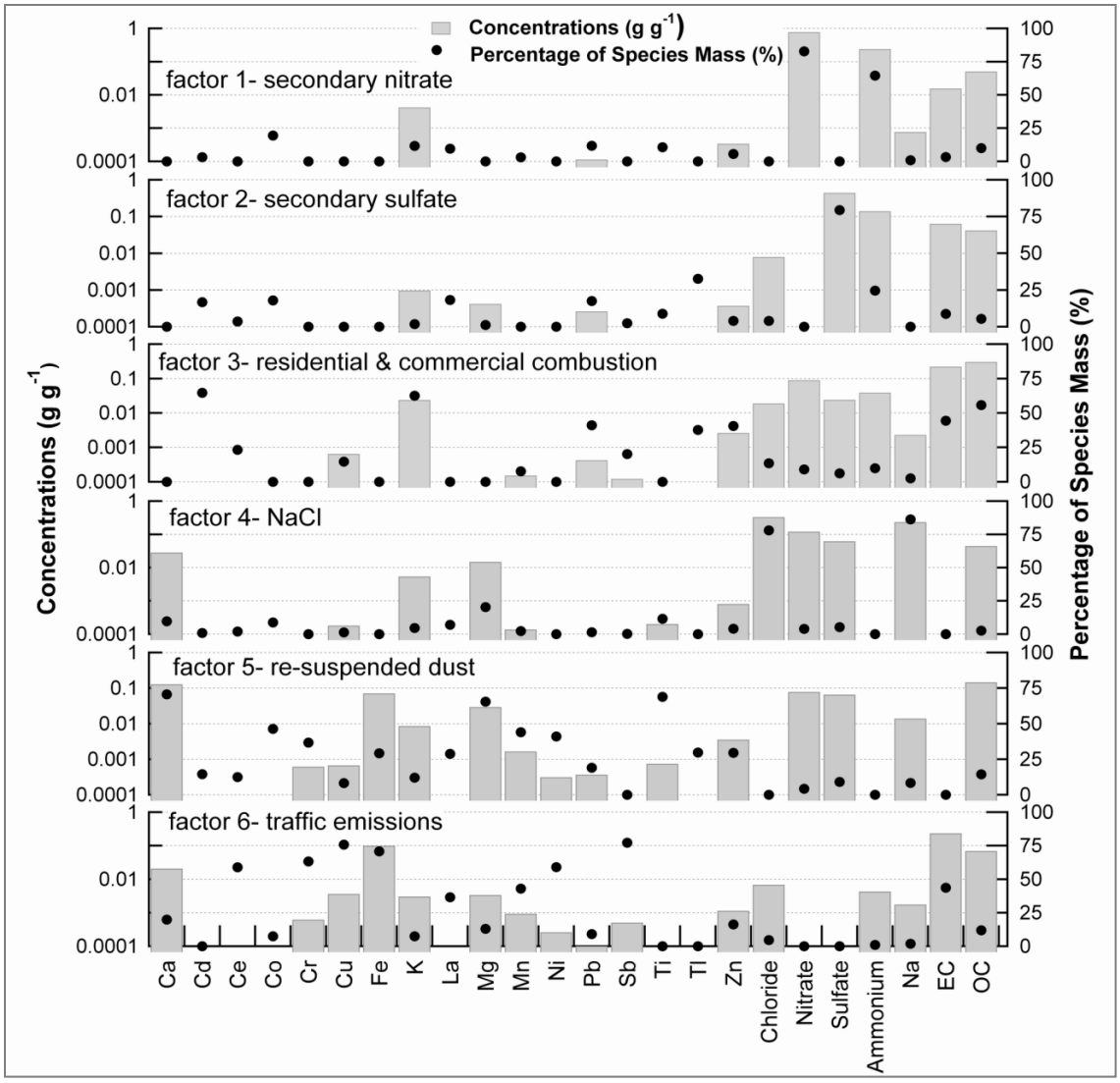

Figure 8-1: PMF factor profiles from chemical composition data in winter 2007/08.

Factor 4- NaCl

Factor 4 was characterized by high concentrations of Na^+ and Cl^- (Figure 8-1), and could explain 86% of Na^+ and 78% of Cl^-. A molar ratio of 1.09 was observed for Na^+ to Cl^-. It is most probably from the de-icing agents. As shown in Table 8-2, this factor was weakly correlated with gaseous pollutants. Some incidences with high NaCl loadings were observed. Between February 14 and February 20, 2008 NaCl was extraordinarily increased at KP and associated with low temperatures and clear and dry days, which are favorable for the re-suspension of the de-icing agent.

Table 8-2: Spearman rank correlations between PMF factors and gaseous pollutants, as well as levoglucosan in winter 2007/08

	nitrate	sulfate	combustion	NaCl	re-suspended dust	traffic
NO	0.13	0.09	0.39	0.16	0.35	0.92
NO_2	0.26	0.16	0.49	0.17	0.43	0.87
CO	0.31	0.27	0.54	0.13	0.25	0.80
SO_2	0.35	0.30	0.56	-0.09	0.10	0.30
LEV	0.60	0.53	0.92	-0.11	0.24	0.37

Factor 5- Re-suspended dust

Factor 5 was considered as re-suspended dust. It contained high concentrations of Ca, Mg and Fe, which are mainly of crustal origin. Besides, a part of trace elements such as Fe, Ti, Mn and Ni were also observed in this factor. They were considered to come from the traffic related dust. The mixture of traffic related dust in the natural dust has been seen in other studies (Amato et al., 2009).

Factor 6- Traffic emission

Factor 6 was characterized by EC, Cu, Sb, Fe, Cr, Ni and OC (shown in Figure 8-1), and can explain 44%, 76%, 77%, 71%, 63%, 59% and 12% of the above species, respectively. It was strongly correlated with NO and NO_2 and CO. This factor was considered to be associated with vehicular tail pipe emission and other traffic related emissions including brake ware and tram lines. Cu and Sb are indicators of brake ware. The Cu : Sb ratio (of ambient concentration) at KP was 7.6, what is in line with the results from studies considering brake ware composition (~5), and much lower than Cu : Sb ratios found in crustal material (~125) (Weckwerth, 2001; Arditsoglou and Samara, 2005). The Cu : Sb ratios at the seven satellite sites were similar and ranged from 5.7 to 7.3.

In addition, high contents of Fe, Cr, Ni and Mn were found in traffic emissions. As discussed in 6.2.1.2, they mainly came from tram lines. Metals including Fe, Cr, Ni and Mn were likely to come from the frictions between the tram wheels and rails or the pantograph and the catenary.

8.2.4 Temporal variation of PM_{10} sources

Figure 8-2 shows the temporal variations of factors at the 8 sites in the intensive campaign between February 13 and March 12, 2008. Figure 8-3 shows the box plot of Spearman rank correlations of each factor between 8 sites. The pair-wise of Spearman rank correlation coefficients are presented in appendix B. In general, secondary nitrate, secondary sulfate and residential and commercial combustion factors showed uniformity among all monitoring sites. NaCl, re-suspended dust and traffic emissions factors showed higher inter-site variability.

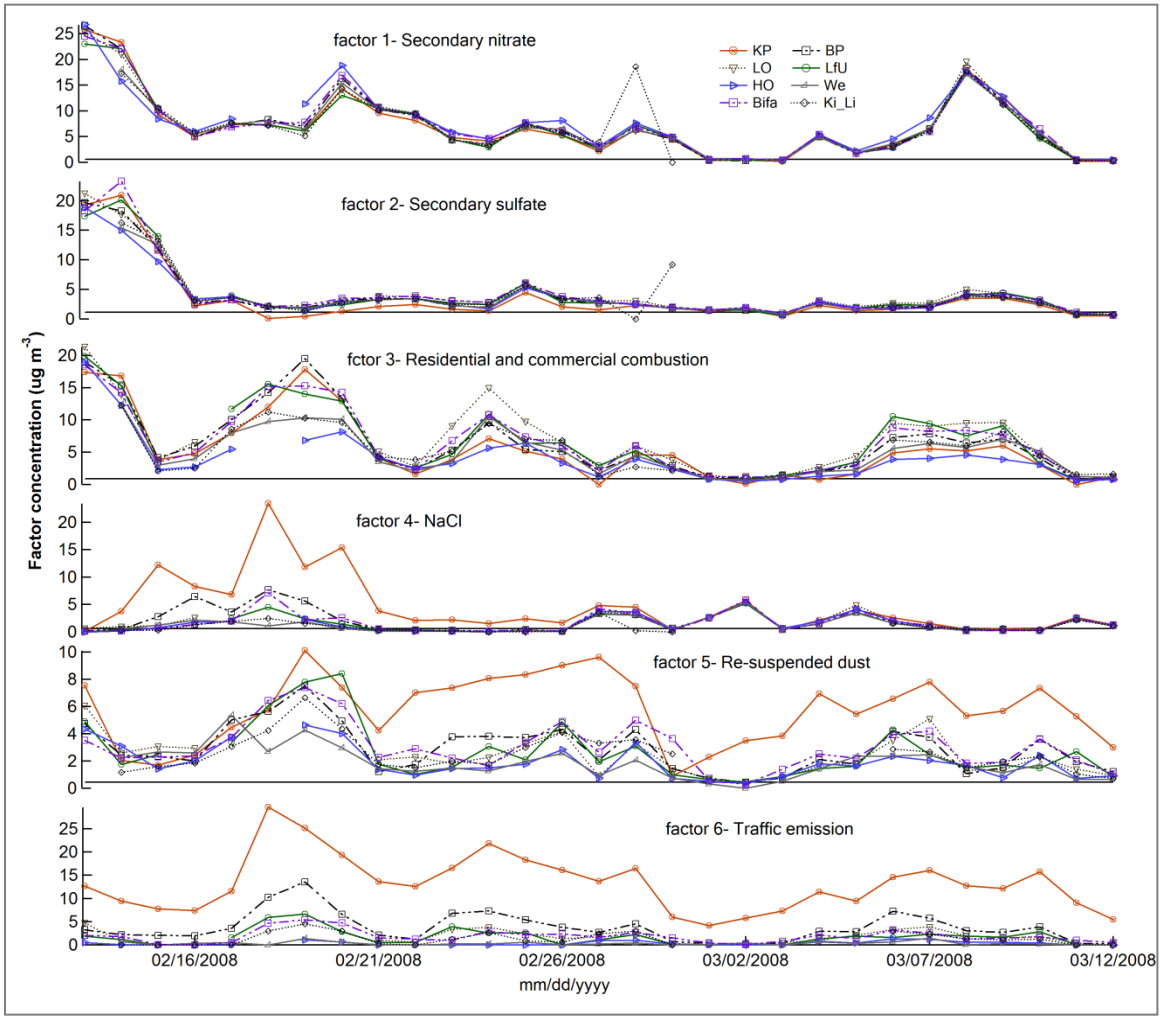

Figure 8-2: Temporal variation of PMF factors from eight sampling sites between February 13, 2008 and March 12, 2008 (the results were obtained from PMF analysis in the winter 2007/08 with all data combined).

Secondary nitrate and secondary sulfate showed very consistent temporal variation among eight sites. Only occasional discrepancies were observed at Ki site. Secondary nitrate and secondary sulfate were highly correlated among 8 sites. Sulfate at KP site had relatively lower correlations with other sites, within the range of 0.81 - 0.91, all fell in the lower 25 percentile range. Residential and commercial combustion factor generally showed similar temporal variation trends among all sampling sites. High correlation coefficients were also observed, and the median correlation coefficient was 0.95.

NaCl showed similar temporal variations among sites except KP. It had a median correlation coefficient of 0.85. Six sites including BP, Lo, LfU, HO, WE and Bi exhibited strong correlations between each other and Spearman's r were in the range of 0.85-0.96. The correlation coefficients between KP and other sites were in the range of 0.44 - 0.77, mostly within the lower 25 percentile. Correlations between Ki and other six sites (excluding KP site) were in the range of 0.72 - 0.80, lower than correlations among the six sites (0.85 – 0.96).

Re-suspended dust had a median correlation coefficient of 0.73 among eight sites. KP site showed different temporal variations than other seven satellite sites. The correlations between KP and the seven sites were in the range of 0.28 - 0.62, lower than the inter-correlations among the other seven sites.

For traffic emissions factor, KP, BP, Lo, LfU, Bi and Ki sites had moderate to strong inter-correlations (r: 0.67 - 0.92). Ho and WE sites showed weaker correlations with other six sites. Weak correlation was also found between Ho and WE sites. It may be due to the fact that Ho is a tower site 100 meters above ground and WE is a suburban site, which are quite different from the other sites that are in or near the urban area.

8.2.5 Spatial variability of PM_{10} sources

Figure 8-3 displays the box plots of Spearman rank correlations and coefficient of divergence (COD) of each factor at eight monitoring sites. The COD value was used in recent studies to examine the degree of discrepancy between data sets from two monitoring sites (Wongphatarakul et al., 1998; Cyrys et al., 2008). If two sampling sites are very similar, COD approaches zero, otherwise, COD approaches one. The COD was

calculated between each pair of monitoring sites. Additionally the Spearman rank correlations were calculated. The pair-wise of COD values are presented in appendix B.

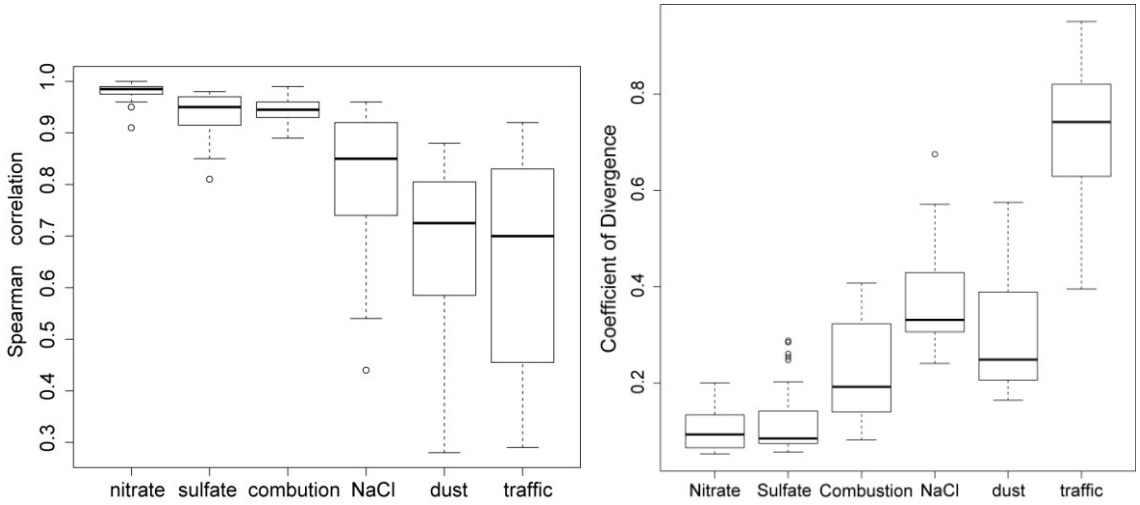

Figure 8-3: Box plots of Spearman rank correlation coefficients (left) and coefficient of divergence (COD, right) for PMF factors between eight different measurement sites (In calculating COD, there are 4 missing data for Lo site, 1 for LfU, Ho and WE site, respectively, and 6 for Ki site.).

As shown in Figure 8-3, secondary nitrate showed the very low COD values, indicating nitrate is homogeneously distributed in the study area. Secondary sulfate also showed very low COD values. The residential and commercial combustion factor had a median COD value of 0.19, and COD values between KP site and other sites were significantly higher.

A median COD value of 0.33 was observed for NaCl. COD values between KP and other sites were significantly higher (0.46 - 0.68, all in the upper 25 percentile range). Higher concentrations were observed at KP site in the first half of intensive campaign before February 27. Concentrations were almost the same among all sites after February 27. It was speculated that there were freshly emitted NaCl as de-icing agent before February 27 at KP site and to a less extent at BP site. In the second half of intensive campaign, de-icing agent seemed no longer to be emitted, probably due to unfavorable weather

conditions, or running out of on road sources, and NaCl exhibited great consistency in concentration levels among all sites.

Re-suspended dust factor had a median COD value of 0.25. Re-suspended dust is considered to be partially related to the local traffic, and showed higher concentrations at KP site than other sites.

Traffic emissions factor was found with much higher concentrations at KP site throughout the study period. Traffic emission showed the highest COD values among eight sites, indicating traffic is highly heterogeneously distributed within the study area. KP site was greatly impacted by traffic emission, which was verified by a factor of 38 times between traffic factor concentrations between KP site and WE site. Apart from KP site, BP site was influenced more by traffic emission than other background sites. BP site is located in a small park but is about 100 meters away from the major roads and a tram line. Though the road and tram line are to the north of BP site, the downwind of prevailing wind direction, vehicle tail pipe emissions as well as tram abrasion products still influenced BP site more than other urban background sites.

8.2.6 Source contributions to PM_{10}

Figure 8-4 shows the factor contribution to PM_{10} mass concentration. The levels of secondary nitrate and secondary sulfate factors were almost the same at all eight sites (ca. 4.0 $\mu g\ m^{-3}$ for sulfate factor and 7.2 $\mu g\ m^{-3}$ for nitrate factor, respectively), which means a homogeneous distribution over the whole city area. It is in line with their strong correlations and low COD values shown above. Note that the contribution of the secondary sulfate and nitrate to the whole PM_{10} fraction depends on the site type. It varied from < 30% at the traffic site (KP) and up to 60 % at a hotel tower site (Ho).

Residential and commercial combustion contributed 4.1 - 6.7 $\mu g\ m^{-3}$ to PM_{10} at eight sites. The contribution of other sources to PM_{10} at different sites differed considerably, especially for NaCl and traffic emission factors. The contribution of traffic emission factor to PM_{10} at KP was more than 30%, whereas the contribution of this factor to PM_{10} levels on the other sites ranged from 2% up to 14%, with the lowest value at Ho and WE sites (2%). Re-suspended dust showed the highest concentration (and contribution to PM_{10} levels) at KP site, whereas at other sites lower concentrations were observed.

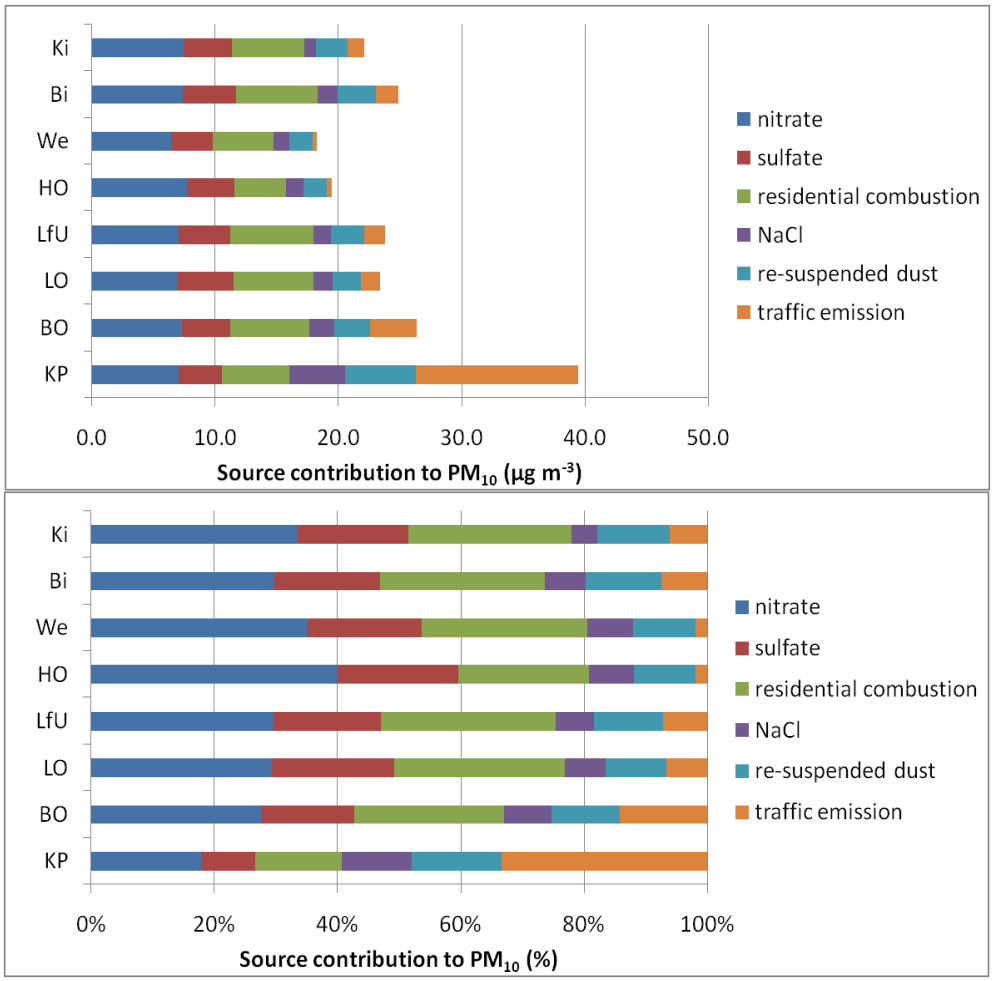

Figure 8-4: Factor contributions to PM_{10} mass concentration at eight measurement sites during February 13, 2008 – March 12, 2008.

In general, the levels of secondary sulfate and nitrate are quite similar at all monitoring sites. The combustion particles represent the most important additional source for PM_{10} at the background sites, whereas traffic emission, NaCl and re-suspended dust contribute significantly to PM_{10} mass concentrations at traffic and traffic influenced sites.

PM_{10} at KP site was higher than other sites. The most important source at KP was traffic emission. The enhanced re-suspended dust and also NaCl contributed to the elevated PM_{10} mass concentration at KP site. According to the factor contribution to PM_{10}, the eight sites can be divided into four groups. KP is an urban traffic site with the traffic emission accounting for 33% of PM_{10} mass concentration. BP is a traffic-influenced

urban background site, with traffic emission accounting for 14% of PM_{10} mass concentration. Lo, LfU, Bi and Ki sites were identified as urban background sites. The PM_{10} mass concentration at the four sites ranged from 22.1 to 23.8 μg m^{-3}, and traffic emission accounted for 6 - 7% of PM_{10} mass concentration. WE and Ho sites were two sites showed different source contributions than other sites with traffic emission accounted for 2% of PM_{10} mass concentration, and were considered as a suburban site and a tower site, respectively.

8.3 Implications for epidemiologic studies

Augsburg is a city where a number of epidemiologic studies were carried out under the framework of KORA (Cooperative Health Research in the Augsburg Region) (Holle et al., 2005; von Klot et al., 2005; Rückerl et al., 2007; Peters et al., 2009; Hampel et al., 2010; von Klot et al., 2011). For short term epidemiologic studies which typically use daily time series of PM pollutants at one central monitoring site or average of a set of monitoring sites, if the particulate pollutants were not highly correlated, exposure misclassification can happen. For long term epidemiologic studies which normally use annual mean concentrations, if the absolute concentration differs substantially across the study area, there is a potential for exposure misclassification for this type of epidemiologic study.

From above results, it can be concluded that particulate sources can differ substantially with regard to their temporal and spatial variation properties. Secondary sulfate and secondary nitrate showed uniformity both temporally and in absolute levels in urban areas. No exposure misclassification will occur for secondary nitrate and sulfate for short term or long term epidemiologic studies. Residential and commercial combustion factor showed good agreement in temporal variations and also similar concentrations across the urban area. NaCl and re-suspended dust factors showed different temporal variations and concentration levels at traffic (or traffic influenced) site relative to urban background sites. But for urban background sites, they showed good temporal variations and similar concentration levels. Traffic emissions factor varied highly across the city. The concentration level was affected highly by how heavily traffic impacted on the

measurement site. However, moderate to strong correlations were found between six sites in or near the city area. This means that traffic emissions generally have good temporal variations in urban area of Augsburg (not including two sites: Ho and We), but differed greatly in concentrations. As a result, long term epidemiologic studies for traffic related emissions must consider the spatial variability of traffic emissions.

8.4 Conclusions

Source apportionment using PMF method in both winters (winter 2006/07 and winter 2007/08) generated the same number of factors and the factor profiles were similar. Six factors were characterized and were associated with secondary nitrate, secondary sulfate, residential and commercial combustion, de-icing agent (NaCl), re-suspended dust and traffic emissions.

Secondary nitrate and secondary sulfate factors were mainly from long range transport and much higher concentrations were observed when air masses came from east and west than from Atlantic. They also showed the highest spatial uniformity across Augsburg. Residential and commercial combustion factor mainly came from the wood combustion for heating, and other combustion types. They showed high correlations and relatively smaller absolute differences in concentration levels among different sites in Augsburg. NaCl was emitted from the re-suspension of de-icing agent, which was used in winter seasons in Augsburg. Re-suspended dust mainly came from the natural dust composed of crustal elements (Ca and Mg), as well as dust from tram abrasions. The tram lines impacted greatly on re-suspended dust at KP site, followed by BP site. Both NaCl and the re-suspended dust factors were elevated at traffic site. The traffic emission factor contained tail-pipe emission and the tracers for brake ware. Traffic emission factor had the highest spatial variability across city Augsburg.

9 Cluster analysis of ambient particulate pollutants: data reduction for epidemiological study

A number of epidemiological studies focusing on the adverse health effect of particulate matter relied on PM mass concentration because such parameters are legally regulated and monitored widely and with simple effort. The PM mass concentration, however, is relatively an unspecific indicator and is mainly correlated with particles in accumulation mode (0.1-1.0 μm). On the other hand, variables including number concentration (dominated by particles < 0.1 μm), surface area concentration etc are also found to have significant adverse health effect.

Due to the fact that a variety of ambient particulate variables can pose threat to human health, a monitoring station was set up in Augsburg since 2004. The long term measurement in particulate matter sampling yielded a number of particulate variables. Size segregated particle number, length, surface and volume concentration, as well as other continuously measured chemical composition were obtained. Apart from the large number of variables, many are inter-correlated with each other. As a result, dimension reduction is necessary before epidemiological studies were undertaken.

In this chapter cluster analysis is applied to a large data set of ambient particulate variables. Representative variables were selected for each cluster (Gu et al., 2012). I then interpret the physical meanings of resolved clusters by associating them with particle sources. In this way the clusters/ selected variables could be associated with specific sources and, thereby, help to identify causal PM components or size fractions, which would be beneficial to policy makers for regulation purpose.

9.1 Methods

9.1.1 Clustering method

Cluster analysis is a technique of finding groups consists of similar patterns within a larger data set. The patterns within one cluster are more similar than the patterns belonging to another cluster. The method was described in detail by Kaufman and

Rousseeuw (1990) and Struyf (1996). It can be divided into hierarchical and partitional clustering. The hierarchical clustering is the cluster algorithm that generates a hierarchy of clusters, which can be displayed by a tree shaped chart, called dendogram. Partitional clustering produces no exact and exclusive clusters. The hierarchical clustering can give the cluster structure or connectivity, while partitional clustering only produces a simple partition of the data. Hierarchical clustering provides more information on how clusters are formed or how variables are merged successively. Such information is important, in the case of this study, to show the inter-relationship among variables. Partitional clustering has the advantage of clustering large amount of data, when calculating the cluster structure is impossible. As a result the hierarchical clustring is chosen.

I used an agglomerative hierarchical cluster method "agnes" to find groups of similar variables within the particle pollutants to reduce variables. The agglomerative method starts with each variable as one cluster and the clusters are merged successively in each step until all variables are merged in one cluster. The open source software R (Version 2.11.1) (Venables et al., 2010) and the package "cluster" (version 1.13.1) were employed (Maechler et al., 2005) in data analysis.

There are several arguments in the "agnes" method,

1) Dissimilarity measurement: metric

The dissimilarity is a measure of the distance between two patterns. It is fundamental to cluster analysis. The dissimilarity metric used here is Euclidean distance,

$$d(x_i, x_j) = \left[\sum_{k=1}^{p}(x_{i,k} - x_{j,k})^2\right]^{0.5}, \quad 9.1$$

where x_i and x_j are the i^{th} and j^{th} rows of a n×p matrix, each row represents an observation and each column represents a variable. $d(x_i, x_j)$ is the Euclidean distance between observations i and j.

2) Sorting method

In agglomerative hierarchical method, the sorting method is a measure of distance between groups of elements, which is used to generate the hierarchy (Lance and Williams, 1966). Among others, there are complete link, single link and average link sorting methods. In complete link, the distance between two clusters is calculated between two

furthest elements. In single link, the nearest two elements in two groups are used. The average link uses the average distance of all elements. The complete link tends to generate tightly bound or compact clusters. Single link suffers from the chaining effect (Nagy, 1968), but it is versatile and can extract concentric clusters (Jain et al., 1999).

9.1.2 Cluster analysis of particulate variables

The cluster analysis of particulate variables was carried out for the measurement between March 14, 2007 and December 17, 2008. Detailed description on the measurement is shown in section 3.2. The variables for cluster analysis were prepared by Dr. Mike Pitz and Dr. Josef Cyrys. First the variables were calculated from number concentration (NC) to length concentration (LC), surface concentration (SC) and mass concentration (MC). Size-segregated LC, SC and MC were calculated from PSD data assuming a spherical shape of particles. In addition, mean particle density of 1.5 g cm^{-3} was assumed (Pitz et al., 2008b) to calculate MC. Equations 9.2 to 9.5 show the calculation method of NC, LC, SC, and MC. They are exponential functions of particle diameter (d_i^x) with x equal to 0, 1, 2 and 3, respectively,

$$NC(d_1 - d_2) = \sum_{d1}^{d2} NC_i, \quad 9.2$$

$$LC\ (d_1 - d_2) = \sum_{d1}^{d2} NC_i \times d_i, \quad 9.3$$

$$SC\ (d_1 - d_2) = \pi \sum_{d1}^{d2} NC_i \times {d_i}^2, \quad 9.4$$

$$MC\ (d_1 - d_2) = \frac{1}{6}\rho\pi \sum_{d1}^{d2} NC_i \times\ d_i^3\ , \quad 9.5$$

where d_1 and d_2 are the lower and upper edge of the size range, respectively. d_i is one of the size bins within the size range $d_1 - d_2$ and ρ is the particle density.

Second, because the PSD data set contains 67 size bins (channels) ranging from 3 nm to 10 µm, it is necessary to combine certain size bins and to reduce the number of size ranges. The size ranges were selected based on the consideration of particle behavior, particle origin and particle deposition in the respiratory tract, which is proposed by Wichmann et al. (2000). As a result NC, LC, SC, and MC were summarized into following size ranges: 3-10 nm, 10-30 nm, 30-50 nm, 50-100 nm, 10-100 nm, 100-500 nm, 100-800 nm, 500-1000 nm, 1000-2500 nm, 2500-10000 nm, 10-800 nm, 3-800 nm,

3-2000 nm, and 3-8200 nm. We subdivided the UFP range into four groups. Range 50-100 nm was introduced because it is considered mainly from agglomerates of particles from combustion processes. Range 3-10 nm was selected because it represents the best particles from nucleation mode. The ranges 10-30 nm and 30-50 nm were chosen because of the increased uncertainty due to electrical charging probability for particles below 30 nm. For particles between 100 nm and 2.5 µm, we subdivided the range into three sections. 100-500 nm was selected due to its likely deposition in the lung, while particles between 500 and 1000 nm are predominantly deposited in the upper respiratory tract. Particles in the range 2500-10000 nm were considered as coarse particles. In addition, the size ranges 10-100 nm and 100-800 nm were introduced to represent the total ultrafine particles and accumulation mode particles, respectively. The cut-points were also selected according to those of previous analyses (Pitz et al., 2011).

Table 9-1 summarizes all variables measured and calculated for the cluster analysis (n=96). Size ranges 10-800 nm, 3-800 nm, 3-2000 nm and 3-8200 nm were included because the upper *aerodynamic diameter* thresholds for PM_1, $PM_{2.5}$ and PM_{10} correspond to 0.8 µm, 2 µm and 8.2 µm *mobility diameter* of the PSD, respectively (Khlystov et al., 2004).

Additionally NC, LC, SC and MC in the same size ranges were also calculated from the PSD after volatilization through a Thermodenuder, which were named with the suffix TD (NC_TD, LC_TD, SC_TD and MC_TD). The TD variables are only available in the size range 10-800 nm. The lower size threshold for particles after Thermodenuder treatment was set to 10 nm because an incomplete removal of volatilized material is possible and this would lead to re-nucleation of gas-phase species in the cooling section of the TD (Birmili et al., 2010).

Table 9-1: Summary of particulate variables measured and calculated between March 14, 2007 and December 17, 2008

PSD variables (n=84)	
Variables	Size ranges
NC, LC, SC and MC	3-10 nm, 10-30 nm, 30-50 nm, 50-100 nm, 10-100 nm 100-500 nm, 100-800 nm, 500-1000 nm, 1000-2500 nm, 2500-10000 nm, 10-800 nm, 3-800 nm, 3-2000 nm, and 3-8200 nm
NC_TD, LC_TD, SC_TD and MC_TD*	10-30 nm, 30-50 nm, 50-100 nm, 10-100 nm 100-500 nm, 100-800 nm, 10-800 nm
Additional variables (n=12)	
TNC, $PM_{2.5}$, $PM_{2.5NV}$, $PM_{2.5V}$, PM_{10}, PM_{10NV}, PM_{10V}, PM_{coarse}, Sulfate, BC, ASC and LC_{EAD}	

*After Thermodenuder treatment

The lower part of Table 9-1 shows the additional variables measured by other instruments. TNC is the total number concentration measured by CPC 3025A. PM mass concentrations together with volatile and non-volatile fractions include $PM_{2.5}$, $PM_{2.5NV}$ (non-volatile $PM_{2.5}$), $PM_{2.5V}$ (volatile $PM_{2.5}$), PM_{10}, PM_{10NV}, PM_{10V} and PM_{coarse} (particle MC in the range of 2.5 to 10 μm, the difference between PM_{10} and $PM_{2.5}$). The other particulate pollutants are particulate sulfate, BC, ASC (active or Fuchs SC) and LC_{EAD} (LC measured by EAD).

The input data for the cluster analysis is a symmetric 96 by 96 Spearman correlation matrix generated from the daily time-series data. Spearman correlation, not Pearson correlation was used due to the non-normal distribution of obtained variables. It contains the signature of the dependency of each variable on all the 96 variables.

For species have different magnitude, standardization should be applied to each column. In this study, no standardization was performed as the data set used is correlation table which is in the range of -1 to 1. I used the Euclidean distance as a measure of the distance

between two variables. I applied the both complete link and the average link methods. The two sorting methods produced the same basic cluster units but there are minor differences in the merging priority or orders. In general, the two methods produced similar results. Because complete link method tends to produce more tightly bound or compact clusters, the results from this method will be discussed in detail.

9.1.3 Positive Matrix Factorization (PMF) analysis

For better interpretation of the meanings of the selected key-variables, the positive matrix factorization (PMF) is used to identify possible particle sources and to build the association between the key-variables and PMF factors. PMF has been successfully applied to PSD data collected at the same monitoring site in Augsburg (Gu et al., 2011; Pitz et al., 2011) and another measurement station in Erfurt in Germany (Yue et al., 2008). PMF 3.0 from the U.S. Environmental Protection Agency (EPA) was used to identify PSD factor profiles and quantify factor contributions.

Detailed description of PMF analysis is shown in Section 7.4. I used hourly mean PSD data covering 64 size bins ranging from 3.8 nm to 8.8 μm (three size bins, 3 nm, 3.4 nm and 10 μm, were excluded because of low data coverage) as input data. The data uncertainty for each size bin was calculated according to Gu et al. (2011). An extra uncertainty of 25% was added to all data points to encompass additional uncertainties arising from the variation of source profiles and physical transformation in the air. Seven size bins, 3.8 nm, 4.3 nm, 4.9 nm, 5.5 nm, 6.9 μm, 7.8 μm and 8.8 μm were poorly modeled and were characterized as "weak" by tripling their uncertainties. Volume profiles were calculated from PSD assuming spherical shape of the particles. In order to choose the right number of factors, a variety of factor numbers were tested and the seven-factor method provided the most meaningful results.

9.2 Results and discussions

9.2.1 Clusters of particulate variables

Figure 9-1 shows the dendrogram of the cluster analysis using 96 variables. The dissimilarity level of the height was set to about 1.7, resulting in 9 clusters, named from "**a**" to "**i**". The information on the numbering of 96 variables is shown in the Appendix C. Table 9-2 shows the nine clusters with all variables included in each cluster. In the following discussion, I use ambient variables representing variables calculated from PSD measured under ambient conditions, while TD variables are variables calculated from PSD after volatilization through a thermodenuder at 300 °C.

Cluster **a** is composed of ambient variables in the size range 30-50 nm, TD variables in the size range 10-30 nm, and NC variables in the summarized size ranges 10-100 nm, 10-800 nm, 3-800 nm, 3-2000 nm, 3-8200 nm, TNC and $LC_{10\text{-}100nm}$. It indicates that the temporal variation of TNC and the summarized particle NC are mostly driven by NC in the size range 30-50 nm. The association between the ambient variables in 30-50 nm and TD variables in 10-30 nm can be explained by the decrease in particle diameter due to volatilization after the passage through the TD (note that a similar shifting could be observed within cluster **c**). Cluster **a** represents the ambient variables in 30-50 nm and total NC.

Cluster **b** consists of ambient variables in the size range 10-30 nm.

Cluster **c** contains TD variables in the size ranges 30-50 nm, 50-100 nm and 10-100 nm, ambient variables in the size range 50-100 nm, LC in the summarized size ranges 10-800 nm, 3-800 nm, 3-2000 nm and 3-8200 nm, $SC_{10\text{-}100nm}$, $MC_{10\text{-}100nm}$, $NC_{100\text{-}500nm}$, $NC_{100\text{-}800nm}$, $NC\_TD_{10\text{-}800nm}$ and $LC\_TD_{10\text{-}800nm}$. As can been seen in Fig. 1, the summarized LC variables (from 10 until 8200 nm), $NC_{100\text{-}500nm}$, $NC_{100\text{-}800nm}$, $SC\_TD_{10\text{-}100nm}$,$MC\_TD_{10\text{-}100nm,}$ and TD variables in the size range 50-100 nm are in one sub-cluster (**c1**). The other variables fall into the other sub-cluster (**c2**). Cluster **c** represents the summarized LC and variables in the size range 50-100 nm.

Cluster **d** consists of all variables except NC in the size ranges 100-500 nm and 100-800 nm, summarized SC and MC variables in the size ranges 10-800 nm, 3-800 nm, 3-2000 nm and 3-8200 nm, $SC\_TD_{10\text{-}800nm}$, $MC\_TD_{10\text{-}800nm}$, PM_{10} and PM_{10NV}. It seems that

particle length, surface and mass concentrations have similar temporal behavior in the size ranges 100-500 nm and 100-800 nm. In spite of this, the SC and MC variables are distributed in respective sub-clusters. As can be seen in Fig. 1, cluster **d** can be divided into two sub-clusters. The first sub-cluster (**d1**) is composed of MC in the size ranges 100-500 nm, 100-800 nm, 10-800 nm, 3-800 nm, 3-2000 nm, and 3-8200 nm, as well as PM_{10} and PM_{10NV}. This indicates that temporal variations of summarized MC variables (in the size ranges 10-800 nm, 3-800 nm, 3-2000 nm and 3-8200 nm) and PM_{10} are mostly driven by $MC_{100\text{-}500nm}$. The other variables in the cluster fall into the second sub-cluster (**d2**), which indicates that the summarized SC variables are relevant to $SC_{100\text{-}500nm}$. Overall, cluster **d** represents SC and MC above 100 nm.

Cluster **e** contains ambient variables in the size range 500-1000 nm, $PM_{2.5,}$ and $PM_{2.5NV}$. It is noticeable that $PM_{2.5}$ (measured by TEOM) is associated with $MC_{500\text{-}1000nm}$, but not with $MC_{3\text{-}2000nm}$ (in cluster **d**). This can be explained by the very high similarity among the summarized MC variables (r: 0.97-0.99). $MC_{3\text{-}2000nm}$ is grouped in cluster **d** instead of cluster e. Cluster **e** represents $PM_{2.5}$ and variables in 500-1000 nm.

Cluster **f** contains BC, $LC_{EAD,}$ and ASC, which are all variables measured by independent instruments. As shown in Fig. 1, LC_{EAD} and ASC are quite similar to each other. Cluster **f** represents combustion related variables.

Cluster **g** consists of ambient variables in the size range 3-10 nm. It represents the nucleation particles.

Cluster **h** contains PM_{coarse}, ambient variables in the size ranges 1000-2500 nm, and 2500-10000 nm. The variables of large particle size fractions 1000-2500 nm and 2500-10000 nm are classified in one cluster and, thereby, represent super-micrometer particle mass concentrations.

Cluster **i** comprises sulfate, $PM_{2.5V}$ and PM_{10V}. Sulfate is a major secondary particulate component. $PM_{2.5V}$ and PM_{10V} are volatile PM fractions (mainly nitrate). Though nitrate was not measured in this study, moderate correlations between nitrate and sulfate could be observed at the same site for other time periods (Gu et al., 2011). This may explain why sulfate is in the same cluster as $PM_{2.5V}$ and PM_{10V}. Cluster **i** represents the secondary aerosols.

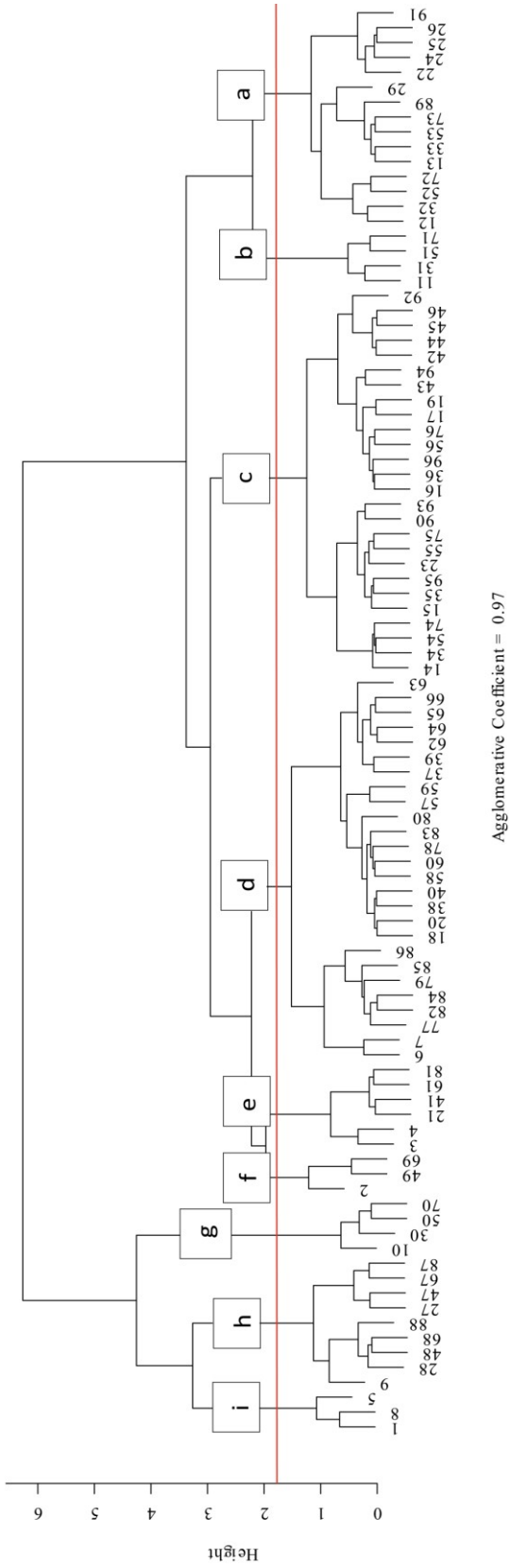

Figure 9-1: The dendrogram obtained from complete link clusters analysis of 96 variables measured at the measurement site in Augsburg in the time period March, 2007 - December, 2008. The height where two clusters are merged represents the distance of the two clusters.

Table 9-2: Clusters and their corresponding variables

Size (nm)	NC	NC_TD	LC	LC_TD	SC	SC_TD	MC	MC_TD
3-10	g		g		g		g	
10-30	b	a	b	a	b	a	b	a
30-50	a	c	a	c	a	c	a	c
50-100	c	c	c	c	c	c	c	c
10-100	a	c	a	c	c	c	c	c
100-500	c	d	d	d	d	d	d	d
100-800	c	d	d	d	d	d	d	d
500-1000	e		e		e		e	
1000-2500	h		h		h		h	
2500-10000	h		h		h		h	
10-800	a	c	c	c	d	d	d	d
3-800	a		c		d		d	
3-2000	a		c		d		d	
3-8200	a		c		d		d	
sulfate	i		BC	f		$PM_{2.5}$	e	
$PM_{2.5V}$	i		LC_{EAD}	f		$PM_{2.5NV}$	e	
PM_{10V}	i		ASC	f		PM_{10}	d	
PM_{coarse}	h		TNC	a		PM_{10NV}	d	

9.2.2 Selecting variables for epidemiological studies

The results of the variable selection are shown in Table 9-3. From the initial 96 variables 15 variables were selected based on the cluster analysis for the use in epidemiological studies. The selection is based on the following principles, 1) the originally measured PSD variables (NC) was preferred over calculated variables (LC, SC and MC), 2) integral variables measured by independent instruments (e.g., BC) were preferred over calculated variables, 3) for UFP, the priority is NC>LC>SC>MC, while for coarse particles, MC has the highest priority, 4) only one key variable was selected to represent one cluster, or two variables were selected to represent two sub-clusters.

Table 9-3: Key-variables selected for epidemiological studies by cluster analysis

Cluster	Key variable	Cluster	Key variable
a	$NC_{30\text{-}50nm}$	e	$PM_{2.5}$
a	$NC_{3\text{-}800nm}$	f	LC_{EAD}
b	$NC_{10\text{-}30nm}$	f	BC
c	$LC_{3\text{-}800nm}$	g	$NC_{3\text{-}10nm}$
c	$NC_{50\text{-}100nm}$	h	$MC_{1000\text{-}2500nm}$
d	$MC_{100\text{-}500nm}$	h	$MC_{2500\text{-}10000nm}$
d	$SC_{100\text{-}500nm}$	i	sulfate
e	$MC_{500\text{-}1000nm}$		

9.2.3 Interpretation of key-variables by means of PMF factors

In order to better understand the physical meaning of the observed clusters, I made a source apportionment analysis of PSD data set using PMF method and analyzed the correlations between variables belonging to different clusters and the PMF factors. Seven factors have been characterized and were associated with re-suspended dust, nucleation particles, fresh traffic emissions, aged traffic emissions, stationary combustion, secondary aerosols and long range transported dust. All factors have very similar profiles as already described by Gu at al. (2011) for an another time period. Briefly, the re-suspended dust factor showed a major volume size distribution peak above 2 µm. The nucleation particles factor showed a major peak <10 nm, and was composed of the smallest particles among all factors. Fresh traffic emissions was mainly composed of particles between 10-40 nm and aged traffic emissions was dominated by particles in the range of 30-100 nm. The stationary combustion factor was mainly in the size range 60-300 nm and 200-500 nm for number size distribution and volume size distribution, respectively. For the secondary aerosols factor a peak at 320 nm for number size distribution and 500 nm for volume size distribution were observed. Whereas for the long range transported dust, a volume peak between 1 and 4 µm was seen.

Table 9-4 shows the range of Spearman correlation coefficients (r) between the temporal variation of all variables in each specific cluster and the PMF factor contributions. Several strong correlations are visible. Cluster **a** is strong correlated with aged traffic emissions factor (r: 0.72-0.91) and the range becomes 0.84-0.91 when excluding TNC. Cluster **b**, composed of ambient variables within 10-30 nm, is strong correlated with

fresh traffic emissions factor (r: 0.93-0.96). For cluster **e**, variables within 500-1000 nm correlate very strong with secondary aerosols (r: 0.95-0.96). Strong correlations are also found for $PM_{2.5}$ and $PM_{2.5NV}$ but to a lesser extent (r: 0.80-0.84), hence this cluster is considered as a good indicator for the secondary aerosols. Cluster **g** is strong correlated with nucleation factor (r: 0.89-0.92), and is considered to represent nucleation particles. Cluster **h** is associated with both the re-suspended dust and the long range transported dust factors. When cluster **h** is divided into two sub-clusters, the picture becomes clearer: variables within 1000-2500 nm are of long range transported dust origin (r: 0.86-0.91), while variables within 2500-10000 nm are of re-suspended dust origin (r: 0.92-0.96).

Table 9-4: Range of Spearman correlation coefficients* between variables belong to each cluster and PMF factors

Cluster (N)	re-suspended dust	nucleation particles	aged traffic emissions	stationary combustion	secondary aerosols	Long range transported dust	fresh traffic emission
a (15)	0.41-0.46	0.09-0.36	**0.72-0.91****	0.47-0.63	0.34-0.52	0.26-0.33	0.55-0.81
b (4)	0.31-0.35	0.44-0.53	0.60-0.68	0.36-0.41	0.42-0.44	<0.3	**0.93-0.96**
c (26)	0.44-0.49	<0	**0.84-0.95**	0.64-0.87	0.43-0.62	0.27-0.33	0.40-0.60
d (26)	0.39-0.53	<0	0.58-0.81	**0.79-0.95**	0.67-0.84	0.19-0.38	0.35-0.49
e (6)	0.28-0.37	<0	0.43-0.51	0.76-0.83	**0.80-0.96**	<0.3	0.31-0.40
f (3)	<0.3	<0	**0.64-0.75**	0.59-0.69	0.53-0.58	0.19-0.32	0.37-0.49
g (4)	<0.1	**0.89-0.92**	<0.3	<0.1	<0.3	<0.1	0.74-0.83
h (9)	**0.50-0.96**	<0	0.42-0.51	0.31-0.35	0.11-0.39	**0.51-0.91**	<0.3
i (3)	<0.2	<0	0.24-0.33	0.59-0.72	**0.73-0.77**	<0.1	<0.3

*The correlation coefficients were calculated between the daily averages of all 96 variables and daily averages of the factor contributions for each of the PMF factors separately. The correlations were then grouped by clusters and their ranges were shown in this table. The correlation was artificially classified as strong, moderate and weak for correlation coefficient r >= 0.80, 0.50 <= r < 0.80 and 0.30 <= r < 0.50, respectively.

**Correlation coefficients in bold represent the strongest correlations of PMF factors with one cluster.

For cluster **c,** variables in first sub-cluster (**c1**, described in 3.1) show strong correlations with aged traffic emissions (r: 0.84-0.92) and mostly strong correlations with stationary combustion factor (r: 0.74-0.87). The second sub-cluster (**c2**) including TD variables

within 30-50 nm and ambient variables within 50-100 nm etc. show strong correlations with aged traffic emissions (r: 0.93-0.95) and moderate correlations to stationary combustion (r: 0.64-0.69).

Cluster **d** contains 26 variables and can be divided into two sub-clusters. The first sub-cluster (**d1**, described in 3.1) comprises MC in the nm size ranges 100-500, 100-800, 10-800, 3-800, 3-2000 and 3-8200, PM_{10}, and PM_{10NV}.These variables are strong correlated with both stationary combustion and secondary aerosols (except PM_{10} and PM_{10NV}, r: 0.71-0.76). The second sub-cluster (**d2**) is strong correlated with stationary combustion and moderately correlated with secondary aerosols.

There are two clusters not strong correlated with PMF factors. Cluster **f**, composed of BC, LC_{EAD} and ASC, is moderately correlated with aged traffic emission (r: 0.64-0.75), stationary combustion (0.59-0.69) and secondary aerosols (0.53-0.58). BC has moderate correlations with aged traffic, stationary combustion and secondary aerosols (r=0.64, 0.59, 0.58, respectively). Compared with winter 2006-2007 (Gu et al., 2011), BC was more strongly correlated with stationary combustion (r=0.87) and secondary aerosols (r=0.85), followed by aged traffic (r=0.77). It seems that in winter 2006-2007, the stationary combustion, other than traffic emission, was the most important contributor to BC. While in a longer time period (e.g., two years in this study), traffic and combustion emissions were both moderately correlated with BC. Cluster **i**, consisting of sulfate, $PM_{2.5V}$ and PM_{10V} is moderately correlated with the secondary aerosols (r: 0.73-0.77). Because the PMF factors were obtained from PSD data, stronger correlations were observed between the PSD variables (NC, LC, SC and MC) and the PMF factors while variables measured with independent measurement methods (e.g. BC, sulfate, $PM_{2.5}$, PM_{10}) showed weaker correlations with PMF factors.

Based on the above correlation analysis, the selected key-variables as well as their associated sources are presented in Table 9-5. 15 out of the total 96 variables were selected by the cluster analysis and each lead variable is associated with PMF factors or with variables already widely used in epidemiological research.

Table 9-5: Key variables selected to represent each cluster for epidemiological studies and their associated sources

Cluster	Key variables	Associated sources
a	$NC_{30\text{-}50nm}$; $NC_{3\text{-}800nm}$	aged traffic emissions; submicron NC
b	$NC_{10\text{-}30nm}$	fresh traffic emissions
c	$LC_{3\text{-}800nm}$; $NC_{50\text{-}100nm}$	aged traffic emissions and/or stationary combustion; aged traffic emissions
d	$MC_{100\text{-}500nm}$; $SC_{100\text{-}500nm}$	stationary combustion and/or secondary aerosols; stationary combustion
e	$MC_{500\text{-}1000nm}$; $PM_{2.5}$	secondary aerosols; $PM_{2.5}$
f	LC_{EAD}; BC	aged traffic emissions; aged traffic emissions and/or stationary combustion
g	$NC_{3\text{-}10nm}$	nucleation particles
h	$MC_{1000\text{-}2500nm}$; $MC_{2500\text{-}10000nm}$	long range transported dust; re-suspended dust
i	sulfate	secondary aerosols

9.3 Conclusions

Size segregated particle NC, LC, SC and MC were calculated from PSD data ranging from 3 nm to 10 μm. In combination with other measured particulate pollutants, 96 different variables for particle characterization were obtained. Agglomerative hierarchy cluster analysis was applied to the whole data set for selecting the key-variables for using in epidemiological analysis. The cluster analysis yielded nine clusters and fifteen parameters were selected, which were believed to best represent each cluster. The relationship between the selected variables and sources were studied by correlation analysis with PMF factors using PSD data. It is demonstrated that cluster analysis is capable of exposure data reduction in terms of using the data in epidemiological studies. It is planned to apply this exposure data reduction method for future epidemiological studies, particularly in the KORA study area.

10 Personal measurement of $PM_{2.5}$, black carbon and particle number concentration in different microenvironments

Personal exposure describes the air pollution levels that a person is in contact with. Epidemiologic studies focus on the personal exposure other than airborne concentration. However, due to the difficulty in accurately assessing the personal exposure among a population, the ambient air pollutants from air quality monitoring networks were often used to approximate the exposure. In most cases, this is appropriate, especially for $PM_{2.5}$ mass concentration and regional aerosols. In spite of this, for air pollutants which are highly variable spatially, personal exposure can differ substantially from stationary measurement. Furthermore, individuals with different daily activity patterns will undergo different microenvironments, thus lead to variations in exposure within a population.

In order to assess the personal exposure in different microenvironments in urban area, personal measurements to $PM_{2.5}$, BC and NC were carried out in a set of pre-designed scenarios. The scenarios were designed as exposure as a pedestrian in traffic, urban background areas, industrial area and home heating area, as well as a passenger in public transport. $PM_{2.5}$, BC and NC were also measured concurrently in a stationary measurement site in urban background area.

In this chapter, personal exposures to $PM_{2.5}$, BC and NC under different scenarios are described. The personal and stationary measurements are compared in different scenarios. Finally the question that how well the stationary measurement can represent the daily personal exposure is discussed respectively for $PM_{2.5}$, BC and NC.

Because the “microenvironments” measured here may contain several sub-microenvironments, the term “scenario” is used hereafter.

10.1 Methods

A microenvironment-targeted personal measurement has been carried out in Augsburg. The tester carrying personal monitors goes through the same designated routes as a pedestrian every day.

10.1.1 Measurement period

The personal measurements were carried out in winter, spring and summer in 2011, respectively to account for the seasonal variation. Measurements lasted 3 weeks (working days) in each season: February 8-25, 2011 in winter, May 2-20, 2011 in spring and July 12-29, 2011 in summer. In total, 45 days' measurements were obtained. The measurement started at about 8:00 am and ended at about 2:00 pm each day.

10.1.2 Scenarios

The measurement was controlled for the pre-designed routes and scenarios, as well as measurement time. Figure 10-1 shows the personal measurement scenarios and the routes. During the 6 hours' sampling period, exposure to 5 major scenarios was measured. The scenarios include A) traffic-related exposure; B) exposure in public transport; C) urban background exposure; D) exposure in industrial area and E) exposure in an area dominated by residential heating. The exposure was measured as pedestrian in all scenarios except in public transport.

Scenario A is exposure along major roads as pedestrian in city centre. In order to differentiate the traffic pollution at morning rush hour and non-rush hours, it was measured twice each day, with one in the morning (A1, ~8:00-8:30 am) and the other in the afternoon (A2, ~1:00-1:30 pm). Scenario C is comprised of two urban background areas with one locates in southwest of the city (C1) and the other locates in northeast of the city (C2), representing upwind and downwind urban background areas, respectively. Scenario D is exposure in the industrial area of Augsburg as pedestrian. Scenario E is locates in a residential area but it is considered to be affected greatly by home heating in winter season. Exposures in scenario A, C, D and E were measured as a pedestrian. Scenario B, the public transport, connected the above scenarios. The major public transport is by tram (B1), except the route between C2 and D which was achieved by bus

(B2). Meanwhile, the activities in indoor environments (café and fast food) were also recorded whenever possible.

Each scenario (A1, C1, C2, D, E, A2) was measured for about 30 minutes. Scenario B accounted for about 100 minutes each day. A field protocol was kept to record the start and end time of each scenario.

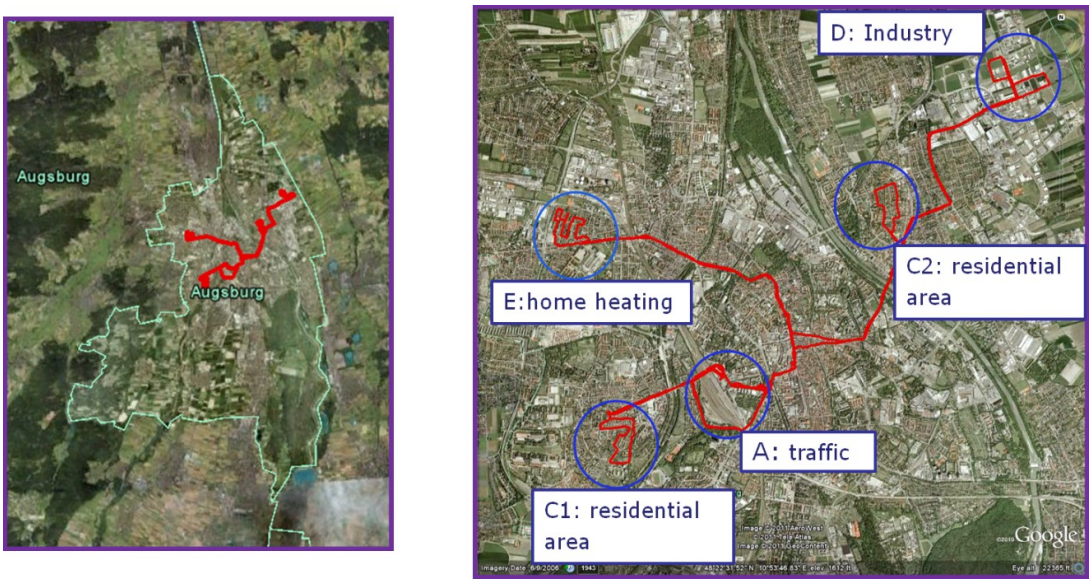

Figure 10-1: Personal measurement routes and scenarios in city Augsburg.

10.1.3 Measurement devices

$PM_{2.5}$ mass concentration, black carbon (BC) and particle number concentration (NC) in the range of 0.01-1.0 µm were measured continuously by portable devices. Personal temperature and relative humidity were also measured by a sensor. Each device can provide real time, 1-minute high resolution data. In addition, a GPS device was used to record the location of the tester. Figure 10-2 shows a picture of the portable devices installed in a bag for the personal measurement.

$PM_{2.5}$ mass concentration was measured by a personal aerosol monitor (pDR-1500, Thermo Scientific, U.S.). It is a sensitive nephelometric monitor which can measure PM mass concentration from 1 µg m^{-3} to 400 mg m^{-3}. The device is factory calibrated against master real-time monitors, which had been adjusted to agree with the reference mass concentration obtained from measurement of gravimetric filters. The test dust used for

the factory calibration is SAE Fine supplied by Power Technology, Inc. It has mass median aerodynamic particle diameter from 2-3 μm, bulk density of 2.60-2.65 g cm^{-3} and a refractive index of 1.54. The pDR-1500 can also be calibrated gravimetrically for a particular aerosol in field conditions. However, such calibration requires a mass collection of 1 mg. In the ambient condition of low PM concentrations, it needs over 300 hours to collect 1 mg of particles. Thus in this study the pDR-1500 monitor was running besides the TEOM (advanced $PM_{2.5}$ monitor) at the central monitoring station concurrently before and after the each personal measurement. The $PM_{2.5}$ measured from TEOM was used to calibrate the pDR-1500 personal monitor.

Figure 10-2: Portable devices measuring $PM_{2.5}$, black carbon and particle number concentration in the personal measurement (left: $PM_{2.5}$, right: number concentration, the other one: black carbon).

BC was measured by a microAeth black carbon monitor (model AE51, Magee Scientific Corporation, U.S.). It measures BC based on the light absorbance (or "Attenuation") method. The aerosol sample was collected on a small area of a quartz filter. A stabilized LED emitted light at 880 nm onto the filter and a detector measured the light attenuation at the sampling spot with respect to a spot where no aerosol was collected. The accumulative attenuation was measured and the microprocessor calculated the real time BC mass concentration in ng m^{-3}.

NC was measured by a condensation particle counter (CPC 3007, TSI Corporation, U.S.). The CPC draws the aerosol sample through a heated saturator where alcohol evaporates and is saturated. The aerosol sample then passes through a condenser where alcohol condensed on the particles and the particle size grows to an extent that can be counted by a laser counter. CPC3007 is driven by 6 AA batteries. Each time a fully soaked Propanol felt cartridge is inserted in the instrument to ensure enough alcohol is provided during measurement. From previous experience the CPC3007 can measure reliable NC concentrations for 6 hours without replacing batteries and Propanol cartridge.

In addition, concurrent $PM_{2.5}$, BC and NC concentrations were measured at a stationary site (UAS site) in an urban background area of Augsburg. Detailed description on the stationary measurement can be seen in section 3.2.

10.1.4 Data correction

Personal devices have been compared with stationary devices before and after each measurement. Each comparison was conducted at the UAS site with personal devices and stationary instruments running simultaneously for about one week.

In order to correct the personal devices against the more advanced stationary instruments, as well as for a direct comparison between personal and stationary measurements, the personal and stationary measurements were compared with each other through logarithmic regression by Dr. Veronika Fensterer. These regression equations act as the final data correction standards in this project, and were used to correct the personal measurement. Detailed correction equations are shown Table 10-1.

Table 10-1: logarithmic correction equations between personal and stationary measurement

Personal measurement (X)	Stationary measurement (Y)	Correction equation
$PM_{2.5}$_p	$PM_{2.5}$_ s	Y= EXP (1.452+0.572×LN(X))
BC_p	BC_s	Y= EXP (0.264+0.802×LN(X))
BC_demo_p*	BC_ s	Y= EXP (0.883+0.467×LN(X))
NC_1_p **	NC_ s	Y= EXP (1.113+0.928×LN(X))
NC_2_p	NC_ s	Y= EXP (1.169+0.924×LN(X))

* BC_demo_p device was only used in winter measurement: BC_p was used in spring and summer.
**NC_1_p was used in winter and summer measurement: NC_2_p was used in spring measurement.

10.2 Results

10.2.1 Descriptive statistics of personal measurement

Figure 10-3 shows the box plots of $PM_{2.5}$, BC and NC under different scenarios in each season. The overall average $PM_{2.5}$ mass concentrations were 33.46, 17.48 and 9.86 μg m^{-3} in winter, spring and summer respectively. Much higher $PM_{2.5}$ mass concentrations were found in winter compared with in spring and summer. This can be explained by the adverse meteorology and additional residential heating in winter. $PM_{2.5}$ showed relatively small differences among different scenarios except in indoor environment (study center: SC). The average $PM_{2.5}$ mass concentrations in different scenarios (not including scenario SC) were in the range of 32.4 - 38.2 μg m^{-3} in winter, 16.4 – 19.9 μg m^{-3} in spring and 7.9 - 11.3 μg m^{-3} in summer.

BC showed a trend with high concentration in winter, and low concentrations in spring and summer. The overall average BC concentrations were 4.57, 2.91 and 2.70 μg m^{-3} in winter, spring and summer respectively. Unlike $PM_{2.5}$ which has minor differences among scenarios, BC showed large differences. In winter high concentrations were observed in morning traffic (A1) and bus (B2). BC concentrations in trams (B1) and traffic in the afternoon (A2) were also elevated (though not as much as in A1 and B2) compared with urban background scenarios (C1 and C2). In spring and summer, BC concentrations in traffic and public transport scenarios (A1, A2, B1 and B2) were significantly higher than urban background and industry microenvironments (C1, C2, D and E).

NC showed highly variable concentrations among scenarios. Highest number concentrations were observed in morning traffic (A1), except in winter when FF scenario also showed very high number concentrations. A factor of 2-3 can be seen for number concentrations between traffic (A1, A2) and urban background scenarios (C1, C2). Lowest concentrations were observed in study center (SC) in winter and spring and in upwind urban background (C1) in summer.

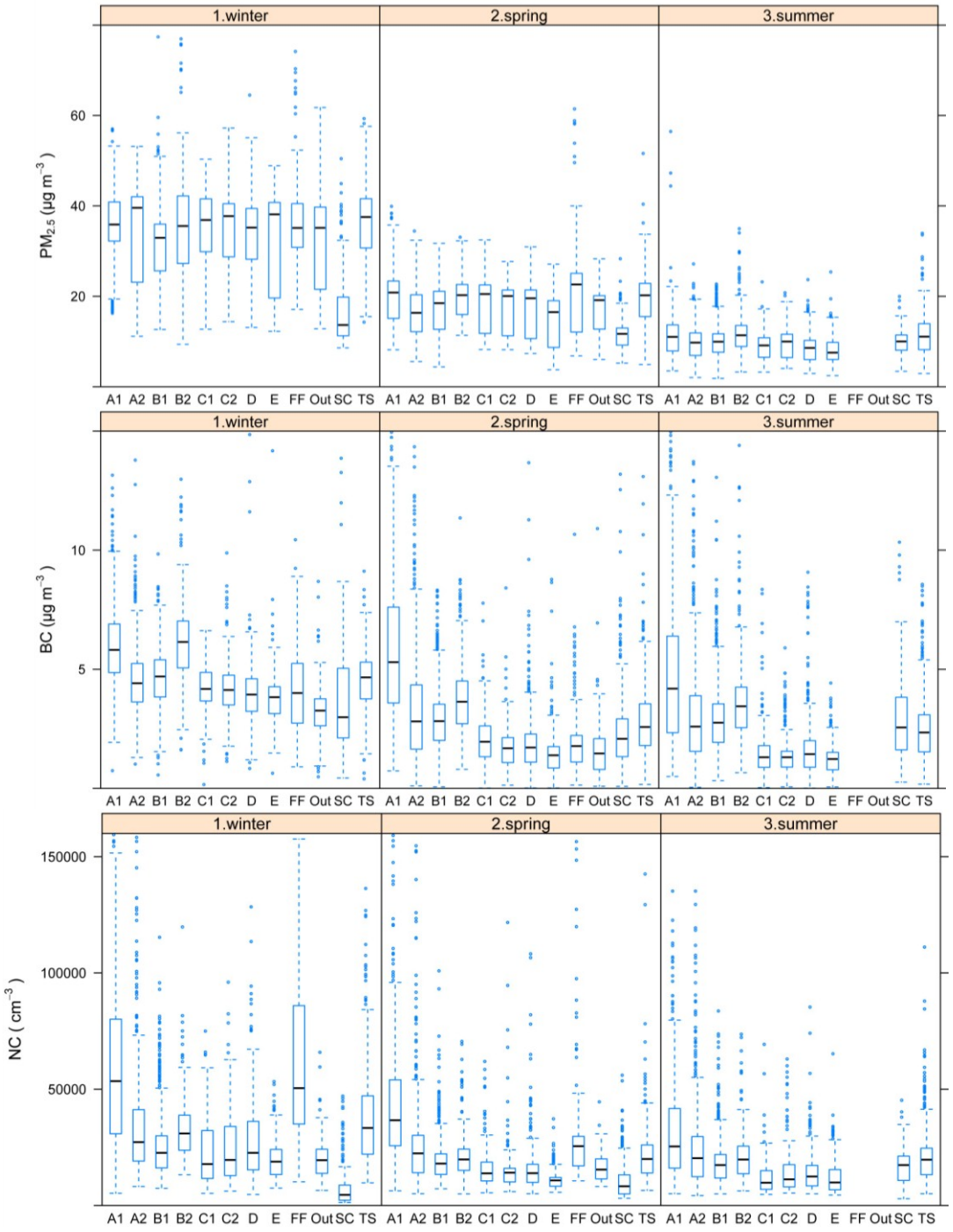

Figure 10-3: Box plots of $PM_{2.5}$, BC and NC concentrations at different scenarios in winter, spring and summer. Data points used are 1-minute in resolution. "FF" indicates the fast food scenario including Bakery and Burger King. Scenario "Out" represents the outdoor in urban background other than C1 and C2. "SC" is the scenario in the study center, normally before 8:00 am and after 1:30 pm for measurement preparation and data download. "TS" is the scenario at tram stations waiting for trams and sometimes buses.

10.2.2 Temporal variation of air pollutants

Figure 10-4 shows the averaged temporal variations of personal and stationary measured $PM_{2.5}$, BC and NC which were averaged for all measurement days (45 days). The frequencies of major scenarios are also shown (0-45).

$PM_{2.5}$ mass concentration at stationary site showed a decreasing trend from morning to the afternoon. The personal $PM_{2.5}$ was overall higher than stationary $PM_{2.5}$, but the increment was quite limited. Moreover, the increment seems independent on the scenarios. As shown in Figure 10-4, the relative increment of personal $PM_{2.5}$ in traffic scenarios (A1 and A2) are similar with in urban background scenarios (C1 and C2).

Stationary BC also showed a slightly decreasing trend from morning to afternoon. Averaged personal BC was higher than stationary BC throughout the time. Personal BC was highly elevated compared with stationary BC at traffic scenarios (A1 and A2). In contrast, the increment was rather small at urban background scenarios (C1 and C2) and home heating scenario (E). Elevated BC was also found in industry scenario (D) and in bus (B2) around 10:30 and 11:10. Personal BC concentrations in trams were relatively higher than in urban background scenarios like C1, C2 and E.

Averaged stationary NC showed a slightly decreasing trend from morning to afternoon. In contrast, personal NC is very dependent on the scenarios. Great NC increase (personal vs. stationary) was observed in morning and afternoon traffic (A1, A2) and fast food (FF) scenarios. Personal NC in scenario C1, C2 and E was less increased or comparable with stationary NC.

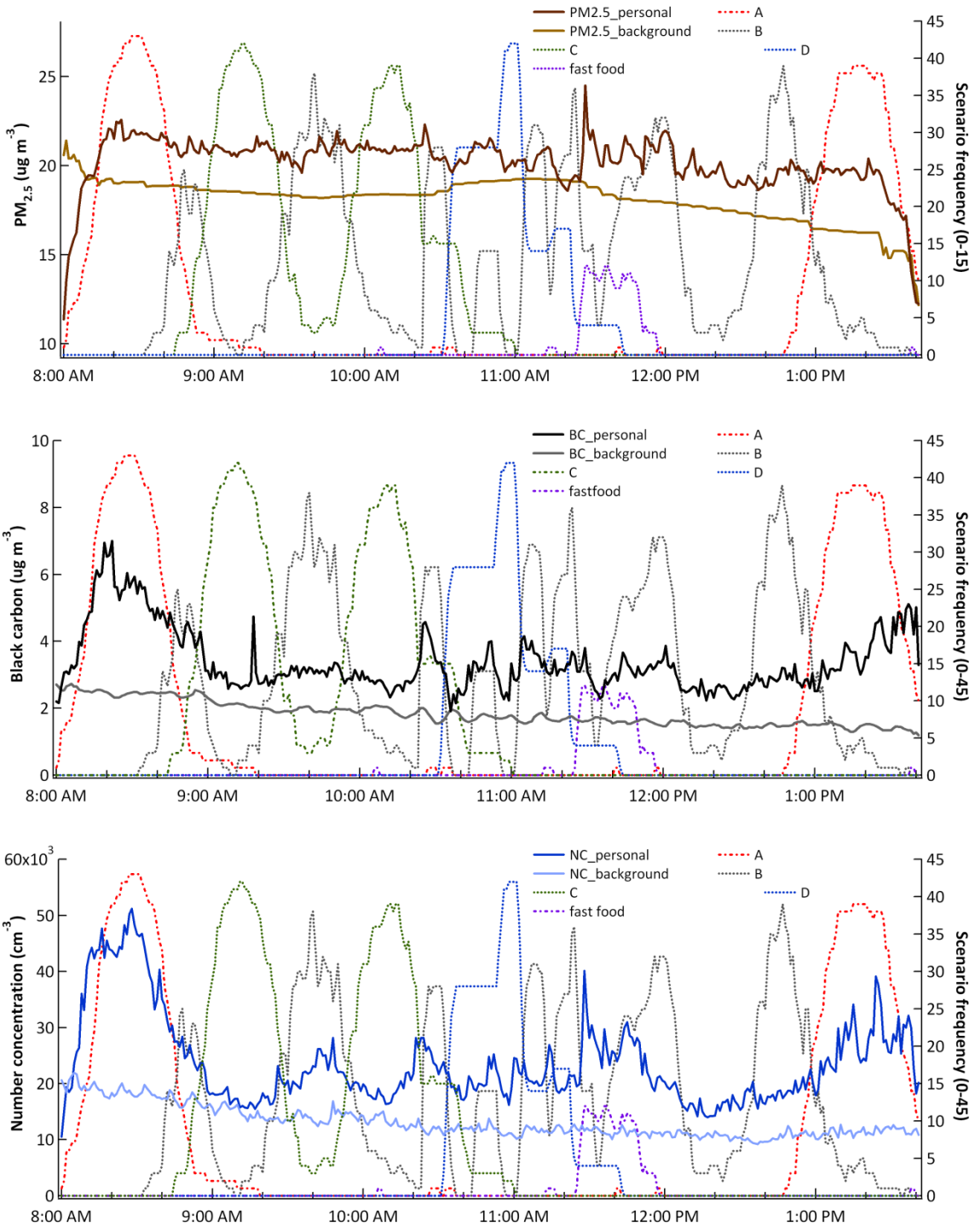

Figure 10-4: Temporal variations of $PM_{2.5}$, BC and NC concentrations from personal measurement and stationary measurement, as well as scenarios frequencies. Data of the same time of day were averaged and a total of 45 days were used.

10.2.3 Ratio of personal to stationary measurement

Table 10-2 shows the ratios of average personal measurement to stationary measurement (short for ratios) under different scenarios. $PM_{2.5}$ showed ratios ranged from 0.98-1.13 (including indoor environment) in winter for all scenarios. It indicated that $PM_{2.5}$ was most insensitive to scenarios in winter and the personal $PM_{2.5}$ mass concentrations were all very close to stationary $PM_{2.5}$. The situation changed substantially in summer when $PM_{2.5}$ in traffic scenarios (A1 and A2) were 1.77 and 2.0 times of stationary $PM_{2.5}$, indicating that traffic emission added a big part to background $PM_{2.5}$ in summer. In contrast, $PM_{2.5}$ in Industry (D) and urban background (C2 and E) scenarios was similar with stationary $PM_{2.5}$ in all three seasons.

Table 10-2: ratios of personal measurement to stationary measurement of $PM_{2.5}$, BC and NC under different microenvironments and seasons

Scenarios	$PM_{2.5}$			BC			NC		
season	winter	spring	summer	winter	spring	summer	winter	spring	summer
A1	1.10	1.17	1.77	1.72	2.94	3.49	2.46	2.74	2.56
A2	1.08	1.22	2.01	2.03	3.37	3.12	2.75	2.28	2.54
B1	0.98	1.15	1.52	1.73	2.05	2.27	1.48	1.68	1.79
B2	1.13	1.24	1.49	2.29	2.92	3.36	2.08	2.18	2.09
C1	1.05	1.14	1.40	1.20	1.25	1.03	1.04	1.25	0.91
C2	1.08	1.12	1.08	1.47	1.15	1.09	1.33	1.42	1.34
D	1.04	1.09	1.02	1.47	1.58	1.58	1.59	1.65	1.57
E	1.04	1.10	1.27	1.59	1.32	1.17	1.49	1.02	1.49
FF	1.05	1.38	-	1.63	1.66	-	5.67	3.26	-
outdoor	1.09	1.10	-	1.36	1.26	-	1.32	1.69	-
TS	1.08	1.25	1.59	1.65	2.00	1.93	2.23	1.94	1.74
SC	0.57	0.77	1.42	1.22	1.40	1.97	0.41	0.71	1.28

BC showed high ratios between personal and stationary measurements in traffic and public transport scenarios. In general, the ratios in traffic and public transport scenarios were higher in warmer seasons and lower in cold season. BC in industrial scenarios was about 50% higher than stationary BC. Lower ratios were observed in urban background scenarios (C1, C2 and E). The BC ratios in home heating scenario (E) decreased from winter to summer (1.59–1.17), which can be explained by the more frequent use of fuel combustion for home heating in colder seasons. Same trend was also observed for

scenario C2, which was also likely influenced by home heating. BC in fast food (FF) scenario was about 63-66% higher than stationary BC. BC exposure in tram stations (TS) was 65%-100% higher than stationary BC.

High NC ratios of personal to stationary measurement were observed in traffic (A1 and A2), bus (B2) and tram station (TS) scenarios. Extraordinary high ratios were found in fast food (FF) scenario, compared with low ratios found in study center (SC), which is also indoor scenario. It indicated that food preparation is a very important NC source for indoor environment. NC in upwind urban background (C1) was less elevated compared with downwind background (C2). NC in industrial area (D) was about 50% higher than stationary NC.

One thing should be noted that for the scenario SC, much higher ratios were observed in summer compared with in winter and spring. This can be partly explained by the room ventilation. As in winter and spring, window in the study center was less frequently opened, while in summer window was opened more frequently for better ventilation and cooling. Considering the study center is located in city center and next to major roads, ventilation can be an important factor determining the indoor concentrations. However, no ventilation record was kept thus this is rather an exploratory explanation.

10.2.4 Correlation between personal and stationary measurement

Figure 10-5 illustrates the scatter plots of daily averaged personal and stationary measurements for $PM_{2.5}$, BC and NC. $PM_{2.5}$ showed a strong correlation between stationary measurement and personal measurement. The linear regression showed an intercept of 5.6 $\mu g\ m^{-3}$ and a ratio of 0.8, with R^2 equals 0.93. This demonstrates that personal exposure to $PM_{2.5}$ is generally in good agreement with stationary $PM_{2.5}$. This is supported by the ratios between personal and stationary measurement (near to 1) which was described in 10.2.3.

BC also showed a strong correlation between stationary and personal measurement, indicating that average BC exposure can be well approximated by stationary measurement. However, combining other information from 10.2.1-10.2.3 that BC is highly variable in different scenarios, the agreement between stationary measurement and personal exposure may be undermined when individuals change the activities.

NC showed a weaker correlation between stationary measurement and personal exposure. The linear regression showed an intercept of 11795 cm^{-3} and a slope of 0.88 with R^2 equals 0.63. Average personal exposure to NC is not well approximated by stationary measurement.

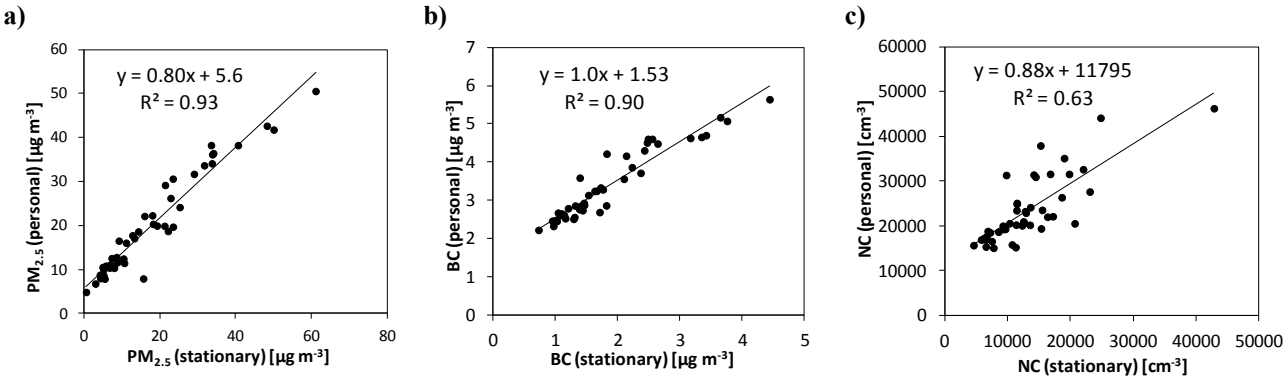

Figure 10-6: Scatter plots and linear regression of daily averaged concentrations of personal measurements and corresponding stationary measurement of $PM_{2.5}$, BC and NC concentrations. The data points are average of daily measurement and a total of 45 days were obtained for each species.

10.3 Discussions

The personal measurement in different scenarios was confined with pre-designed sequences. The measurement for each scenario was not undertaken simultaneously but in sequence. Thus the measured exposure to each scenario can be affected by the diurnal pattern of meteorology. Scenario A1 and A2 were measured at the same route but at different time. Exposures in scenario A1 were always higher in A2, particularly for BC and NC. The difference can be partially explained by the average diurnal variation of background concentrations. For $PM_{2.5}$, the average stationary concentration decreased from ~20 µg m^{-3} at 8:00 am to about ~15 µg m^{-3} at 13:30, indicating a decrease of 25%. For stationary measured BC and NC, a decrease of 40% was estimated from morning to afternoon. Thus in addition to look at the absolute personal exposure, it is important to discuss personal exposure together with stationary measurement, such as Figure 10-4 and

Table 10-2. By calculating the ratio of personal exposure to stationary measurement, the impact of meteorology on scenario exposure can be largely eliminated.

In general, high exposures were found in traffic and public transport scenarios. Interestingly, the ratios between personal and stationary measurement for $PM_{2.5}$ and BC had an increasing trend from winter to spring to summer. Much Higher ratios for $PM_{2.5}$ and BC were observed in summer than in winter. Assuming the traffic density and emission inventory kept roughly the same from winter to summer, the major differences were the urban background concentrations (from stationary measurement) between winter ($PM_{2.5}$: 32.3 μg m^{-3}; BC: 2.8 μg m^{-3}) and summer ($PM_{2.5}$: 7.0 μg m^{-3}; BC: 1.3 μg m^{-3}). Then the percentage of mass added by traffic emission should be less in winter compared with in summer. Ratio of NC, in contrast, did not show clear trend from winter to summer and it seems that above explanation for mass concentrations of $PM_{2.5}$ and BC is not suitable for number concentration.

Here both personal exposure and stationary measurement were conducted. Overall how well the stationary measurements represent the personal exposure on the daily basis? From the summarized daily average between personal and stationary measurement, $PM_{2.5}$ and BC from stationary measurement were highly correlated with personal exposure, while personal NC was moderately correlated with stationary measurement. When looking at the absolute concentration level, $PM_{2.5}$ showed rather small differences between personal and stationary measurement. For BC, a factor of 1.6-2.1 (by season) was observed between personal and stationary measurement. While for NC, this factor was 1.78. This demonstrates that stationary $PM_{2.5}$ is a good indicator of personal $PM_{2.5}$, both for temporal variation and absolute concentration. Personal NC is not well represented by stationary NC, neither temporal variation nor absolute concentration. Stationary BC is in good agreement with personal BC in terms of temporal variation (correlation) but there exists large discrepancies in absolute concentrations.

10.4 Conclusions

Personal measurement of $PM_{2.5}$, BC and NC were carried out in different pre-designed scenarios by a tester as pedestrian and through public transport in city Augsburg in three seasons (winter, spring and summer) in 2011. In the same time, $PM_{2.5}$, BC and NC were also measured at a stationary site in urban background of Augsburg.

Personal $PM_{2.5}$ and BC showed high concentrations in winter and low concentrations in spring and summer. Small differences were found for $PM_{2.5}$ among scenarios while BC and NC were highly variable among scenarios. High BC and NC concentrations were associated with traffic and public transport scenarios (A1, A2, B1 and B2). Low concentrations were found in urban background scenarios.

Personal $PM_{2.5}$ showed limited increase relative to stationary $PM_{2.5}$ in all scenarios. This is particularly significant in winter when ratios (personal: stationary) for all scenarios were in the range of 0.98-1.10. Personal NC and BC were highly elevated in traffic and transport scenarios compared to stationary measurement (with ratios from 1.5-3.5).

On a daily average basis, stationary $PM_{2.5}$ is a good indicator of personal $PM_{2.5}$, both in correlation and absolute concentration. Daily averaged stationary BC correlated well with personal BC, but there is a large discrepancy in absolute concentrations, however stationary BC underestimated the personal exposure to BC. Stationary NC correlated moderately with personal NC, but underestimated the personal exposure to NC substantially.

11 Summary and outlook

This thesis utilizes a huge dataset collected at the aerosol measurement sites in Augsburg. The analyses focused on the identification of the main sources for ambient particulate matter in Augsburg for a better understanding of the temporal variation of PM concentration. In addition the spatial variation of the source structure was analyzed. An important part of this thesis is dedicated to the relatively new approaches of source apportionment (PMF based on particle size distribution data) and comparison with the more traditional PMF analysis applied on particulate chemical composition data. A development of a method for data reduction of particulate variables in order to select key variables for the use in epidemiological study was a further focus of this thesis. Last but not least I presented the measurement of personal exposure to particulate pollutants under different microenvironments in urban area.

In the beginning I used data collected at the aerosol measurement site for a general description of the air quality in Augsburg and I analyzed the concentrations and variations of particulate pollutants in four winter seasons. It indicated that the four winters (2004-2008) can be grouped into two groups, the cold winters (2004/05 & 2005/06) and warm winters (2006/07 & 2007/08). PM mass concentration, sulfate, nitrate and BC showed higher concentrations in cold winters than in warm winters. NC, PAHs and BC was highly elevated in morning rush hour on weekdays but no elevations in weekends, indicating the great impact of traffic emissions to NC, PAHs and BC on working days.

Source apportionment analyses using positive matrix factorization (PMF) model were carried out for both particulate chemical composition (PCC, at urban traffic site) and particle size distribution (PSD, at urban background site) data. In general, six PCC factors were obtained and were associated with secondary nitrate, secondary sulfate, residential and commercial combustion, NaCl deicing agent, re-suspended dust and traffic emission. Seven PSD factors were characterized and were associated with re-suspended dust, fresh traffic emission, aged traffic emission, stationary combustion, long range transported dust and secondary aerosols. The factors from two methods (PCC and PSD) were compared with each other in winter 2006/07. Both methods produced four similar pairs of factors.

Traffic factors and re-suspended dust factor showed weak agreement due to the influence of local traffic emissions, whereas secondary aerosols, which are mostly originated from long-range transport, showed a better temporal agreement and a minor spatial discrepancy.

The temporal and spatial variations of particulate sources were evaluated by source apportionment of PCC data from eight sampling sites across the urban area. Six factors were obtained of which secondary nitrate and secondary sulfate factors showed high temporal and spatial consistencies. On the contrary, traffic emission showed the greatest temporal and spatial variability. Other factors which were associated with traffic (re-suspended dust, NaCl de-icing agent) were also elevated at the sites with high traffic density. Residential and commercial combustion factor was in general distributed homogeneously across the urban area.

The measurement of particulate matter in Augsburg yielded a number of (96) particulate variables including size segregated particle NC, LC, SC and MC, and other continuously measured particulate pollutants. Agglomerative hierarchy cluster method was used to the whole data set for selecting the key-variables for using in epidemiological study. Nine clusters were produced and among which fifteen variables were selected, which were believed to best represent each cluster. For a better understanding of selected variables, the relationship between the selected variables and particle sources were studied by correlation analysis with PSD source factors. The cluster analysis is proved to be an effective way for data reduction.

Due to the great spatial variability of certain particulate sources, as well as to assess the personal exposure in different microenvironments in urban area, personal measurements to $PM_{2.5}$, BC and NC were carried out in a set of pre-designed scenarios. Limited differences were found for personal exposure to $PM_{2.5}$ mass concentrations among different scenarios. $PM_{2.5}$ mass concentrations are more likely driven by meteorology which varies with seasons. BC and NC, in contrast, were highly elevated in traffic and public transport scenarios (especially morning traffic and bus), and were comparable to stationary measurement in urban background scenarios. On the daily average basis, stationary $PM_{2.5}$ is a good indicator for personal $PM_{2.5}$, both in temporal variations and

absolute concentrations. Stationary BC and NC underestimated the personal exposures to BC and NC substantially.

By summarizing the thesis I found the following points which deserve further study.

1) Source apportionment with a combination of PCC and PSD data. A combination of PCC and PSD in source apportionment model is not suitable in this thesis as both data sets were measured at different types of measurement stations. However, it may yield some new sources combining both data sets, when PCC and PSD were measured at the same site.

2) Comparing PCC and PSD factors at the same measurement site. In the thesis I compared PCC and PSD factors at different measurement sites. In spite of this, a direct comparison of PCC and PSD factors at the same measurement site is preferred in the future. This will give even more confidence of how well the two methods agreed with each other.

3) Development of further methods for data reduction and comparison with the cluster analysis. I used cluster analysis for reducing the data dimensions and to select the key variables for epidemiological study. The comparison between cluster analysis and other methods are welcomed. Not shown in the thesis, but the comparison between cluster analysis and heat map is in process. Some other methods like partial correlation analysis also deserve trying.

4) Geographic visualized personal exposure. The personal exposure measurement recorded the geographic coordinates but such information has not been incorporated in the personal exposure. The combination of personal exposure, geographic coordinates or even land use information, could provide further understanding on the personal exposure.

Appendix

A. The sensitivity analysis of Potassium in winter 2006/07

This source apportionment result of residential and commercial combustion factor in winter 2006/07 differs from what has been found using levoglucosan and K as tracers of wood combustion, which assumed almost all K was emitted from wood combustion (Schnelle-Kreis et al., 2010). A sensitivity analysis of K was carried out to evaluate the K in this factor in winter 2006/07. First, PMF was run with K excluded (No_K). Second PMF was run with the K signal/noise (S/N) ratio increased from original value of 3.6 to 9.8 by decreasing the uncertainties (50 to 20 ng m^{-3}) and error fractions (8% to 4%), while other settings remained the same (High_K). The factor contributions from above two methods were compared with the results from the base run. In addition, correlation analyses were conducted between this factor and major species contained in the factor. The correlation coefficients are shown in table 3.

Table A1: Spearman correlation coefficients between residential and commercial combustion factor from different methods and major chemical species

Methods	No_K	High_K	base run	Cd	K	Pb	Zn	LEV	EC	OC
No_K		0.84	0.99	**0.85** [b]	0.70	0.70	0.69	0.74	0.74	0.76
High_K	0.84		0.84	0.83	0.85	0.81	0.70	**0.89**	0.73	0.81
base run	0.99	0.84		**0.85**	0.70	0.70	0.68	0.76	0.72	0.75
wood	0.70	0.85	0.70	0.83	**1.00**	0.90	0.84	0.91	0.85	0.92

[a] wood combustion factor is calculated by mass balance method using K as indicator

[b] bold font represents the highest correlation between factor and chemical species

This factor had almost the same temporal variations when K was not included (no_K method) with the base run, and a correlation coefficient of 0.99 was obtained. In High_K method a higher fraction of 41% for K was observed (27% for base run). Though the factor contribution was strongly correlated with base run, the correlation coefficient was

0.84. From table A1 it can be seen that this factor in the base run and No_K method was less correlated with more dependent on Cd (r=0.85), while in High_K method it was more dependent on LEV (r=0.89) and K (r=0.85). This factor, therefore, is considered not only influenced by biomass burning, but also partly by other combustion sources, like residential and commercial combustion.

Additionally I compared the results from the base run with the primary wood combustion factor which calculated by mass balance method using K as tracer,

$$PM_{10}\ (\text{wood combustion}) = (cK\_ambient - cK\_background)/\ cK\_emission, \quad (2)$$

where cK_ambient is the ambient concentration of K, and cK_background is the background concentration of K, obtained from the intercept of regression fit between K and LEV. cK_emission is the emission ratio of K from wood combustion (Schnelle-Kreis et al. 2010).

The correlation coefficient between primary wood combustion and base run was 0.70 and the factor mass concentration from PMF was much higher than the mass balance method (4.2 vs. 2.3 μg m^{-3}). This is because the factor obtained by PMF included not only primary wood combustion particles, but also secondary aerosols from wood combustion and material from other combustion sources.

The analysis above indicated that due to the low S/N ratio, the importance of K as an inorganic biomass burning tracer in winter 2006/07 was weakened in the PMF analysis. Also the S/N ratio is crucial thus one need to be more cautious in altering the species uncertainties.

B. Pair-wise COD values and Spearman's rank correlation coefficients between measurement sites

Table B1: COD values between eight sites between February 13, 2008 and March 12, 2008

COD	Nitrate	Sulfate	combustion	NaCl	dust	traffic
KP-BP	0.11	0.25	0.34	0.46	0.42	0.65
KP-LO	0.13	0.20	0.41	0.50	0.49	0.82
KP-LfU	0.14	0.25	0.36	0.56	0.48	0.83
KP-HO	0.20	0.18	0.35	0.56	0.54	0.95
KP-WE	0.15	0.26	0.34	0.57	0.58	0.95
KP-Bi	0.14	0.28	0.36	0.53	0.42	0.78
KP-Ki	0.13	0.29	0.36	0.68	0.45	0.88
BP-LO	0.07	0.09	0.14	0.29	0.16	0.49
BP-LfU	0.08	0.06	0.09	0.31	0.18	0.58
BP-HO	0.15	0.06	0.24	0.32	0.25	0.82
BP-WE	0.10	0.06	0.13	0.35	0.34	0.84
BP-Bi	0.09	0.08	0.08	0.28	0.18	0.45
BP-Ki	0.08	0.07	0.19	0.39	0.20	0.72
LO-LfU	0.06	0.08	0.14	0.35	0.18	0.56
LO-HO	0.12	0.10	0.31	0.33	0.22	0.75
LO-WE	0.06	0.09	0.19	0.33	0.29	0.80
LO-Bi	0.06	0.08	0.11	0.32	0.20	0.40
LO-Ki	0.05	0.08	0.23	0.39	0.22	0.65
LfU-HO	0.14	0.09	0.25	0.30	0.23	0.70
LfU-WE	0.07	0.08	0.15	0.30	0.32	0.74
LfU-Bi	0.08	0.09	0.09	0.31	0.22	0.55
LfU-Ki	0.06	0.08	0.19	0.31	0.21	0.65
HO-WE	0.10	0.06	0.18	0.24	0.24	0.63
HO-Bi	0.10	0.10	0.25	0.26	0.28	0.74
HO-Ki	0.14	0.06	0.22	0.29	0.25	0.82
WE-Bi	0.06	0.08	0.14	0.33	0.36	0.79
WE-Ki	0.06	0.07	0.13	0.39	0.25	0.81
Bi-Ki	0.09	0.10	0.19	0.31	0.17	0.63

Table B2: Spearman rank correlations between eight sites between February 13, 2008 and March 12, 2008

Spearman' r	nitrate	sulfate	combustion	NaCl	dust	traffic
KP-BP	0.99	0.87	0.96	0.77	0.61	0.92
KP-LO	1	0.91	0.93	0.58	0.41	0.83
KP-LfU	0.99	0.9	0.94	0.68	0.55	0.81
KP-HO	0.97	0.91	0.93	0.54	0.45	0.29
KP-WE	0.99	0.85	0.95	0.56	0.28	0.33
KP-Bi	0.98	0.81	0.95	0.65	0.52	0.82
KP-Ki	0.98	0.87	0.89	0.44	0.62	0.83
BP-LO	0.99	0.98	0.96	0.89	0.83	0.9
BP-LfU	0.99	0.97	0.99	0.91	0.88	0.86
BP-HO	0.96	0.96	0.92	0.87	0.84	0.41
BP-WE	0.99	0.98	0.96	0.86	0.79	0.48
BP-Bi	0.99	0.97	0.98	0.85	0.8	0.81
BP-Ki	0.98	0.93	0.91	0.77	0.78	0.85
LO-LfU	0.99	0.98	0.95	0.93	0.76	0.85
LO-HO	0.98	0.97	0.94	0.88	0.81	0.4
LO-WE	1	0.97	0.96	0.95	0.86	0.46
LO-Bi	0.99	0.96	0.97	0.91	0.75	0.76
LO-Ki	0.99	0.96	0.91	0.78	0.44	0.87
LfU-HO	0.96	0.94	0.93	0.95	0.71	0.44
LfU-WE	0.99	0.95	0.96	0.93	0.78	0.49
LfU-Bi	0.98	0.95	0.98	0.95	0.72	0.67
LfU-Ki	0.99	0.95	0.94	0.8	0.7	0.73
HO-WE	0.97	0.97	0.94	0.96	0.87	0.6
HO-Bi	0.97	0.92	0.94	0.94	0.72	0.53
HO-Ki	0.91	0.97	0.9	0.76	0.58	0.64
WE-Bi	0.98	0.95	0.96	0.85	0.73	0.45
WE-Ki	0.98	0.96	0.95	0.72	0.59	0.39
Bi-Ki	0.95	0.92	0.94	0.77	0.86	0.79

C. The table of variables used in cluster analysis

Table C: The number and variable names used in cluster analysis

N.	variable	N.	variable	N.	variable	N.	variable
1	sulfate	25	$NC_{3\text{-}2000nm}$	49	LC_{EAD}	73	$MC_{30\text{-}50nm}$
2	BC	26	$NC_{3\text{-}8200nm}$	50	$SC_{3\text{-}10nm}$	74	$MC\_TD_{30\text{-}50nm}$
3	$PM_{2.5}$	27	$NC_{1000\text{-}2500nm}$	51	$SC_{10\text{-}30nm}$	75	$MC_{50\text{-}100nm}$
4	$PM_{2.5NV}$	28	$NC_{2500\text{-}10000nm}$	52	$SC\_TD_{10\text{-}30nm}$	76	$MC\_TD_{50\text{-}100nm}$
5	$PM_{2.5V}$	29	TNC	53	$SC_{30\text{-}50nm}$	77	$MC_{100\text{-}500nm}$
6	PM_{10}	30	$LC_{3\text{-}10nm}$	54	$SC\_TD_{30\text{-}50nm}$	78	$MC\_TD_{100\text{-}500nm}$
7	PM_{10NV}	31	$LC_{10\text{-}30nm}$	55	$SC_{50\text{-}100nm}$	79	$MC_{100\text{-}800nm}$
8	PM_{10V}	32	$LC\_TD_{10\text{-}30nm}$	56	$SC\_TD_{50\text{-}100nm}$	80	$MC\_TD_{100\text{-}800nm}$
9	PM_{coarse}	33	$LC_{30\text{-}50nm}$	57	$SC_{100\text{-}500nm}$	81	$MC_{500\text{-}1000nm}$
10	$NC_{3\text{-}10nm}$	34	$LC\_TD_{30\text{-}50nm}$	58	$SC\_TD_{100\text{-}500nm}$	82	$MC_{10\text{-}800nm}$
11	$NC_{10\text{-}30nm}$	35	$LC_{50\text{-}100nm}$	59	$SC_{100\text{-}800nm}$	83	$MC\_TD_{10\text{-}800nm}$
12	$NC\_TD_{10\text{-}30nm}$	36	$LC\_TD_{50\text{-}100nm}$	60	$SC\_TD_{100\text{-}800nm}$	84	$MC_{3\text{-}800nm}$
13	$NC_{30\text{-}50nm}$	37	$LC_{100\text{-}500nm}$	61	$SC_{500\text{-}1000nm}$	85	$MC_{3\text{-}2000nm}$
14	$NC\_TD_{30\text{-}50nm}$	38	$LC\_TD_{100\text{-}500nm}$	62	$SC_{10\text{-}800nm}$	86	$MC_{3\text{-}8200nm}$
15	$NC_{50\text{-}100nm}$	39	$LC_{100\text{-}800nm}$	63	$SC\_TD_{10\text{-}800nm}$	87	$MC_{1000\text{-}2500nm}$
16	$NC\_TD_{50\text{-}100nm}$	40	$LC\_TD_{100\text{-}800nm}$	64	$SC_{3\text{-}800nm}$	88	$MC_{2500\text{-}10000nm}$
17	$NC_{100\text{-}500nm}$	41	$LC_{500\text{-}1000nm}$	65	$SC_{3\text{-}2000nm}$	89	NC10-100nm
18	$NC\_TD_{100\text{-}500nm}$	42	$LC_{10\text{-}800nm}$	66	$SC_{3\text{-}8200nm}$	90	$NC\_TD_{10\text{-}100nm}$
19	$NC_{100\text{-}800nm}$	43	$LC\_TD_{10\text{-}800nm}$	67	$SC_{1000\text{-}2500nm}$	91	$LC_{10\text{-}100nm}$
20	$NC\_TD_{100\text{-}800nm}$	44	$LC_{3\text{-}800nm}$	68	$SC_{2500\text{-}10000nm}$	92	$LC\_TD_{10\text{-}100nm}$
21	$NC_{500\text{-}1000nm}$	45	$LC_{3\text{-}2000nm}$	69	ASC	93	$SC_{10\text{-}100nm}$
22	$NC_{10\text{-}800nm}$	46	$LC_{3\text{-}8200nm}$	70	$MC_{3\text{-}10nm}$	94	$SC\_TD_{10\text{-}100nm}$
23	$NC\_TD_{10\text{-}800nm}$	47	$LC_{1000\text{-}2500nm}$	71	$MC_{10\text{-}30nm}$	95	$MC_{10\text{-}100nm}$
24	$NC_{3\text{-}800nm}$	48	$LC_{2500\text{-}10000nm}$	72	$MC\_TD_{10\text{-}30nm}$	96	$MC\_TD_{10\text{-}100nm}$

References

Aatmeeyata, Sharma M. Contribution of Traffic-Generated Nonexhaust PAHs, Elemental Carbon, and Organic Carbon Emission to Air and Urban Runoff Pollution. Journal of Environmental Engineering-Asce 2010; 136: 1447-1450.

Alleman LY, Lamaison L, Perdrix E, Robache A, Galloo JC. PM(10) metal concentrations and source identification using positive matrix factorization and wind sectoring in a French industrial zone. Atmospheric Research 2010; 96: 612-625.

Allen AG, Nemitz E, Shi JP, Harrison RM, Greenwood JC. Size distributions of trace metals in atmospheric aerosols in the United Kingdom. Atmospheric Environment 2001; 35: 4581-4591.

Amato F, Hopke PK. Source apportionment of the ambient PM(2.5) across St. Louis using constrained positive matrix factorization. Atmospheric Environment 2012; 46: 329-337.

Amato F, Pandolfi M, Escrig A, Querol X, Alastuey A, Pey J, Perez N, Hopke PK. Quantifying road dust resuspension in urban environment by Multilinear Engine: A comparison with PMF2. Atmospheric Environment 2009; 43: 2770-2780.

Andersen ZJ, Wahlin P, Raaschou-Nielsen O, Scheike T, Loft S. Ambient particle source apportionment and daily hospital admissions among children and elderly in Copenhagen. Journal of Exposure Science and Environmental Epidemiology 2007; 17: 625-636.

Anderson HR. Air pollution and mortality: A history. Atmospheric Environment 2009; 43: 142-152.

Ansari AS, Pandis SN. Response of inorganic PM to precursor concentrations. Environmental Science & Technology 1998; 32: 2706-2714.

Arditsoglou A, Samara C. Levels of total suspended particulate matter and major trace elements in Kosovo: a source identification and apportionment study. Chemosphere 2005; 59: 669-678.

Baumann K, Jayanty RKM, Flanagan JB. Fine particulate matter source apportionment for the Chemical Speciation Trends Network site at Birmingham, Alabama, using Positive Matrix Factorization. Journal of the Air & Waste Management Association 2008; 58: 27-44.

Bhugwant C, Cachier H, Bessafi M, Leveau J. Impact of traffic on black carbon aerosol concentration at la Reunion Island (Southern Indian Ocean). Atmospheric Environment 2000; 34: 3463-3473.

Birmili W, Heinke K, Pitz M, Matschullat J, Wiedensohler A, Cyrys J, Wichmann HE, Peters A. Particle number size distributions in urban air before and after volatilisation. Atmospheric Chemistry and Physics 2010; 10: 4643-4660.

Blanco A, De Tomasi F, Filippo E, Manno D, Perrone MR, Serra A, Tafuro AM, Tepore A. Characterization of African dust over southern Italy. Atmospheric Chemistry and Physics 2003; 3: 2147-2159.

Bond TC, Streets DG, Yarber KF, Nelson SM, Woo JH, Klimont Z. A technology-based global inventory of black and organic carbon emissions from combustion. Journal of Geophysical Research-Atmospheres 2004; 109.

Brook RD, Rajagopalan S, Pope CA, Brook JR, Bhatnagar A, Diez-Roux AV, Holguin F, Hong YL, Luepker RV, Mittleman MA, Peters A, Siscovick D, Smith SC, Whitsel L, Kaufman JD. Particulate Matter Air Pollution and Cardiovascular Disease An Update to the Scientific Statement From the American Heart Association. Circulation 2010; 121: 2331-2378.

Brown DM, Wilson MR, MacNee W, Stone V, Donaldson K. Size-dependent proinflammatory effects of ultrafine polystyrene particles: A role for surface area and oxidative stress in the enhanced activity of ultrafines. Toxicology and Applied Pharmacology 2001; 175: 191-199.

Brown SG, Frankel A, Raffuse SM, Roberts PT, Hafner HR, Anderson DJ. Source apportionment of fine particulate matter in Phoenix, AZ, using positive matrix factorization. Journal of the Air & Waste Management Association 2007; 57: 741-752.

Bruckmann P, Birmili W, Straub W, Pitz M, Gladtke D, Pfeffer U, Hebbinghaus H, Wurzler S, Olschewski A. An outbreak of Saharan dust causing high PM10 levels north of the Alps. Gefahrstoffe Reinhaltung der Luft 2008; 68: 490-498.

Burton RM, Suh HH, Koutrakis P. Spatial variation in particulate concentrations within metropolitan Philadelphia. Environmental Science & Technology 1996; 30: 400-407.

Cabada JC, Rees S, Takahama S, Khlystov A, Pandis SN, Davidson CI, Robinson AL. Mass size distributions and size resolved chemical composition of fine particulate matter at the Pittsburgh supersite. Atmospheric Environment 2004; 38: 3127-3141.

Cass GR, Hughes LA, Bhave P, Kleeman MJ, Allen JO, Salmon LG. The chemical composition of atmospheric ultrafine particles. Philosophical Transactions of the Royal Society of London Series A-Mathematical Physical and Engineering Sciences 2000; 358: 2581-2592.

Charron A, Harrison RM. Primary particle formation from vehicle emissions during exhaust dilution in the roadside atmosphere. Atmospheric Environment 2003; 37: 4109-4119.

Chen LWA, Watson JG, Chow JC, Dubois DW, Herschberger L. Chemical mass balance source apportionment for combined PM(2) (5) measurements from U S non-urban and urban long-term networks. Atmospheric Environment 2010; 44: 4908-4918.

Clarke AD, Collins WG, Rasch PJ, Kapustin VN, Moore K, Howell S, Fuelberg HE. Dust and pollution transport on global scales: Aerosol measurements and model predictions. Journal of Geophysical Research-Atmospheres 2001; 106: 32555-32569.

Costabile F, Birmili W, Klose S, Tuch T, Wehner B, Wiedensohler A, Franck U, Konig K, Sonntag A. Spatio-temporal variability and principal components of the particle number size distribution in an urban atmosphere. Atmospheric Chemistry and Physics 2009; 9: 3163-3195.

Curtius J. Nucleation of atmospheric aerosol particles. Comptes Rendus Physique 2006; 7: 1027-1045.

Cyrys J, Heinrich J, Brauer M, Wichmann HE. Spatial variability of acidic aerosols, sulfate and PM10 in Erfurt, Eastern Germany. Journal of Exposure Analysis and Environmental Epidemiology 1998; 8: 447-464.

Cyrys J, Pitz M, Heinrich J, Wichmann HE, Peters A. Spatial and temporal variation of particle number concentration in Augsburg, Germany. Science of the Total Environment 2008; 401: 168-175.

DeGaetano AT, Doherty OM. Temporal, spatial and meteorological variations in hourly PM2.5 concentration extremes in New York City. Atmospheric Environment 2004; 38: 1547-1558.

Delfino RJ, Sioutas C, Malik S. Potential role of ultrafine particles in associations between airborne particle mass and cardiovascular health. Environmental Health Perspectives 2005; 113: 934-946.

Dominici F, McDermott A, Daniels M, Zeger SL, Samet JM. Revised analyses of the National Morbidity, Mortality, and Air Pollution Study: Mortality among residents of 90 cities. Journal of Toxicology and Environmental Health-Part A-Current Issues 2005; 68: 1071-1092.

Dominici F, Peng RD, Barr CD, Bell ML. Protecting Human Health From Air Pollution Shifting From a Single-pollutant to a Multipollutant Approach. Epidemiology 2010; 21: 187-194.

Dons E, Panis LI, Van Poppel M, Theunis J, Willems H, Torfs R, Wets G. Impact of time-activity patterns on personal exposure to black carbon. Atmospheric Environment 2011; 45: 3594-3602.

Draxler R, Hess GD. NOAA Technical Memorandum ERL ARL-224-Description of the HYSPLIT_4 modelling system. 1997; 1-6.

Draxler R, Stunder B, Rolph G, Stein A, Taylor A. HYSPLIT4 User's Guide. 2009.

Duan FK, He KB, Ma YL, Yang FM, Yu XC, Cadle SH, Chan T, Mulawa PA. Concentration and chemical characteristics of PM2.5 in Beijing, China: 2001-2002. Science of the Total Environment 2006; 355: 264-275.

Duan N. Models for human exposure to air pollution. Environmental International 1982; 8: 305-309.

Duce RA, Hoffman GL, Zoller WH. Atmospheric Trace-Metals at Remote Northern and Southern-Hemisphere Sites - Pollution Or Natural. Science 1975; 187: 59-61.

EC. Council Directive of 15 July 1980 on air quality limit values and guide values for sulphur dioxide and suspended particulates. 1980. Official Journal of the European Communities. Accessed in January 2012 at http://eur-lex.europa.eu/LexUriServ/LexUriServ.do?uri=CELEX:31980L0779:EN:NOT.

EC. Council Directive 96/62/EC of 27 September 1996 on ambient air quality assessment and management. The Council of the European Union. 1996. Accessed in January 2012 at http://europa.eu/legislation_summaries/other/l28031a_en.htm.

EC. Council Directive 1999/30/EC of 22 April 1999: relating to limit values for sulphur dioxide, nitrogen dioxide and oxides of nitrogen, particulate matter and lead in ambient air. 1999. Official Journal of the European Communities. Accessed in January 2012 at http://eur-lex.europa.eu/LexUriServ/LexUriServ.do?uri=OJ:L:1999:163:0041:0060:EN:PDF.

EC. Directive 2008/50/EC of the European Parliament and of The Council of 21 May 2008 on ambient air quality and cleaner air for Europe. Official Journal of the European Union. 2008.

Accessed in January 2012 at http://eur-lex.europa.eu/LexUriServ/LexUriServ.do?uri=CELEX:32008L0050:EN:NOT.

Eldering A, Cass GR, Moon KC. An Air Monitoring Network Using Continuous Particle-Size Distribution Monitors - Connecting Pollutant Properties to Visibility Via Mie Scattering Calculations. Atmospheric Environment 1994; 28: 2733-2749.

Ferin J. Pulmonary Retention and Clearance of Particles. Toxicology Letters 1994; 72: 121-125.

Finlayson-pitts BJ, Pitts JN. Chemistry of the upper and lower atmosphere: theory, experments, and applications. Academic Press, San diego, California, USA, 2000.

Fissan H, Neumann S, Trampe A, Pui DYH, Shin WG. Rationale and principle of an instrument measuring lung deposited nanoparticle surface area. Journal of Nanoparticle Research 2007; 9: 53-59.

Flagan RC. Differential Mobility Analysis of Aerosols: A Tutorial. Kona Powder and Particle Journal 2008; 26: 254-268.

Formenti P, Schutz L, Balkanski Y, Desboeufs K, Ebert M, Kandler K, Petzold A, Scheuvens D, Weinbruch S, Zhang D. Recent progress in understanding physical and chemical properties of African and Asian mineral dust. Atmospheric Chemistry and Physics 2011; 11: 8231-8256.

Furusjo E, Sternbeck J, Cousins AP. PM10 source characterization at urban and highway roadside locations. Science of the Total Environment 2007; 387: 206-219.

Furuta N, Iijima A, Kambe A, Sakai K, Sato K. Concentrations, enrichment and predominant sources of Sb and other trace elements in size classified airborne particulate matter collected in Tokyo from 1995 to 2004. Journal of Environmental Monitoring 2005; 7: 1155-1161.

Gehring U, Heinrich J, Kramer U, Grote V, Hochadel M, Sugiri D, Kraft M, Rauchfuss K, Eberwein HG, Wichmann HE. Long-term exposure to ambient air pollution and cardiopulmonary mortality in women. Epidemiology 2006; 17: 545-551.

Grahame T, Hidy G. Using factor analysis to attribute health impacts to particulate pollution sources. Inhalation Toxicology 2004; 16: 143-152.

Grahame TJ, Schlesinger RB. Health effects of airborne particulate matter: do we know enough to consider regulating specific particle types or sources? Inhalation Toxicology 2007; 19: 457-481.

Griffin RJ, Cocker DR, Seinfeld JH, Dabdub D. Estimate of global atmospheric organic aerosol from oxidation of biogenic hydrocarbons. Geophysical Research Letters 1999; 26: 2721-2724.

Grivas G, Chaloulakou A, Samara C, Spyrellis N. Spatial and temporal variation of PM10 mass concentrations within the Greater Area of Athens, Greece. Water Air and Soil Pollution 2004; 158: 357-371.

Gu J, Pitz M, Schnelle-Kreis J, Diemer J, Reller A, Zimmermann R, Soentgen J, Stoelzel M, Wichmann HE, Peters A, Cyrys J. Source apportionment of ambient particles: Comparison of positive matrix factorization analysis applied to particle size distribution and chemical composition data. Atmospheric Environment 2011; 45: 1849-1857.

Gu J, Pitz M, Breitner S, Birmili W, von Klot S, Schneider A, Soentgen J, Reller A, Peters A, Cyrys J. Selection of key ambient particulate variables for epidemiological studies — Applying cluster and heatmap analyses as tools for data reduction. Science of the Total Environment 2012; 435-436: 541-550.

Hallquist M, Wenger JC, Baltensperger U, Rudich Y, Simpson D, Claeys M, Dommen J, Donahue NM, George C, Goldstein AH, Hamilton JF, Herrmann H, Hoffmann T, Iinuma Y, Jang M, Jenkin ME, Jimenez JL, Kiendler-Scharr A, Maenhaut W, McFiggans G, Mentel TF, Monod A, Prevot ASH, Seinfeld JH, Surratt JD, Szmigielski R, Wildt J. The formation, properties and impact of secondary organic aerosol: current and emerging issues. Atmospheric Chemistry and Physics 2009; 9: 5155-5236.

Hampel R, Schneider A, Brüske I, Zareba W, Cyrys J, Rückerl R, Breitner S, Korb H, Sunyer J, Wichmann HE, Peters A. Altered cardiac repolarization in association with air pollution and air temperature among myocardial infarction survivors. Environmental Health Perspectives 2010; 18: 1755-1761.

Hanninen O, Zauli-Sajani S, De Maria R, Lauriola P, Jantunen M. Integrated Ambient and Microenvironment Model for Estimation of PM(10) Exposures of Children in Annual and Episode Settings. Environmental Modeling & Assessment 2009; 14: 419-429.

Hansen HK, Pedersen AJ, Ottosen LM, Villumsen A. Speciation and mobility of cadmium in straw and wood combustion fly ash. Chemosphere 2001; 45: 123-128.

Harrison RM, Beddows DCS, Dall'Osto M. PMF Analysis of Wide-Range Particle Size Spectra Collected on a Major Highway. Environmental Science & Technology 2011; 45: 5522-5528.

Haywood J, Francis P, Osborne S, Glew M, Loeb N, Highwood E, Tanre D, Myhre G, Formenti P, Hirst E. Radiative properties and direct radiative effect of Saharan dust measured by the C-130 aircraft during SHADE: 1. Solar spectrum. Journal of Geophysical Research-Atmospheres 2003; 108.

Hazi Y, Heikkinen MSA, Cohen BS. Size distribution of acidic sulfate ions in fine ambient particulate matter and assessment of source region effect. Atmospheric Environment 2003; 37: 5403-5413.

Heo JB, Hopke PK, Yi SM. Source apportionment of PM(2.5) in Seoul, Korea. Atmospheric Chemistry and Physics 2009; 9: 4957-4971.

Hering S, Eldering A, Seinfeld JH. Bimodal character of accumulation mode aerosol mass distributions in Southern California. Atmospheric Environment 1997; 31: 1-11.

Hering SV, Flagan RC, Friedlander SK. Design and Evaluation of New Low-Pressure Impactor .1. Environmental Science & Technology 1978; 12: 667-673.

Hering SV, Friedlander SK, Collins JJ, Richards LW. Design and Evaluation of A New Low-Pressure Impactor .2. Environmental Science & Technology 1979; 13: 184-188.

Hewitt CN. The atmospheric chemistry of sulphur and nitrogen in power station plumes. Atmospheric Environment 2001; 35: 1155-1170.

Hildemann LM, Markowski GR, Cass GR. Chemical-Composition of Emissions from Urban Sources of Fine Organic Aerosol. Environmental Science & Technology 1991; 25: 744-759.

Hillamo RE, Kauppinen EI. On the Performance of the Berner Low-Pressure Impactor. Aerosol Science and Technology 1991; 14: 33-47.

Hoek G, Brunekreef B, Goldbohm S, Fischer P, van den Brandt PA. Association between mortality and indicators of traffic-related air pollution in the Netherlands: a cohort study. Lancet 2002a; 360: 1203-1209.

Hoek G, Meliefste K, Cyrys J, Lewne M, Bellander T, Brauer M, Fischer P, Gehring U, Heinrich J, van Vliet P, Brunekreef B. Spatial variability of fine particle concentrations in three European areas. Atmospheric Environment 2002b; 36: 4077-4088.

Holle R, Happich M, Löwel H, Wichmann HE. KORA - A Research Platform for Population Based Health Research. Das Gesundheitswesen 2005; S01: s19-s25.

Holmes NS. A review of particle formation events and growth in the atmosphere in the various environments and discussion of mechanistic implications. Atmospheric Environment 2007; 41: 2183-2201.

Holmes NS, Morawska L. A review of dispersion modelling and its application to the dispersion of particles: An overview of different dispersion models available. Atmospheric Environment 2006; 40: 5902-5928.

Hopke PK, Ito K, Mar T, Christensen WF, Eatough DJ, Henry RC, Kim E, Laden F, Lall R, Larson TV, Liu H, Neas L, Pinto J, Stolzel M, Suh H, Paatero P, Thurston GD. PM source apportionment and health effects: 1. Intercomparison of source apportionment results. Journal of Exposure Science and Environmental Epidemiology 2006; 16: 275-286.

Hopke, Philip. K. A Guide to Positive matrix factorization; In Workshop on UNMIX and PMF as Applied to PM2.5; 600/A-00/048; Willis, R.D., Ed. U.S. Environmental Protection Agency: Research Triangle Park, NC. 2000.

Hueglin C, Gehrig R, Baltensperger U, Gysel M, Monn C, Vonmont H. Chemical characterisation of PM2.5, PM10 and coarse particles at urban, near-city and rural sites in Switzerland. Atmospheric Environment 2005; 39: 637-651.

Iijima A, Sato K, Yano K, Tago H, Kato M, Kimura H, Furuta N. Particle size and composition distribution analysis of automotive brake abrasion dusts for the evaluation of antimony sources of airborne particulate matter. Atmospheric Environment 2007; 41: 4908-4919.

Ito K, Christensen WF, Eatough DJ, Henry RC, Kim E, Laden F, Lall R, Larson TV, Neas L, Hopke PK, Thurston GD. PM source apportionment and health effects: 2. An investigation of intermethod variability in associations between source-apportioned fine particle mass and daily mortality in Washington, DC. Journal of Exposure Science and Environmental Epidemiology 2006; 16: 300-310.

Jain AK, Murty MN, Flynn PJ. Data clustering: A review. Acm Computing Surveys 1999; 31: 264-323.

Jeong CH, Evans GJ, Dann T, Graham M, Herod D, Dabek-Zlotorzynska E, Mathieu D, Ding L, Wang D. Influence of biomass burning on wintertime fine particulate matter: Source contribution at a valley site in rural British Columbia. Atmospheric Environment 2008; 42: 3684-3699.

Jeong CH, Evans GJ, Hopke PK, Chalupa D, Utell MJ. Influence of atmospheric dispersion and new particle formation events on ambient particle number concentration in Rochester, United States, and Toronto, Canada. Journal of the Air & Waste Management Association 2006; 56: 431-443.

Jeong CH, Hopke PK, Chalupa D, Utell M. Characteristics of nucleation and growth events of ultrafine particles measured in Rochester, NY. Environmental Science & Technology 2004; 38: 1933-1940.

Jerrett M, Buzzelli M, Burnett RT, DeLuca PF. Particulate air pollution, social confounders, and mortality in small areas of an industrial city. Social Science & Medicine 2005; 60: 2845-2863.

John W, Wall SM, Ondo JL, Winklmayr W. Modes in the Size Distributions of Atmospheric Inorganic Aerosol. Atmospheric Environment Part A-General Topics 1990; 24: 2349-2359.

Kanamitsu M. Description of the NMC global data assimilation and forecast system. Weather and Forcast 1989; 4: 335-342.

Karnae S, John K. Source apportionment of fine particulate matter measured in an industrialized coastal urban area of South Texas. Atmospheric Environment 2011; 45: 3769-3776.

Katsouyanni K, Touloumi G, Spix C, Schwartz J, Balducci F, Medina S, Rossi G, Wojtyniak B, Sunyer J, Bacharova L, Schouten JP, Ponka A, Anderson HR. Short term effects of ambient sulphur dioxide and particulate matter on mortality in 12 European cities: Results from time series data from the APHEA project. British Medical Journal 1997; 314: 1658-1663.

Kaufman L, Rousseuw PJ. Finding Groups in Data. John Wiley & Sons, New York, 1990.

Kaur S, Nieuwenhuijsen MJ. Determinants of Personal Exposure to PM(2.5), Ultrafine Particle Counts, and CO in a Transport Microenvironment. Environmental Science & Technology 2009; 43: 4737-4743.

Kaur S, Nieuwenhuijsen MJ, Colvile RN. Pedestrian exposure to air pollution along a major road in Central London, UK. Atmospheric Environment 2005; 39: 7307-7320.

KBA. Emissionen, Kraftstoffe - Deutschland und seine Laender am 1. Januar 2009. Kraftfahrt-Bundesamt Report, The Kraftfahrt-Bundesamt (Federal Motor Transport Authority), Flensburg, Germany. 2009.

Khlystov A, Stanier C, Pandis SN. An algorithm for combining electrical mobility and aerodynamic size distributions data when measuring ambient aerosol. Aerosol Science and Technology 2004; 38: 229-238.

Kim E, Hopke PK. Comparison between conditional probability function and nonparametric regression for fine particle source directions. Atmospheric Environment 2004; 38: 4667-4673.

Kim E, Hopke PK. Source characterization of ambient fine particles at multiple sites in the Seattle area. Atmospheric Environment 2008; 42: 6047-6056.

Kim E, Hopke PK, Edgerton ES. Source identification of Atlanta aerosol by positive matrix factorization. Journal of the Air & Waste Management Association 2003a; 53: 731-739.

Kim E, Hopke PK, Edgerton ES. Improving source identification of Atlanta aerosol using temperature resolved carbon fractions in positive matrix factorization. Atmospheric Environment 2004a; 38: 3349-3362.

Kim E, Hopke PK, Kenski DM, Koerber M. Sources of fine particles in a rural Midwestern US area. Environmental Science & Technology 2005a; 39: 4953-4960.

Kim E, Hopke PK, Larson TV, Covert DS. Analysis of ambient particle size distributions using unmix and positive matrix factorization. Environmental Science & Technology 2004b; 38: 202-209.

Kim E, Hopke PK, Paatero P, Edgerton ES. Incorporation of parametric factors into multilinear receptor model studies of Atlanta aerosol. Atmospheric Environment 2003b; 37: 5009-5021.

Kim E, Hopke PK, Pinto JP, Wilson WE. Spatial variability of fine particle mass, components, and source contributions during the regional air pollution study in St. Louis. Environmental Science & Technology 2005b; 39: 4172-4179.

Kim E, Turkiewicz K, Zulawnick SA, Magliano KL. Sources of fine particles in the South Coast area, California. Atmospheric Environment 2010; 44: 3095-3100.

Kim M, Deshpande SR, Crist KC. Source apportionment of fine particulate matter (PM2.5) at a rural Ohio River Valley site. Atmospheric Environment 2007; 41: 9231-9243.

Kittelson DB, Watts WF, Johnson JP. On-road and laboratory evaluation of combustion aerosols - Part 1: Summary of diesel engine results. Journal of Aerosol Science 2006; 37: 913-930.

Kleeman MJ, Robert MA, Riddle SG, Fine PM, Hays MD, Schauer JJ, Hannigan MP. Size distribution of trace organic species emitted from biomass combustion and meat charbroiling. Atmospheric Environment 2008; 42: 3059-3075.

Kleeman MJ, Schauer JJ, Cass GR. Size and composition distribution of fine particulate matter emitted from wood burning, meat charbroiling, and cigarettes. Environmental Science & Technology 1999; 33: 3516-3523.

Klems JP, Pennington MR, Zordan CA, McFadden L, Johnston MV. Apportionment of Motor Vehicle Emissions from Fast Changes in Number Concentration and Chemical Composition of Ultrafine Particles Near a Roadway Intersection. Environmental Science & Technology 2011; 45: 5637-5643.

Kok JF. Does the size distribution of mineral dust aerosols depend on the wind speed at emission? Atmospheric Chemistry and Physics 2011; 11: 10149-10156.

Kroll JH, Seinfeld JH. Chemistry of secondary organic aerosol: Formation and evolution of low-volatility organics in the atmosphere. Atmospheric Environment 2008; 42: 3593-3624.

Krudysz MA, Froines JR, Fine PM, Sioutas C. Intra-community spatial variation of size-fractionated PM mass, OC, EC, and trace elements in the Long Beach, CA area. Atmospheric Environment 2008; 42: 5374-5389.

Krzyzanowski M, Cohen A. Update of WHO air quality guidelines. Air Quality, Atmosphere & Health 2008; 1: 7-13.

Kumar P, Ketzel M, Vardoulakis S, Pirjola L, Britter R. Dynamics and dispersion modelling of nanoparticles from road traffic in the urban atmospheric environment-A review. Journal of Aerosol Science 2011; 42: 580-603.

Kumar P, Robins A, Vardoulakis S, Britter R. A review of the characteristics of nanoparticles in the urban atmosphere and the prospects for developing regulatory controls. Atmospheric Environment 2010; 44: 5035-5052.

Lance GN, Williams WT. A Generalized Sorting Strategy for Computer Classifications. Nature 1966; 212: 218-&.

Larson TV, Covert DS, Kim E, Elleman R, Schreuder AB, Lumley T. Combining size distribution and chemical species measurements into a multivariate receptor model of PM2.5. Journal of Geophysical Research-Atmospheres 2006; 111.

Lee E, Chan CK, Paatero P. Application of positive matrix factorization in source apportionment of particulate pollutants in Hong Kong. Atmospheric Environment 1999; 33: 3201-3212.

Lenschow P, Abraham HJ, Kutzner K, Lutz M, Preuss JD, Reichenbacher W. Some ideas about the sources of PM10. Atmospheric Environment 2001; 35: S23-S33.

LfU. Luftreinhalte-/Aktionsplan für die Stadt Augsburg mit Einbeziehung der Umlandgemeinden (in German). 2009: 33.

Li JJ, Wang GH, Zhou BH, Cheng CL, Cao JJ, Shen ZX, An ZS. Chemical composition and size distribution of wintertime aerosols in the atmosphere of Mt. Hua in central China. Atmospheric Environment 2011; 45: 1251-1258.

Lim JM, Lee JH, Moon JH, Chung YS, Kim KH. Source apportionment of PM10 at a small industrial area using Positive Matrix Factorization. Atmospheric Research 2010; 95: 88-100.

Liu S, Hu M, Slanina S, He LY, Niu YW, Bruegemann E, Gnauk T, Herrmann H. Size distribution and source analysis of ionic compositions of aerosols in polluted periods at Xinken in Pearl River Delta (PRD) of China. Atmospheric Environment 2008; 42: 6284-6295.

Liu W, Hopke PK, Han YJ, Yi SM, Holsen TM, Cybart S, Kozlowski K, Milligan M. Application of receptor modeling to atmospheric constituents at Potsdam and Stockton, NY. Atmospheric Environment 2003; 37: 4997-5007.

Maechler, M, Rousseeuw, P, Struyf, A., and Hubert, M. Cluster Analysis Basics and Extensions. 2005.

Mage DT. Concepts of Human Exposure Assessment for Airborne Particulate Matter. Environment International 1985; 11: 407-412.

Mansurov ZA. Soot formation in combustion processes (review). Combustion Explosion and Shock Waves 2005; 41: 727-744.

Marcazzan GM, Vaccaro S, Valli G, Vecchi R. Characterisation of PM10 and PM2.5 particulate matter in the ambient air of Milan (Italy). Atmospheric Environment 2001; 35: 4639-4650.

Maring H, Savoie DL, Izaguirre MA, Custals L, Reid JS. Mineral dust aerosol size distribution change during atmospheric transport. Journal of Geophysical Research-Atmospheres 2003; 108.

Marple VA, Rubow KL, Behm SM. A Microorifice Uniform Deposit Impactor (Moudi) - Description, Calibration, and Use. Aerosol Science and Technology 1991; 14: 434-446.

Martello DV, Pekney NJ, Anderson RR, Davidson CI, Hopke PK, Kim E, Christensen WF, Mangelson NF, Eatough DJ. Apportionment of ambient primary and secondary fine particulate matter at the Pittsburgh National Energy Laboratory particulate matter characterization site using positive matrix factorization and a potential source contributions function analysis. Journal of the Air & Waste Management Association 2008; 58: 357-368.

Maykut NN, Lewtas J, Kim E, Larson TV. Source apportionment of PM2.5 at an urban IMPROVE site in Seattle, Washington. Environmental Science & Technology 2003; 37: 5135-5142.

Maynard AD, Maynard RL. A derived association between ambient aerosol surface area and excess mortality using historic time series data. Atmospheric Environment 2002; 36: 5561-5567.

Milford JB, Davidson CI. The Sizes of Particulate Trace-Elements in the Atmosphere - A Review. Journal of the Air Pollution Control Association 1985; 35: 1249-1260.

Monn C. Exposure assessment of air pollutants: a review on spatial heterogeneity and indoor/outdoor/personal exposure to suspended particulate matter, nitrogen dioxide and ozone. Atmospheric Environment 2001; 35: 1-32.

Mooibroek D, Schaap M, Weijers EP, Hoogerbrugge R. Source apportionment and spatial variability of PM(2.5) using measurements at five sites in the Netherlands. Atmospheric Environment 2011; 45: 4180-4191.

Mori I, Nishikawa M, Tanimura T, Quan H. Change in size distribution and chemical composition of kosa (Asian dust) aerosol during long-range transport. Atmospheric Environment 2003; 37: 4253-4263.

Nagy G. State of the Art in Pattern Recognition. PROCEEDINGS OF THE IEEE 1968; 56: 836-857.

Narodoslawsky M, Obernberger I. From waste to raw material - The route from biomass to wood ash for cadmium and other heavy metals. Journal of Hazardous Materials 1996; 50: 157-168.

Nerriere E, Zmirou-Navier D, Blanchard O, Momas I, Ladner J, Le Moullec Y, Personnaz MB, Lameloise P, Delmas W, Target A, Desqueyroux H. Can we use fixed ambient air monitors to estimate population long-term exposure to air pollutants? The case of spatial variability in the Genotox ER study. Environmental Research 2005; 97: 32-42.

Norris, Gary, Vedantham, Ram, Wade, Katie, Brown, steve, Pouty, Jeff, Foley, Chuck, and Martin, Lockheed. EPA Positive Matrix Factorization (PMF) 3.0 Fundamentals & User Guide. 2008.

Oberdorster G, Oberdorster E, Oberdorster J. Nanotoxicology: An emerging discipline evolving from studies of ultrafine particles. Environmental Health Perspectives 2005; 113: 823-839.

Oglesby L, Kunzli N, Roosli M, Braun-Fahrlander C, Mathys P, Stern W, Jantunen M, Kousa A. Validity of ambient levels of fine particles as surrogate for personal exposure to outdoor air pollution - Results of the European EXPOLIS-EAS study (Swiss Center Basel). Journal of the Air & Waste Management Association 2000; 50: 1251-1261.

Ogulei D, Hopke PK, Chalupa DC, Utell MJ. Modeling source contributions to submicron particle number concentrations measured in Rochester, New York. Aerosol Science and Technology 2007a; 41: 179-201.

Ogulei D, Hopke PK, Ferro AR, Jaques PA. Factor analysis of submicron particle size distributions near a major United States-Canada trade bridge. Journal of the Air & Waste Management Association 2007b; 57: 190-203.

Ogulei D, Hopke PK, Wallace LA. Analysis of indoor particle size distributions in an occupied townhouse using positive matrix factorization. Indoor Air 2006a; 16: 204-215.

Ogulei D, Hopke PK, Zhou LM, Pancras JP, Nair N, Ondov JM. Source apportionment of Baltimore aerosol from combined size distribution and chemical composition data. Atmospheric Environment 2006b; 40: S396-S410.

Oh MS, Lee TJ, Kim DS. Quantitative Source Apportionment of Size-segregated Particulate Matter at Urbanized Local Site in Korea. Aerosol and Air Quality Research 2011; 11: 247-264.

Paatero P, Tapper U. Positive matrix factorization: a non-negative factor model with optimal utilization of error estimates of data values. Environmetrics 1994; 5: 111-126.

Paatero P. Least squares formulation of robust non-negative factor analysis. Chemometrics and Intelligent Laboratory Systems 1997; 37: 23-35.

Paatero P. The multilinear engine - A table-driven, least squares program for solving multilinear problems, including the n-way parallel factor analysis model. Journal of Computational and Graphical Statistics 1999; 8: 854-888.

Paatero P. User's Guide for Positive Matrix Factorization programs PMF2 and PMF3, Part 2: reference. Personal Communication 2007; 18-22.

Parekh PP, Husain L. Trace element concentrations in summer aerosols at rural sites in New York state and their possible sources. Atmospheric Environment 1981; 15: 1717-1725.

Park SS, Ondov JM, Harrison D, Nair NP. Seasonal and shorter-term variations in particulate atmospheric nitrate in Baltimore. Atmospheric Environment 2005; 39: 2011-2020.

Pekkanen J, Peters A, Hoek G, Tiittanen P, Brunekreef B, de Hartog J, Heinrich J, Ibald-Mulli A, Kreyling WG, Lanki T, Timonen KL, Vanninen E. Particulate air pollution and risk of ST-segment depression during repeated submaximal exercise tests among subjects with coronary

heart disease - The exposure and risk assessment for fine and ultrafine particles in ambient air (ULTRA) study. Circulation 2002; 106: 933-938.

Pere-Trepat E, Kim E, Paatero P, Hopke PK. Source apportionment of time and size resolved ambient particulate matter measured with a rotating DRUM impactor. Atmospheric Environment 2007; 41: 5921-5933.

Peters A, Greven S, Heid IM, Baldari F, Breitner S, Bellander T, Chrysohoou C, Illig T, Jacquemin B, Koenig W, Lanki T, Nyberg F, Pekkanen J, Pistelli R, R 點 kerl R, Stefanadis C, Schneider A, Sunyer J, Wichmann HE. Fibrinogen genes modify the fibrinogen response to ambient particulate matter. American Journal of Respiratory and Critical Care Medicine 2009; 179: 484-491.

Peters A, Skorkovsky J, Kotesovec F, Brynda J, Spix C, Wichmann HE, Heinrich J. Associations between mortality and air pollution in Central Europe. Environmental Health Perspectives 2000; 108: 283-287.

Peters A, Wichmann HE, Tuch T, Heinrich J, Heyder J. Respiratory effects are associated with the number of ultrafine particles. Am J Respir Crit Care Med 1997; 155: 1376-1383.

Pey J, Querol X, Alastuey A, Rodriguez S, Putaud JP, Van Dingenen R. Source apportionment of urban fine and ultra-fine particle number concentration in a Western Mediterranean city. Atmospheric Environment 2009; 43: 4407-4415.

Pinto JP, Lefohn AS, Shadwick DS. Spatial variability of PM2.5 in urban areas in the United States. Journal of the Air & Waste Management Association 2004; 54: 440-449.

Pitz M, Birmili W, Schmid O, Peters A, Wichmann HE, Cyrys J. Quality control and quality assurance for particle size distribution measurements at an urban monitoring station in Augsburg, Germany. Journal of Environmental Monitoring 2008a; 10: 1017-1024.

Pitz M, Gu J, Soentgen J, Peters A, Cyrys J. Particle size distribution factor as an indicator for the impact of the Eyjafjallajokull ash plume at ground level in Augsburg, Germany. Atmospheric Chemistry and Physics 2011; 11: 9367-9374.

Pitz M, Schmid O, Heinrich J, Birmili W, Maguhn J, Zimmermann R, Wichmann HE, Peters A, Cyrys J. Seasonal and diurnal variation of PM2.5 apparent particle density in urban air in Augsburg, Germany. Environmental Science & Technology 2008b; 42: 5087-5093.

Plaza J, Pujadas M, Gomez-Moreno FJ, Sanchez M, Artinano B. Mass size distributions of soluble sulfate, nitrate and ammonium in the Madrid urban aerosol. Atmospheric Environment 2011; 45: 4966-4976.

Polissar AV, Hopke PK, Paatero P. Atmospheric aerosol over Alaska - 2. Elemental composition and sources. Journal of Geophysical Research-Atmospheres 1998; 103: 19045-19057.

Pope CA, Burnett RT, Thun MJ, Calle EE, Krewski D, Ito K, Thurston GD. Lung cancer, cardiopulmonary mortality, and long-term exposure to fine particulate air pollution. Jama-Journal of the American Medical Association 2002; 287: 1132-1141.

Putaud JP, Van Dingenen R, Alastuey A, Bauer H, Birmili W, Cyrys J, Flentje H, Fuzzi S, Gehrig R, Hansson HC, Harrison RM, Herrmann H, Hitzenberger R, Huglin C, Jones AM, Kasper-Giebl

A, Kiss G, Kousa A, Kuhlbusch TAJ, Loschau G, Maenhaut W, Molnar A, Moreno T, Pekkanen J, Perrino C, Pitz M, Puxbaum H, Querol X, Rodriguez S, Salma I, Schwarz J, Smolik J, Schneider J, Spindler G, ten Brink H, Tursic J, Viana M, Wiedensohler A, Raes F. A European aerosol phenomenology-3: Physical and chemical characteristics of particulate matter from 60 rural, urban, and kerbside sites across Europe. Atmospheric Environment 2010; 44: 1308-1320.

Puxbaum H, Wopenka B. Chemical-Composition of Nucleation and Accumulation Mode Particles Collected in Vienna, Austria. Atmospheric Environment 1984; 18: 573-580.

Quass, U, Kuhlbusch, T, and Koch, M. Identification of source groups for fine dust. Public report to the Environment Ministry of North Rhine, Westphalia, Germany.IUTA-Report LP15. 2004.

Ramadan Z, Eickhout B, Song XH, Buydens LMC, Hopke PK. Comparison of Positive Matrix Factorization and Multilinear Engine for the source apportionment of particulate pollutants. Chemometrics and Intelligent Laboratory Systems 2003; 66: 15-28.

Raunemaa T, Kuuspalo K, Alander T, Mirme A, Tamm E. Age estimation of atmospheric black carbon over Finland from combined aerosol size distribution and radon progeny measurements. Journal of Aerosol Science 1996; 27: 455-465.

Ravindra K, Bencs L, Wauters E, de Hoog J, Deutsch F, Roekens E, Bleux N, Berghmans P, Van Grieken R. Seasonal and site-specific variation in vapour and aerosol phase PAHs over Flanders (Belgium) and their relation with anthropogenic activities. Atmospheric Environment 2006; 40: 771-785.

Ravindra K, Sokhi R, Van Grieken R. Atmospheric polycyclic aromatic hydrocarbons: Source attribution, emission factors and regulation. Atmospheric Environment 2008; 42: 2895-2921.

Reche C, Querol X, Alastuey A, Viana M, Pey J, Moreno T, Rodriguez S, Gonzalez Y, Fernandez-Camacho R, de la Campa AMS, de la Rosa J, Dall'Osto M, Prevot ASH, Hueglin C, Harrison RM, Quincey P. New considerations for PM, Black Carbon and particle number concentration for air quality monitoring across different European cities. Atmospheric Chemistry and Physics 2011; 11: 6207-6227.

Reiss R, Anderson EL, Cross CE, Hidy G, Hoel D, McClellan R, Moolgavkar S. Evidence of health impacts of sulfate- and nitrate-containing particles in ambient air. Inhalation Toxicology 2007; 19: 419-449.

Rückerl R, Greven S, Ljungman P, Aalto P, Antoniades C, Bellander T, Berglind N, Chrysohoou C, Forastiere F, Jacquemin B, von Klot S, Koenig W, Kuchenhoff H, Lanki T, Pekkanen J, Perucci CA, Schneider A, Sunyer J, Peters A. Air pollution and inflammation (interleukin-6,C-reactive protein, fibrinogen) in myocardial infarction survivors. Environmental Health Perspectives 2007; 115: 1072-1080.

RVS. Luftreinhalte-/Aktionsplan für die Stadt Augsburg mit Einbeziehung der Umlandgemeinden, 1. Fortschreibung, Erarbeitet von der Regierung von Schwaben (in German). Bayerisches Staatsministerium für Umwelt und Gesundheit. 2009.

Sager TM, Castranova V. Surface area of particle administered versus mass in determining the pulmonary toxicity of ultrafine and fine carbon black: comparison to ultrafine titanium dioxide. Particle and Fibre Toxicology 2009; 6.

Sajani SZ, Scotto F, Lauriola P, Galassi F, Montanari A. Urban air pollution monitoring and correlation properties between fixed-site stations. Journal of the Air & Waste Management Association 2004; 54: 1236-1241.

Salam A, Bauer H, Kassin K, Ullah SM, Puxbaum H. Aerosol chemical characteristics of a mega-city in Southeast Asia (Dhaka-Bangladesh). Atmospheric Environment 2003; 37: 2517-2528.

Samoli E, Analitis A, Touloumi G, Schwartz J, Anderson HR, Sunyer J, Bisanti L, Zmirou D, Vonk JM, Pekkanen J, Goodman P, Paldy A, Schindler C, Katsouyanni K. Estimating the exposure-response relationships between particulate matter and mortality within the APHEA multicity project. Environmental Health Perspectives 2005; 113: 88-95.

Schauer JJ, Kleeman MJ, Cass GR, Simoneit BRT. Measurement of emissions from air pollution sources. 1. C-1 through C-29 organic compounds from meat charbroiling. Environmental Science & Technology 1999a; 33: 1566-1577.

Schauer JJ, Kleeman MJ, Cass GR, Simoneit BRT. Measurement of emissions from air pollution sources. 2. C-1 through C-30 organic compounds from medium duty diesel trucks. Environmental Science & Technology 1999b; 33: 1578-1587.

Schauer JJ, Kleeman MJ, Cass GR, Simoneit BRT. Measurement of emissions from air pollution sources. 3. C-1-C-29 organic compounds from fireplace combustion of wood. Environmental Science & Technology 2001; 35: 1716-1728.

Schauer JJ, Kleeman MJ, Cass GR, Simoneit BRT. Measurement of emissions from air pollution sources. 4. C-1-C-27 organic compounds from cooking with seed oils. Environmental Science & Technology 2002a; 36: 567-575.

Schauer JJ, Kleeman MJ, Cass GR, Simoneit BRT. Measurement of emissions from air pollution sources. 5. C-1-C-32 organic compounds from gasoline-powered motor vehicles. Environmental Science & Technology 2002b; 36: 1169-1180.

Schauer JJ, Rogge WF, Hildemann LM, Mazurek MA, Cass GR. Source apportionment of airborne particulate matter using organic compounds as tracers. Atmospheric Environment 1996; 30: 3837-3855.

Schneider J, Hock N, Weimer S, Borrmann S. Nucleation particles in diesel exhaust: Composition inferred from in situ mass spectrometric analysis. Environmental Science & Technology 2005; 39: 6153-6161.

Schneider J, Kirchner U, Borrmann S, Vogt R, Scheer V. In situ measurements of particle number concentration, chemically resolved size distributions and black carbon content of traffic-related emissions on German motorways, rural roads and in city traffic. Atmospheric Environment 2008; 42: 4257-4268.

Schnelle-Kreis J, Kunde R, Schmoecker G, Abbaszade G, Diemer J, Ott H, Zimmermann R. Anteil von Partikelemissionen aus Holzverbrennung an PM10-Feinstaubimmissionen im st 錠tischen Umfeld am Beispiel von Augsburg ?Teil 1: Emissions- und Immissionsmessungen (in German). Gefahrstoffe Reinhaltung der Luft 2010; 5: 203-209.

Schnelle-Kreis J, Sklorz M, Orasche J, Stolzel M, Peters A, Zimmermann R. Semi volatile organic compounds in ambient PM2.5. Seasonal trends and daily resolved source contributions. Environmental Science & Technology 2007; 41: 3821-3828.

Schwartz J. Air pollution and hospital admissions for heart disease in eight US counties. Epidemiology 1999; 10: 17-22.

Schwartz J, Litonjua A, Suh H, Verrier M, Zanobetti A, Syring M, Nearing B, Verrier R, Stone P, MacCallum G, Speizer FE, Gold DR. Traffic related pollution and heart rate variability in a panel of elderly subjects. Thorax 2005; 60: 455-461.

Shao Y, Ishizuka M, Mikami M, Leys JF. Parameterization of size-resolved dust emission and validation with measurements. Journal of Geophysical Research-Atmospheres 2011; 116.

Simoneit BRT. A review of biomarker compounds as source indicators and tracers for air pollution. Environmental Science and Pollution Research 1999; 6: 159-169.

Slinn SA, Slinn WGN. Predictions for Particle Deposition on Natural-Waters. Atmospheric Environment 1980; 14: 1013-1016.

Smith JN, Dunn MJ, VanReken TM, Iida K, Stolzenburg MR, McMurry PH, Huey LG. Chemical composition of atmospheric nanoparticles formed from nucleation in Tecamac, Mexico: Evidence for an important role for organic species in nanoparticle growth. Geophysical Research Letters 2008; 35.

Smith JN, Moore KF, Eisele FL, Voisin D, Ghimire AK, Sakurai H, McMurry PH. Chemical composition of atmospheric nanoparticles during nucleation events in Atlanta. Journal of Geophysical Research-Atmospheres 2005; 110.

Song Y, Zhang YH, Xie SD, Zeng LM, Zheng M, Salmon LG, Shao M, Slanina S. Source apportionment of PM2.5 in Beijing by positive matrix factorization. Atmospheric Environment 2006; 40: 1526-1537.

Sow M, Alfaro SC, Rajot JL, Marticorena B. Size resolved dust emission fluxes measured in Niger during 3 dust storms of the AMMA experiment. Atmospheric Chemistry and Physics 2009; 9: 3881-3891.

Spindler G, Muller K, Bruggemann E, Gnauk T, Herrmann H. Long-term size-segregated characterization of PM10, PM2.5, and PM1 at the IfT research station Melpitz downwind of Leipzig (Germany) using high and low-volume filter samplers. Atmospheric Environment 2004; 38: 5333-5347.

Stoeger T, Reinhard C, Takenaka S, Schroeppel A, Karg E, Ritter B, Heyder J, Schulz H. Instillation of six different ultrafine carbon particles indicates a surface area threshold dose for acute lung inflammation in mice. Environmental Health Perspectives 2006; 114: 328-333.

Stoelzel M, Breitner S, Cyrys J, Pitz M, Woelke G, Kreyling W, Heinrich J, Wichmann HE, Peters A. Daily mortality and particulate matter in different size classes in Erfurt, Germany. Journal of Exposure Science and Environmental Epidemiology 2007; 17: 458-467.

Struyf, Anja, Hubert, Mia, and Rousseeuw, Peter J. Clustering in an Object-Oriented Environment. 1996.

Thimmaiah D, Hovorka J, Hopke PK. Source Apportionment of Winter Submicron Prague Aerosols from Combined Particle Number Size Distribution and Gaseous Composition Data. Aerosol and Air Quality Research 2009; 9: 209-236.

Tran CL, Buchanan D, Cullen RT, Searl A, Jones AD, Donaldson K. Inhalation of poorly soluble particles. II. Influence of particle surface area on inflammation and clearance. Inhalation Toxicology 2000; 12: 1113-1126.

Vaattovaara P, Huttunen PE, Yoon YJ, Joutsensaari J, Lehtinen KEJ, O'Dowd CD, Laaksonen A. The composition of nucleation and Aitken modes particles during coastal nucleation events: evidence for marine secondary organic contribution. Atmospheric Chemistry and Physics 2006; 6: 4601-4616.

Vallejo M, Lerma C, Infante O, Hermosillo AG, Riojas-Rodriguez H, Cardenas M. Personal exposure to particulate matter less than 2.5 mu m in Mexico City: a pilot study. Journal of Exposure Analysis and Environmental Epidemiology 2004; 14: 323-329.

Vega E, Mugica V, Carmona R, Valencia E. Hydrocarbon source apportionment in Mexico City using the chemical mass balance receptor model. Atmospheric Environment 2000; 34: 4121-4129.

Venables WN, Smith DM, the R development core team. An Introduction to R. Notes on R: A Programming Environment for Data Analysis and Graphics. 2010.

Viana M, Kuhlbusch TAJ, Querol X, Alastuey A, Harrison RM, Hopke PK, Winiwarter W, Vallius A, Szidat S, Prevot ASH, Hueglin C, Bloemen H, Wahlin P, Vecchi R, Miranda AI, Kasper-Giebl A, Maenhaut W, Hitzenberger R. Source apportionment of particulate matter in Europe: A review of methods and results. Journal of Aerosol Science 2008a; 39: 827-849.

Viana M, Pandolfi M, Minguillon MC, Querol X, Alastuey A, Monfort E, Celades I. Inter-comparison of receptor models for PM source apportionment: Case study in an industrial area. Atmospheric Environment 2008b; 42: 3820-3832.

von Klot S, Cyrys J, Hoek G, Kühnel B, Pitz M, Kuch B, Meisinger C, Hörmann A, Wichmann HE, Peters A. Estimated personal soot exposure is associated with acute myocardial infarction onset in a case-crossover study. Progress in Cardiovascular Diseases 2011; 53: 361-368.

von Klot S, Peters A, Aalto P, Bellander T, Berglind N, D'Ippoliti D, Elosua R, Hormann A, Kulmala M, Lanki T, Lowel H, Pekkanen J, Picciotto S, Sunyer J, Forastiere F. Ambient air pollution is associated with increased risk of hospital cardiac readmissions of myocardial infarction survivors in five European cities. Circulation 2005; 112: 3073-3079.

Waheed A, Li XL, Tan MG, Bao LM, Liu JF, Zhang YX, Zhang GL, Li Y. Size Distribution and Sources of Trace Metals in Ultrafine/Fine/Coarse Airborne Particles in the Atmosphere of Shanghai. Aerosol Science and Technology 2011; 45: 163-171.

Wahlin P, Palmgren F, Van Dingenen R. Experimental studies of ultrafine particles in streets and the relationship to traffic. Atmospheric Environment 2001; 35: S63-S69.

Watson JG, Chow JC, Lu ZQ, Fujita EM, Lowenthal DH, Lawson DR, Ashbaugh LL. Chemical Mass-Balance Source Apportionment of Pm(10) During the Southern California Air-Quality Study. Aerosol Science and Technology 1994; 21: 1-36.

Watson JG, Cooper JA, Huntzicker JJ. The Effective Variance Weighting for Least-Squares Calculations Applied to the Mass Balance Receptor Model. Atmospheric Environment 1984; 18: 1347-1355.

Watson JG, Robinson NF, Chow JC, Henry RC, Kim BM, Pace TG, Meyer EL, Nguyen Q. The USEPA/DRI chemical mass balance receptor model, CMB 7.0. Environmental Software 1990; 5: 38-49.

Weckwerth G. Verification of traffic emitted aerosol components in the ambient air of Cologne (Germany). Atmospheric Environment 2001; 35: 5525-5536.

Westerlund, K. G. Metal Emissions from Stockholm Traffic-wear of brake Linings. Report from SLB. No.3. 2001.

Whitby KT, Husar RB, Liu BYH. The aerosol size distribution of Los Angeles smog. Journal of Colloid and Interface Science 1972a; 39: 177-204.

Whitby KT, Liu BYH, Husar RB, Barsic NJ. The minnesota aerosol-analyzing system used in the Los Angeles smog project. Journal of Colloid and Interface Science 1972b; 39: 136-164.

Whitby KT. The physical characteristics of sulfur aerosols. Atmospheric Environment 1978; 41, Supplement: 25-49.

WHO. WHO Air quality guidelines for particulate matter,ozone, nitrogen dioxide and sulfur dioxide, Global update 2005, Summary of risk assessment. 2006.

Wichmann HE, Spix C, Tuch T, Woelke G, Peters A, Heinrich J, Kreyling WG, Heyder J. Daily Mortality and Fine and Ultrafine Particles in Erfurt, Germany, Part A: Role of Particle Number and Particle Mass. Health effects Institute Research Report 98 2000; 5-86.

Wilson JC, Liu BYH. Aerodynamic Particle-Size Measurement by Laser-Doppler Velocimetry. Journal of Aerosol Science 1980; 11: 139-150.

Wilson WE, Stanek J, Han HS, Johnson T, Sakurai H, Pui DYH, Turner J, Chen DR, Duthie S. Use of the electrical aerosol detector as an indicator of the surface area of fine particles deposited in the lung. Journal of the Air & Waste Management Association 2007; 57: 211-220.

Wilson WE, Suh HH. Fine particles and coarse particles: Concentration relationships relevant to epidemiologic studies. Journal of the Air & Waste Management Association 1997; 47: 1238-1249.

Withby KT. The physical characteristics of sulfur aerosols. Atmospheric Environment 1978; 12: 135-159.

Wongphatarakul V, Friedlander SK, Pinto JP. A comparative study of PM2.5 ambient aerosol chemical databases. Environmental Science & Technology 1998; 32: 3926-3934.

Yue W, Schneider A, Stozel M, Rückerl R, Cyrys J, Pan XC, Zareba W, Koenig WG, Wichmann HE, Peters A. Ambient source-specific particles are associated with prolonged repolarization and increased levels of inflammation in male coronary artery disease patients. Mutation Research-Fundamental and Molecular Mechanisms of Mutagenesis 2007; 621: 50-60.

Yue W, Stolzel M, Cyrys J, Pitz M, Heinrich J, Kreyling WG, Wichmann HE, Peters A, Wang S, Hopke PK. Source apportionment of ambient fine particle size distribution using positive matrix factorization in Erfurt, Germany. Sci Total Environ 2008; 398: 133-144.

Zhang DZ, Iwasaka Y, Matsuki A, Ueno K, Matsuzaki T. Coarse and accumulation mode particles associated with Asian dust in southwestern Japan. Atmospheric Environment 2006; 40: 1205-1215.

Zhang KM, Wexler AS, Zhu YF, Hinds WC, Sioutas C. Evolution of particle number distribution near roadways. Part II: the 'road-to-ambient' process. Atmospheric Environment 2004; 38: 6655-6665.

Zhang WJ, Zhuang GS, Guo JH, Xu DQ, Wang W, Baumgardner D, Wu ZY, Yang W. Sources of aerosol as determined from elemental composition and size distributions in Beijing. Atmospheric Research 2010; 95: 197-209.

Zhou LM, Hopke PK, Paatero P, Ondov JM, Pancras JP, Pekney NJ, Davidson CI. Advanced factor analysis for multiple time resolution aerosol composition data. Atmospheric Environment 2004a; 38: 4909-4920.

Zhou LM, Hopke PK, Stanier CO, Pandis SN, Ondov JM, Pancras JP. Investigation of the relationship between chemical composition and size distribution of airborne particles by partial least squares and positive matrix factorization. Journal of Geophysical Research-Atmospheres 2005; 110.

Zhou LM, Kim E, Hopke PK, Stanier CO, Pandis S. Advanced factor analysis on Pittsburgh particle size-distribution data. Aerosol Science and Technology 2004b; 38: 118-132.

Zhuang H, Chan CK, Fang M, Wexler AS. Size distributions of particulate sulfate, nitrate, and ammonium at a coastal site in Hong Kong. Atmospheric Environment 1999; 33: 843-853.

Curriculum Vitae

Name:	Jianwei Gu
Date of Birth:	10.01.1983
Place of Birth:	Jiangyin, Jiangsu
Nationality:	Chinese

9/1989 - 7/1993	Elemental school at Xinzhuang, Zhutang, Jiangyin
9/1993 – 7/1995	Central elemental school in Zhutang, Jiangyin
9/1995 – 7/1998	Junior high school in Zhutang, Jiangyin
9/1998 – 7/2001	Senior high school in Jiangyin
9/2001 – 7/2005	Studies of Environmental Sciences in the School of Resource and Environmental Science, Wuhan University (undergraduate)
9/2005 – 7/2008	Studies of Environmental Sciences in the College of Environmental Sciences and Engineering, Peking University (graduate student)
	Thesis: Study on the variations of water-soluble ions and related gases
10/2008 – 10/2012	PhD study in Environmental Science Center, University of Augsburg & Institute of Epidemiology II, Helmholtz Zentrum München, German Research Center for Environmental Health